HELLENIC REPUBLIC

National and Kapodistrian University of Athens

EST. 1837

MEDICAL SCHOOL

Master of Science Program

«MOLECULAR AND APPLIED PHYSIOLOGY»

Examination of PRKN mRNA levels in peripheral blood as a tool to identify PRKN-related Parkinson's Disease

MSc Thesis

ELINA SILIOGKA

7450202200016

ATHENS, 2025

ΑΚΑΔΗΜΙΑ ΑΘΗΝΩΝ

ΙΙΒΕΑΑ

ΙΔΡΥΜΑ ΙΑΤΡΟΒΙΟΛΟΓΙΚΩΝ ΕΡΕΥΝΩΝ ΑΚΑΔΗΜΙΑΣ ΑΘΗΝΩΝ

ONASSIS FOUNDATION

ΕΛΛΗΝΙΚΗ ΔΗΜΟΚΡΑΤΙΑ
Εθνικόν και Καποδιστριακόν Πανεπιστήμιον Αθηνών

ΙΑΤΡΙΚΗ ΣΧΟΛΗ

Πρόγραμμα Μεταπτυχιακών Σπουδών

«ΜΟΡΙΑΚΗ ΚΑΙ ΕΦΑΡΜΟΣΜΕΝΗ ΦΥΣΙΟΛΟΓΙΑ»

Examination of PRKN mRNA levels in peripheral blood as a tool to identify PRKN-related Parkinson's Disease

ΔΙΠΛΩΜΑΤΙΚΗ ΕΡΓΑΣΙΑ

ΕΛΙΝΑ ΣΙΛΙΟΓΚΑ

ΑΜ: 7450202200016

ΑΘΗΝΑ, 2025

ΑΚΑΔΗΜΙΑ ΑΘΗΝΩΝ
ΙΙΒΕΑΑ
ΙΔΡΥΜΑ ΙΑΤΡΟΒΙΟΛΟΓΙΚΩΝ ΕΡΕΥΝΩΝ ΑΚΑΔΗΜΙΑΣ ΑΘΗΝΩΝ
ONASSIS FOUNDATION

HELLENIC REPUBLIC
National and Kapodistrian University of Athens
EST. 1837

MEDICAL SCHOOL

Master of Science Program

«MOLECULAR AND APPLIED PHYSIOLOGY»

Direction: Fundamental Research (Neurosciences)

Examination of PRKN mRNA levels in peripheral blood as a tool to identify PRKN-related Parkinson's Disease

MSc Thesis

ELINA SILIOGKA

7450202200016

Committee Members:

1st: Leonidas Stefanis, *Professor of Neurology- Neurobiology, NKUA (Supervisor)*

2nd: Antonios Chatzigeorgiou, *Associate Professor of Physiology , NKUA*

3rd: Spiros Efthimiopoulos, *Professor of Physiology- Neurobiology , NKUA*

ATHENS, 2025

ΑΚΑΔΗΜΙΑ ΑΘΗΝΩΝ
ΙΙΒΕΑΑ ΙΔΡΥΜΑ ΙΑΤΡΟΒΙΟΛΟΓΙΚΩΝ ΕΡΕΥΝΩΝ ΑΚΑΔΗΜΙΑΣ ΑΘΗΝΩΝ
ONASSIS FOUNDATION

ΕΛΛΗΝΙΚΗ ΔΗΜΟΚΡΑΤΙΑ
Εθνικόν και Καποδιστριακόν Πανεπιστήμιον Αθηνών

ΙΑΤΡΙΚΗ ΣΧΟΛΗ

Πρόγραμμα Μεταπτυχιακών Σπουδών

«ΜΟΡΙΑΚΗ ΚΑΙ ΕΦΑΡΜΟΣΜΕΝΗ ΦΥΣΙΟΛΟΓΙΑ»

Κατεύθυνση: Βασική Έρευνα (Νευροεπιστήμες)

Examination of PRKN mRNA levels in peripheral blood as a tool to identify PRKN-related Parkinson's Disease

ΔΙΠΛΩΜΑΤΙΚΗ ΕΡΓΑΣΙΑ

ΕΛΙΝΑ ΣΙΛΙΟΓΚΑ

ΑΜ: 7450202200016

Μέλη Συμβουλευτικής Επιτροπής:

1ο : Λεωνίδας Στεφανής, Καθηγητής Νευρολογίας, ΕΚΠΑ / ΙΙΒΕΑΑ (Επιβλέπων)

2ο : Αντώνιος Χατζηγεωργίου, *Αναπληρωτής Καθηγητής Φυσιολογίας, ΕΚΠΑ*

3ο : Σπύρος Ευθυμιόπουλος, *Καθηγητής Φυσιολογίας Ζώων & Ανθρώπου , ΕΚΠΑ*

ΑΘΗΝΑ, 2025

ΑΚΑΔΗΜΙΑ ΑΘΗΝΩΝ

ΙΙΒΕΑΑ
ΙΔΡΥΜΑ ΙΑΤΡΟΒΙΟΛΟΓΙΚΩΝ ΕΡΕΥΝΩΝ ΑΚΑΔΗΜΙΑΣ ΑΘΗΝΩΝ

ONASSIS FOUNDATION

Abstract

Parkinson's Disease (PD), the second most prevalent neurodegenerative disorder , is characterized by the degeneration of dopaminergic neurons in the substantia nigra pars compacta (SNpc) and the formation of Lewy bodies. Mitochondrial dysfunction, particularly involving the PINK1/Parkin-mediated quality control system, is central to PD pathogenesis..

PRKN, encoding the E3 ubiquitin ligase Parkin, plays a critical role in mitophagy and mitochondrial maintenance. Mutations in *PRKN* are a leading cause of early-onset autosomal recessive PD. Genetic identification of *PRKN* mutations is difficult, requiring a battery of sophisticated tests. It would be valuable to have a screening test to identify with high sensitivity and specificity potential *PRKN* mutation carriers. In previous work, based on a small number of samples, Papagiannakis et al. (2024) suggested that *PRKN* mRNA expression levels in Peripheral Blood Mononuclear Cells (PBMCs) separated with high accuracy patients with PRKN-related PD from idiopathic PD (iPD) and healthy controls. In the current work, we have sought to validate and extend these findings to additional samples using an alternative set of primers for the performance of RT-PCR of the *PRKN* gene.

This thesis analyzed PBMC samples from 7 *PRKN*-related PD patients (3 biallelic, 4 heterozygous), 8 idiopathic PD patients, and 7 healthy controls of an already established cohort at the 1st Department of Neurology of the National and Kapodistrian University of Athens at Eginition Hospital. Experiments were undertaken largely in the Laboratory of Neurodegenerative Disorders of the Biomedical Research Foundation of the Academy of Athens. The expression levels of *PRKN* mRNA were quantified by RT-PCR using a novel pair of primers, while genetic analysis employed MLPA, Sanger Sequencing and Whole Exome Sequencing (WES).

A statistically significant difference in *PRKN* expression was founded between these groups (healthy controls, idiopathic PD, PD *PRKN*–carriers, omnibus p-value<0.0001). *PRKN* expression levels were decreased in biallelic and heterozygous *PRKN*-carrier PD patients, compared to healthy controls (4.3

times lower, p-value=0.0004) and to iPD patients (3.25 times lower , p-value=0.0210). *PRKN* mRNA levels were uniformly undetectable or very low in all *PRKN* carriers, even heterozygotes. ROC analysis revealed a sensitivity of 100% and specificity of 100%, as well as the PPV of low PRKN expression levels for the presence of heterozygote or biallelic *PRKN*–variants was 100% (72,3%-100%)

In conclusion, our study highlights the diagnostic potential of *PRKN*-mRNA expression levels in differentiating *PRKN*-variant carriers from non- carriers in PD, demonstrating reduced *PRKN* mRNA expression in *PRKN*-associated PD patients. These findings pave the way for the integration of *PRKN* expression profile in peripheral blood as a useful screening tool into the clinical workflow of diagnostics and therapeutics of PD. Furthermore, the uniformly low *PRKN* mRNA levels in heterozygote carriers suggest that additional mechanisms of reducing *PRKN* mRNA levels beyond the single allele genetic defect may be at play.

Keywords: PD, Parkin, mitochondria, PRKN, mRNA, PBMCs, RT-PCR

Acknowledgements

I would like to express my deepest gratitude to everyone who has supported and guided me throughout the journey of completing this thesis. Without the encouragement, patience and contributions, this work would not have been possible.

First and foremost, I extend my heartfelt appreciation to my supervisor, Professor Leonidas Stefanis and my advisor Dr Maria Xilouri, for their invaluable guidance, constructive feedback and unwavering support. Their expertise and mentorship have been instrumental in shaping my research and academic growth.

I am also immensely grateful to my thesis committee members, for their insightful comments, encouragement and for dedicating their time to reviewing my work.

A special thanks to Dr Nikolaos Papagiannakis for his kind support and guidance throughout the project, as well to Dr Matina Maniati, Dr Athanasios Stavropoulos, Niki Kotoula and Maria Fouka, for their valuable help, experience and support to the technical part of this study.

Also, I would like to thank all my professors of this Master Program, for their educational support throughout these years, my lab colleagues of Biomedical Research Foundation of the Academy of Athens and Medical School colleagues of National and Kapodistrian University of Athens for their sharing experiences, valuable comments and stimulating discussions, as well Dr Xenia Gaitanari for the valuable administrative support of this Master Program.

I extend my deepest appreciation to my family and friends for their unconditional help and encouragement throughout the process. Their continuous support has given me the strength to persevere through challenges and accomplish this milestone.

Finally, I acknowledge the funding and institutional support provided by Onassis Foundation Scholarship, which made this academic journey and research possible.

And to all those who have contributed to this work, whether directly or indirectly, I am sincerely grateful. Thank you!

ABBREVIATIONS

ACMG : American College of Medical Genetics and Genomics

ARPD: Autosomal Recessive Parkinson's Disease

CNS: Central Nervous System

CNVs: Copy Number Variations

Cq: Quantification Cycle

cRNA: corrected RNA

Ct: Cycle Threshold

DA: Dopamine

DMSO: Dimethyl Sulfoxide

EDTA: Ethylenediaminetetraacetic Acid

FBS: Fetal Bovine Serum

iPD: Idiopathic Parkinson's Disease

iPSC: Induced Pluripotent Stem Cells

IMM: Inner Mitochondrial Membrane

KO: Knockout

LB: Lewy Body

LC: Locus Coeruleus

MDV: Mitochondria- Derived Vesicles

MQC: Mitochondrial Quality Control

mtDNA: Mitochondrial DNA

MPTP: 1-Methyl-4-phenyl-1,2,3,6-tetrahydropyridine

NGS: Next Generation Sequencing

NKUA: National and Kapodistrian University of Athens

OMM: Outer Mitochondrial Membrane

PARIS: Parkin-Interacting Substrate

PD: Parkinson's Disease

PPV: Positive Predictive Value

REM: Rapid Eye Movement

ROC: Receiver Operating Characteristic

RPMI: Rosewell Park Memorial Institute (culture medium)

RT-PCR: Reverse Transcription Polmerase Chain Reaction

SNpc: Substantia Nigra Pars Compacta

Tm: Melting Temperature

UKPDSBBC: United Kingdom Parkinson's Disease Society Brain Bank Criteria

WES: Whole Exome Sequencing

CONTENTS

1. GENERAL SECTION

1.1 Introduction

1.1.1 Parkinson's Disease (PD)

Parkinson's disease (PD) is the second most common neurodegenerative disorder and the most prevalent neurodegenerative movement disorder. It is characterized by the progressive loss of neuromelanin containing dopaminergic neurons in substantia nigra pars compacta (SNpc)[1,2]

PD primarily manifests as a movement disorder with cardinal motor symptoms such as bradykinesia, resting tremor, and rigidity[3]. However, it has become apparent that non-motor symptoms, which include constipation, REM –sleep disorder, depression and hyposmia, may precede the motor symptoms by several years. Other non-motor symptoms may also occur, and at late disease stages, postural instability and dementia are seen[4]. The motor symptoms appear when approximately 50-60% of the dopaminergic neurons have degenerated, thereby lowering the amount of dopamine in the striatum by 70-80%, which causes dysregulation of basal ganglia activity[5].

In industrialized countries, PD affects at least 0,3% of the general population, but this increases with age such that the incidence is 1% in people older than 60 years and over 3% in people older than 80 years[6,7]. While 5-10% of PD patients have a monogenic variant with Mendelian inheritance, the remaining 90-95 % is sporadic with unknown etiology[8]. Today, 23 loci and 19 disease-causing genes have been associated with PD, reflecting the heterogeneity in phenotype, age at onset and inheritance[9]. A mutation in the *PARK2* gene is the most common cause of autosomal recessive PD (ARPD), which accounts for 50% of early-onset parkinsonism[10] and is the main focus of this diploma thesis.

1.1.2 Pathophysiology of PD

PD has traditionally been viewed as a disease caused by the selective degeneration of dopamine (DA) neurons found in the substantia nigra pars compacta (SNpc)[11]. However, systematic, large-scale characterization of

post-mortem PD brains has provided a contrasting image of disease progression based on the presence of Lewy bodies (LB). LB are intraneuronal eosinophilic proteinaceous inclusions, which were first described by the German-born American neurologist Friedrich Heinrich Lewy in 1912. A study in 1997 by Spillantini et al revealed that a-synuclein was the primary component of Lewy bodies. Since then, proteome studies have shown that Lewy bodies consist of more than 300 proteins of which approximately 90 have been confirmed by immunohistochemistry in post-mortem studies. However, the process by which Lewy body pathology occurs and their role in the neurodegenerative process in PD remains to be determined[12]. Pathologic staining of LB has revealed widespread involvement of most major subdivisions of the central nervous system (CNS), ranging from brainstem nuclei to cortex. A growing body of evidence in both human patients and preclinical animal models suggest that LBs may initially appear in the brainstem or enteric nervous system and spread across the brain in a prion-like manner[13-21].

The realization that PD pathology is not solely confined to the SNpc and can spread across the CNS has altered our understanding of PD pathogenesis and disease progression. However, despite evidence of widespread pathology, not all cell populations are equally affected. Certain populations of neurons remain more vulnerable to developing LB pathology and neurodegeneration in PD, suggesting that cell-intrinsic factors can gate selective vulnerability. The most vulnerable neuronal subpopulations include SNpc DA neurons, cholinergic neurons in the pedunculopontine nucleus, nucleus basalis of Meynert, and dorsal motor nucleus of vagus, noradrenergic neurons in the locus coeruleus, and serotoninergic neurons in the raphe nucleus[22,23]. While the factors regulating regional heterogeneity in disease susceptibility are not fully known, mitochondrial stress and failure of mitochondrial quality control pathways are thought to contribute to regional differences in pathology and neurodegeneration[22].

1.1.3 Mitochondria and CNS

Mitochondria are membrane-bound organelles that perform a range of critical cellular functions. They are double-membraned structures, with outer and inner mitochondrial membranes (OMM and IMM respectively) separated by an intermembrane space and a central matrix enclosed by the IMM. Reflecting their evolutionary origins as endosymbiotic bacteria, mitochondria carry their own unique circular genome (mt DNA) at copy numbers upwards of 10-100 per mitochondrion[24]. Their genome encodes two unique rRNAs, 22 tRNAs, and 13 polypeptides required to assemble the mitochondrial ribosome and parts of the electron transport chain, while the nuclear genome encodes more than 1000 mitochondrial genes[24,25]. Mitochondria exist as dynamic networks shifting from innumerable punctuate organelles to cell-wide tubular networks governed by a complex fission/fusion machinery. Mitochondria are highly multifunctional. They not only generate the bulk of ATP in most cell types through oxidative phosporylation, but also metabolize and synthesize complex macromolecules (e.g lipids, amino-acids and nucleotides), buffer reactive oxygen species (ROS) and cytoplasmic Ca^{2+} , regulate cellular balances, control apoptosis, and act as sensors for key anchoring scaffolds for intracellular networks[24,26,28].

Though critical for survival, these energetically demanding processes generate reactive intermediate and oxidizing agents that damage nucleic acids, proteins, and lipids, necessitating various waste removal and damage control mechanisms such as the urea cycle, glutathione, antioxidants, and H2S detoxification[26-27]. While these mechanisms perform detoxification of reactive metabolic intermediaries and end products, mitochondria also possess several sophisticated systems for maintaining structural integrity and proper protein function. These systems, collectively known as mitochondrial quality control (MQC), include AAA proteases that degrade proteins in the matrix and intermembrane space, the ubiquitin-proteasome system for removing OMM proteins, the removal of larger portions of mitochondria through mitochondria derived vesicles (MDVs) and mitophagy, and regulation of fission/fusion dynamics[25,28].

Mitochondria within the CNS exist in a unique metabolic environment, due to the sheer energetic demand of neural activity and the structural polarization of CNS cells. The brain comprises roughly 2% of total body mass yet consumes 20% of the body's oxygen intake and 25% of glucose supply, of which the bulk goes towards sustaining membrane potentials and facilitating neurotransmission[28,29]. Neuronal mitochondria must meet the immense energetic demands of neuronal signaling while also buffering waves of Ca^{2+} entry, which leads to the generation of excitotoxic ROS if left unchecked[29]. Furthermore, neuronal architecture is complex and exquisitely polarized, with some neurons carrying the vast majority of their cytoplasm and mitochondria in long dendrites and axons that can be as far as a meter away from the soma. Given the functional specialization of these cellular subcomponents, it is likely that such structural polarization leads to local metabolic needs that may require sub-specialization of mitochondrial function, such as increased Ca^{2+} buffering at the pre- and post synaptic termini and increased biosynthetic functions at the soma[25,30]. While other somatic cells can oftentimes rely on cell division to generate fresh mitochondria, neurons are postmitotic cells that must overcome the aforementioned challenges for an entire lifetime.

These bioenergetic demands are particularly evident in the neuronal populations selectively vulnerable in PD, including most of the nuclei described above. Many of these neurons send extensive, branching axons throughout the brain and influence large diffuse brain areas. The axons of SNpc DA neurons, for example, form a vast branching net that has been estimated to form up to 100-400 thousand synapses within the striatum and extend on average around 30-46 cm in length in rats[31-33]. In humans, they have been estimated to form up to 1-2 million synapses[25]. When compared to the less vulnerable neighboring DA neurons in the ventral tegmental area, SNpc DA neurons have more complex axons, a higher density of axonal mitochondria, higher rates of oxidative phosphorylation, and increased superoxide production[34]. Furthermore, many of these vulnerable populations extend unmyelinated axons[30], which likely demand even more energy than myelinated neurons due to the need to regenerate the membrane potential along the entire axon rather than just at nodes of Ranvier. Thus, the extreme

cytoarchitectural specialization of these neuronal subpopulation places a large bioenergetic burden on their mitochondria and may contribute to their selective vulnerability in PD.

1.1.4 Mitochondrial dysfunction in PD

The idea that mitochondria may be involved in the pathogenesis of PD was first suggested by observing the effects of MPTP, a byproduct of illicit synthesis of the opioid drug desmethylprodine. MPTP is metabolized to the mitochondrial complex I inhibitor MPP+, which in turn causes acute onset parkinsonism with selective destruction of SNpc neurons[35]. Since the discovery of MPTP, three major lines of evidence – epidemiological, pathological and genetic- have pointed to mitochondrial dysfunction as a central driver of disease. First, mitochondrial toxins have either been shown to cause or correlate with increased risk of PD. In addition to MPTP, exposure to the pesticide rotenone, a complex I inhibitor, has been associated with increased risk of PD in epidemiological studies[36-38]. Second, post-mortem studies of human PD patients have found widespread evidence of mitochondrial dysfunction. Complex I dysfunction has been consistently identified in the SNpc of deceased patients, with some reports of more generalized complex dysfunction that may affect other tissues as well[39-42].

In addition to these bioenergetic defects, mitochondria in postmortem tissue also show evidence of genetic defects, with greater age-dependent accumulation of mtDNA deletions and somatic mosaicism than control subjects[41-44]. Numerous other studies have identified dysregulation in the expression of various mitochondrial proteins, such as the molecular chaperone prohibitin, OMM protein VDAC1, mitochondrial import protein Tom40, and serine protease HtrA2, as well as increased oxidative damage to mitochondrial proteins[45]. Third, mutations in genes that cause monogenic PD have been linked to mitochondrial dysfunction. For example, the PD associated gene VPS35, which encodes a key subunit of the retromer complex responsible for sorting proteins between membranous organelles, contributes to the formation of MDVs and regulates fission/fusion dynamics[46-48]. The mutant proteins encoded by other genes that cause monogenic PD,

such as LRRK2, SNCA, ATP13A2, have likewise been found to cause mitochondrial pathologies ranging from increased fragmentation, disruption of ER-mitochondrial interactions, impaired Ca^{2+} buffering, elevated numbers of mtDNA mutations, and increased ROS production[49-53].

Most prominent of the monogenic PD-associated genes involved in mitochondrial function are *PINK1*, encoding the PTEN-induced serine/threonine kinase 1 , and *PRKN*, encoding an E3 ubiquitin ligase Parkin[54]. Following these findings, genetic studies in Drosophila implicated a shared biological pathway for Parkin and PINK1 function, with further mechanistic work establishing their function in detecting mitochondrial damage and recruiting mechanisms to remove and replace dysfunctional mitochondrial components[55-57]. The activation and function of the PINK1/Parkin system of MQC are some of the most well-studied pathways of PD pathogenesis and will be reviewed in detail below. Collectively, these findings firmly establish mitochondrial dysfunction as a core pathologic feature of at least these rare cases of autosomal recessive PD. The contribution of mitochondrial dysfunction to neurodegeneration relative to other mechanisms is not fully known, though it likely differs between monogenic versus familial PD and is dependent on the brain region in question.

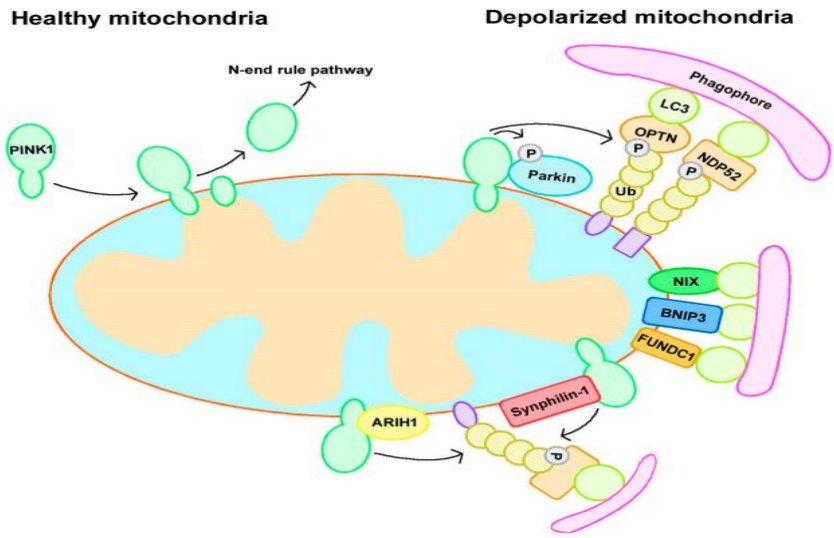

Picture 1: Mitophagy pathways. Mitophagy can be divided into Parkin-dependent or independent pathways. (*Cells* 2019)

1.1.5 PINK1/Parkin pathway in PD

Loss of function mutation in *PINK1* and *PRKN* are the most common known causes of autosomal recessive and early onset PD (before the age of 45)[58]. Despite an earlier age of onset, PD associated with *PINK1* or *PRKN* mutations is usually more benign with slower progression, high L-DOPA responsiveness, and normal cognition, but with high likelihood of dyskinesias, dystonia, hyperreflexia, and psychiatric symptoms[58-60]. The clinical presentation of *PINK1/PRKN* PD is intriguing in its relatively pure motor phenotype compared to other cases of PD and the robust and long-lasting (sometimes in the range of decades) responsiveness to dopamine replacement therapy, suggesting that these patients may experience a disease process that is largely confined to the SNpc DA system. This hypothesis is consistent with postmortem pathology in seventeen cases of PRKN and one-case of PINK1 PD, which is striking for the highly specific loss of SNpc neurons with elective sparing of the locus coeruleus (LC) and other brain regions[61]. Whereas LB pathology is found in virtually all cases of sPD, it was found only inconsistently in *PINK1/PRKN*–PD, suggesting that α-synuclein may be a minor player in these cases. In contrast, the clinical – pathologic features of sporadic PD and other monogenic causes of PD tend to exhibit significantly greater variation and wider involvement of other cell population[61]. While it is important to note that the limited availability of autopsy cases may cause an underestimation of the pathological heterogeneity of *PRKN* and *PINK1* PD, the combined clinical-pathological evidence of highly selective SNpc DA neuron loss suggest that these genes may represent critical regulator of SNpc DA neurons and that studying downstream pathological pathways may be critical for yielding insights into the vulnerability of this neuronal population in PD.

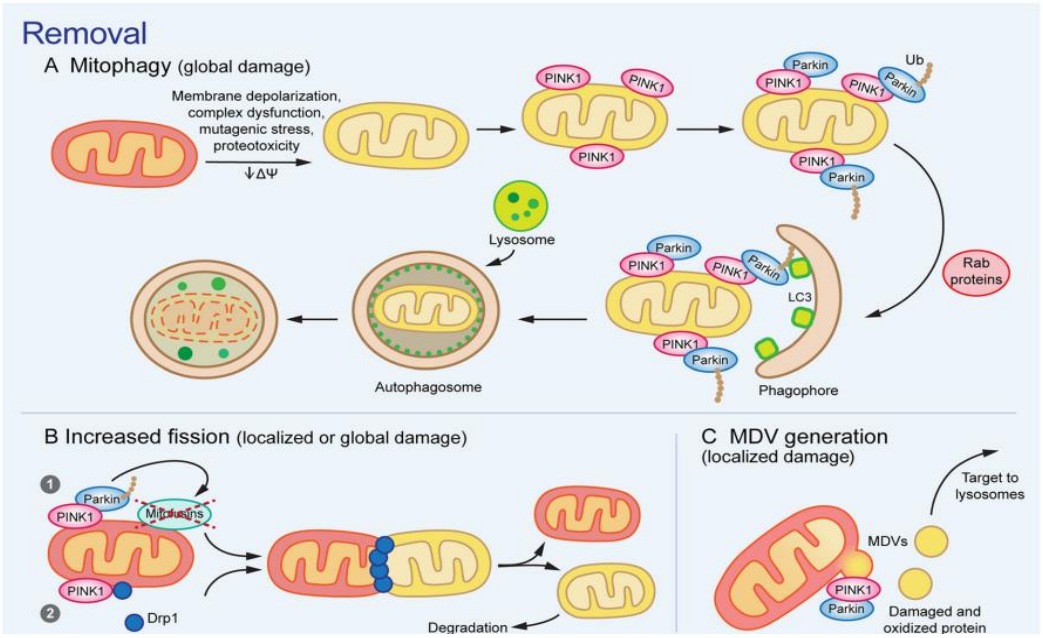

Picture 2 [Ge et al. *Molecular Neurodegeneration* (2020)]

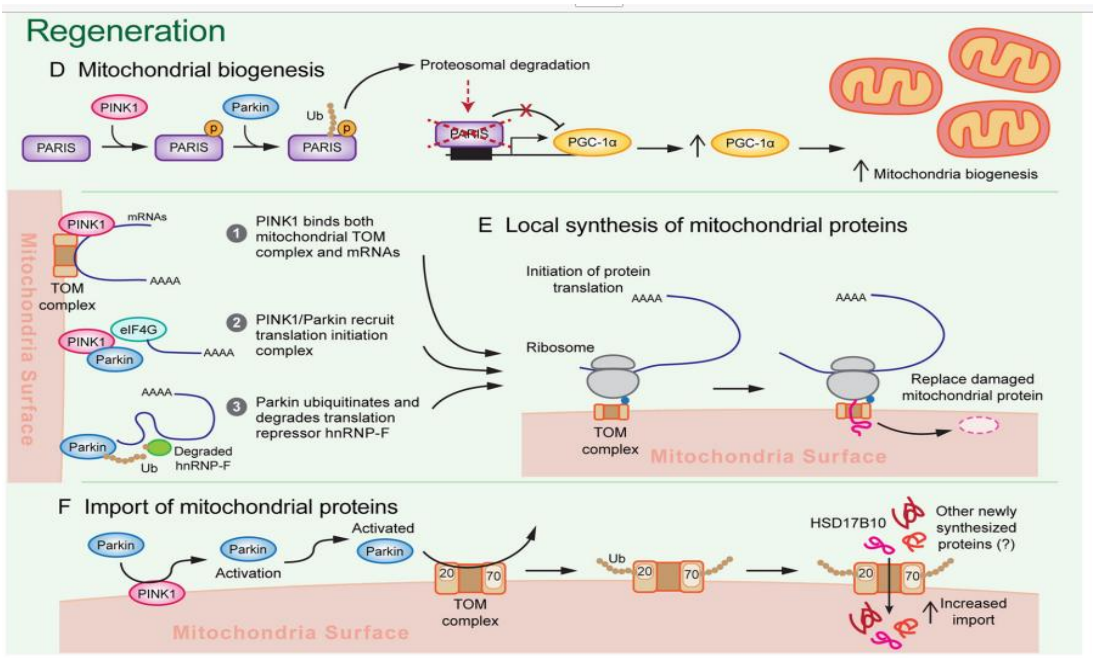

Picture 3 (and Picture 2 above): Model for the multifunctional role of PINK1/Parkin in mitochondrial quality control . Activation of PINK1/ Parkin triggers multiple mechanisms of **a-c** mitochondrial removal and **d,e** mitochondrial regeneration. Different mechanisms of mitochondrial removal are engaged depending in the severity of damage. [Ge et al. *Molecular Neurodegeneration* (2020)]

1.1.6 Mechanism of PINK1/Parkin activation

PINK1 and Parkin function as the first steps of a signaling pathway that activates mitochondrial quality control pathways in response to mitochondrial damage[62]. Under basal conditions, PINK1'*s* N-terminus is transferred across the OMM to the IMM, with the kinase domains located closer to the C-terminus protruding out into the cytosol. PINK1 is then cleansed by IMM-bound proteases and subsequently degraded by the proteasome, leading to undetectable basal levels of PINK1[63,64]. Stressors such as membrane depolarization, mitochondrial complex dysfunction, mutagenic stress, and proteotoxicity lead to accumulation of PINK1 on the OMM by impairing intermembrane transport of the N-terminus domain to the IMM. Subsequent homodimerization of PINK1 on the OMM leads to autophosphorylation, which promotes kinase activation and facilitates binding to substrates Parkin and ubiquitin[65,66]. Thus, PINK1'*s* ability to rapidly accumulate and activate in response to mitochondrial stressors allows it to function as a sensor of mitochondrial damage.

1.1.7 Parkin

The *PARK2* gene encodes the 52kDA protein parkin, which consists of 12 exons and 465 amino acids[67,68]. Mutations in the *PARK2* gene cause an autosomal recessive form of PD and is the most frequent cause of early-onset PD found in several distinct families with distinct ethnicities[69]. Parkin functions as an E3-ubiquitin ligase and has a broad range of neuroprotective functions including the maintenance of mitochondrial metabolism[70] and the ubiquitin-proteasome system, where parkin plays an essential role in the ubiquitin – mediated degradation of misfolded or damaged proteins and in removal of dysfunctional mitochondria via mitophagy[71]. The protein is widely expressed throughout the brain and abundant expression of parkin mRNA has been observed in other tissues such as the heart and skeletal muscles.

Parkin is a RING-in-between-RING (RBR) type E3 ubiquitin that catalyses the mono and poly-ubiquitylation of several structurally and functionally distinct proteins, including itself[72,73]. Parkin consists of an N-terminal ubiquitin-like (UBL) domain that is followed by four cysteine-rich regions, each of which

binds two Zn^{2+} atoms[74]. Three of those regions are the new gene (RING) domain designated as RINGO-2, the last two of which are separated by a 51 –residue-in-between-RING (IBR) domain in the C-terminal part[75].

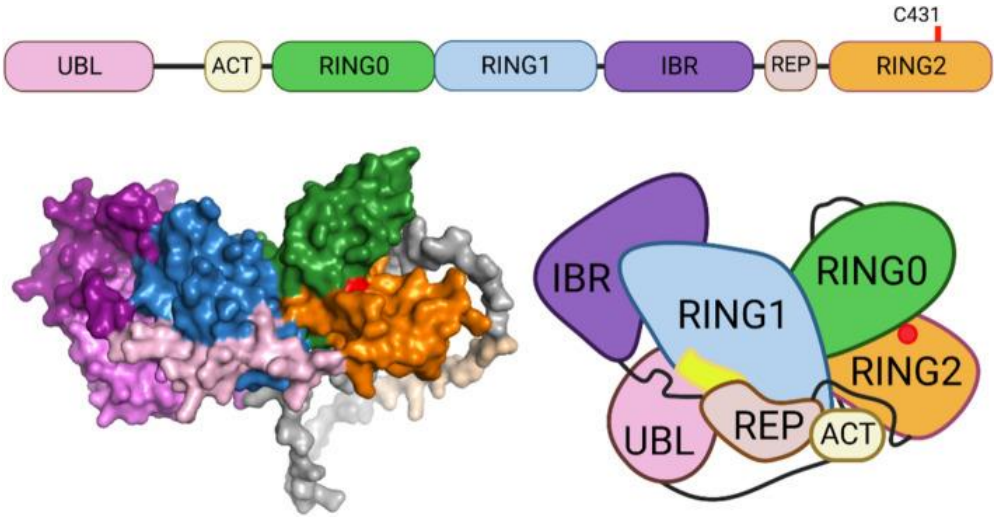

Picture 4: Parkin domain organization and auto-inhibited conformation (Clausen et al, 2024)

1.1.8 Parkin function

Parkin functions as an E3-ubiquitin ligase that is engaged in monoubiquitylation[76] and multiple monoubiquitylation[77], as well as K48 –linked and K63-linked polyubiquitylation[78]. The classical K48-linked polyubiquitylation is involved in proteasomal degradation[79], whereas the K63-linked polyubiquitylation plays a proteasomal-independent role in the regulation of protein trafficking for lysosomal degradation and targeting whole organelles for autophagic degradation[80]. The proteasomal-mediated degradation of proteins involves the sequential action of three enzymes, i.e. ubiquitin-activating (EI), ubiquitin-conjugating (E2), and ubiquitin-ligase (E3), which cooperate in adding ubiquitin molecules to proteins destined for degradation[81]. Through a sequential and repetitive action of these enzymes, ubiquitin molecules are attached to substrate proteins via a covalent isopeptide between the glycine at residue 76 (G76) in the C-terminal part of ubiquitin and lysine at residue 48 (K48) at the N-terminal part of the substrate proteins targeting them for proteasomal degradation[82,83].

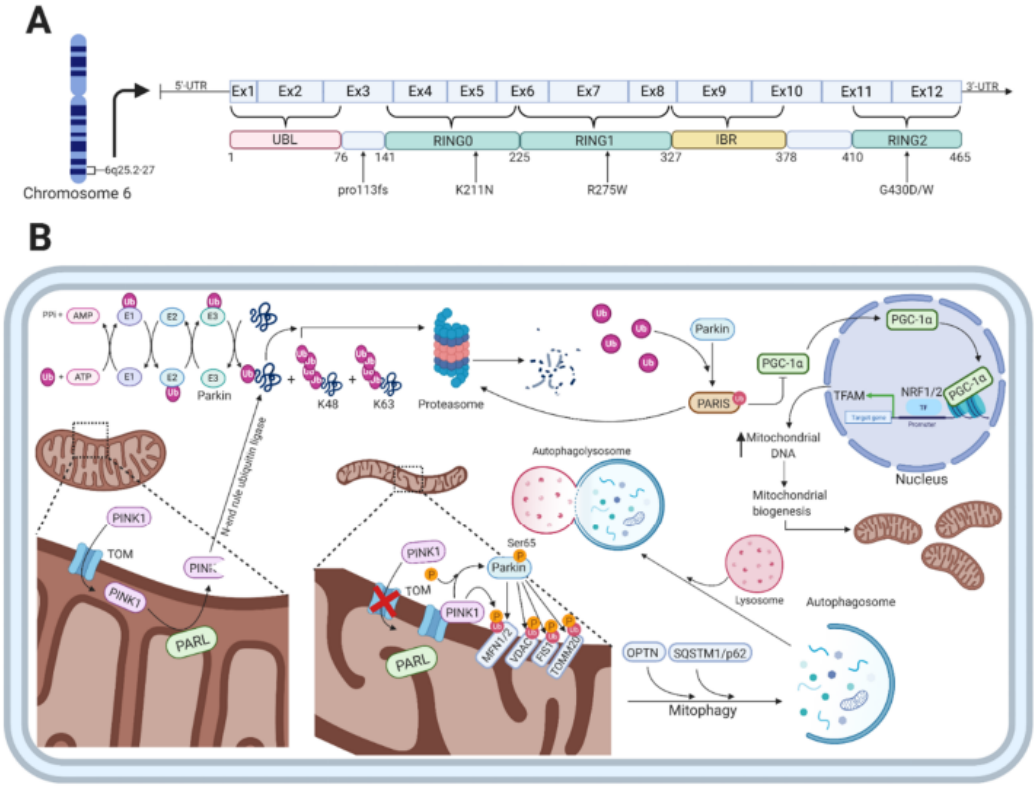

Picture 5: The function of parkin and *PARK2*-related mutation. **(A)** Shows a schematic representation of parkin on transcripti level, color-coded functional domains, and *PARK2* related mutations**. (B)** Shows the various cellular functions of parkin, which is involved in the ubiquitin-proteasome system as an E3–ubiquitin ligase, regulation of mitophagy, and mitochondrial biogenesis. (*Cells*, 2021)

Besides the function of parkin in the ubiquitin proteasomal system, several studies have shown that parkin specifically translocates from the cytosol to dysfunctional mitochondria upon an impaired electrochemical membrane potential leading to mitochondria depolarization[84-86]. Mitophagy, the autophagy-mediated degradation of mitochondria, is in part mediated by the PD-associated proteins parkin and PINK1 in a ubiquitin-dependent mechanism[87]. In the parkin-dependent mitophagy process, PINK1 functions as the mitochondrial damage sensor, parkin as a signal amplifier, and the ubiquitin chains as the signal effector[88]. When healthy mitochondria are present, PINK1 is transported through the translocase of the outer membrane (TOM) complex to the inner mitochondrial membrane (IMM), mediated by its N-terminal mitochondrial targeting sequence. This is followed by its subsequent cleavage by presenilin-associated rhomboid-like protein (PARL),

a protease in the IMM, which leads to the production of a 52kDA PINK1 protein fragment[90,91]. The protein fragment is released to the cytosol where it is rapidly ubiquitylated for proeasomal degradation by an N-end rule ubiquitin ligase. Thus, the intracellular levels of PINK1 are low on healthy mitochondria. Basal activity of Parkin is also minimal due to intramolecular interactions that block the active site and compete with E2 ligase binding.

When mitochondria are damaged, they become depolarized, leading to inhibition of PINK1 translocation and processing in the IMM[92]. This results in the accumulation of unprocessed PINK1 bound to the TOM complex on the OMM and the subsequent Parkin activation through two mechanisms. First, it phosphorylates ubiquitin on S65, which competes with an autoinhibitory domain with Parkin and stabilizes it in an active conformation. Second, PINK1 directly phsosporylates Parkin on S65 in Parkin's ubiquitin-like-domain, which induces conformational changes that allow for binding of the charged E2 ligase[93-101]. These mechanisms increase Parkin's E3 ubiquitin ligase activity, with both required for full activation, through it is unclear whether either mechanism contributes differentially to activation[102]. Thus, Parkin amplifies a damage detection signal from PINK1 by facilitating the formation of ubiquitin chains, which recruit more Parkin to the mitochondria[103].

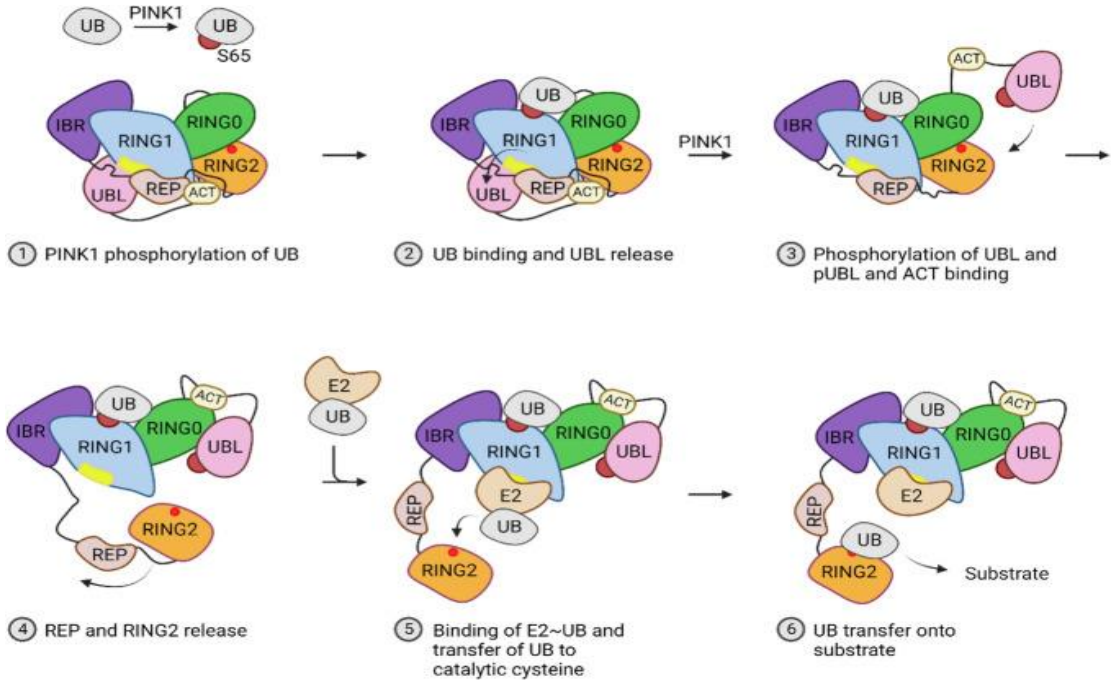

Picture 6: Parkin activation (Clausen et al, 2024)

Once recruited to the mitochondria, Parkin exhibits two waves of ubiquitination: the first wave targets many outer OMM and mitochondrial matrix proteins within the first 2 hours of activation, whereas the second wave targets IMM proteins[103,104]. The parkin-mediated ubiquitylation of proteins located on the OMM includes mitofusin ½ (MEN ½) , voltage-dependent anion-selective channel (VDAC) proteins, mitochondrial fission 1 protein (FIS1), and mitochondrial import receptor subunit TOM20 homologue (TOMM20). The formation of these chains of ubiquitin molecules on OMM proteins is served by autophagic cargo receptors such as optineurin (OPTN) and sequestrine 1 (SQSTMI/p62) that will initiate the degradation of damaged mitochondria. Parkin has also been found to ubiquitinate many cytosolic targets, though it is unclear whether these targets are phosphorylated by mitochondrial bound Parkin or whether may be cytosolic activation of Parkin[104].

Among these cytosolic targets are AIMP2, whose accumulation leads to PARP1 and MIF-dependent cell death of nigral DA neurons, and Parkin Interacting Substrate (PARIS, ZNF746), which causes neurotoxicity by suppressing mitochondrial biogenesis[105-112]. The density of Parkin substrates and the formation of multiple types of ubiquitin linkages (K6, K11, K48, K63), poses the question of whether Parkin ubiquitination may have diverse effects on cellular signaling beyond targeting proteins for degradation[113]. Substrate specificity and chain formation may show some cell-type dependence. Thus, it is possible that differences in Parkin substrate recognition and targeting may lead to divergent Parkin function in a cell-type specific manner.

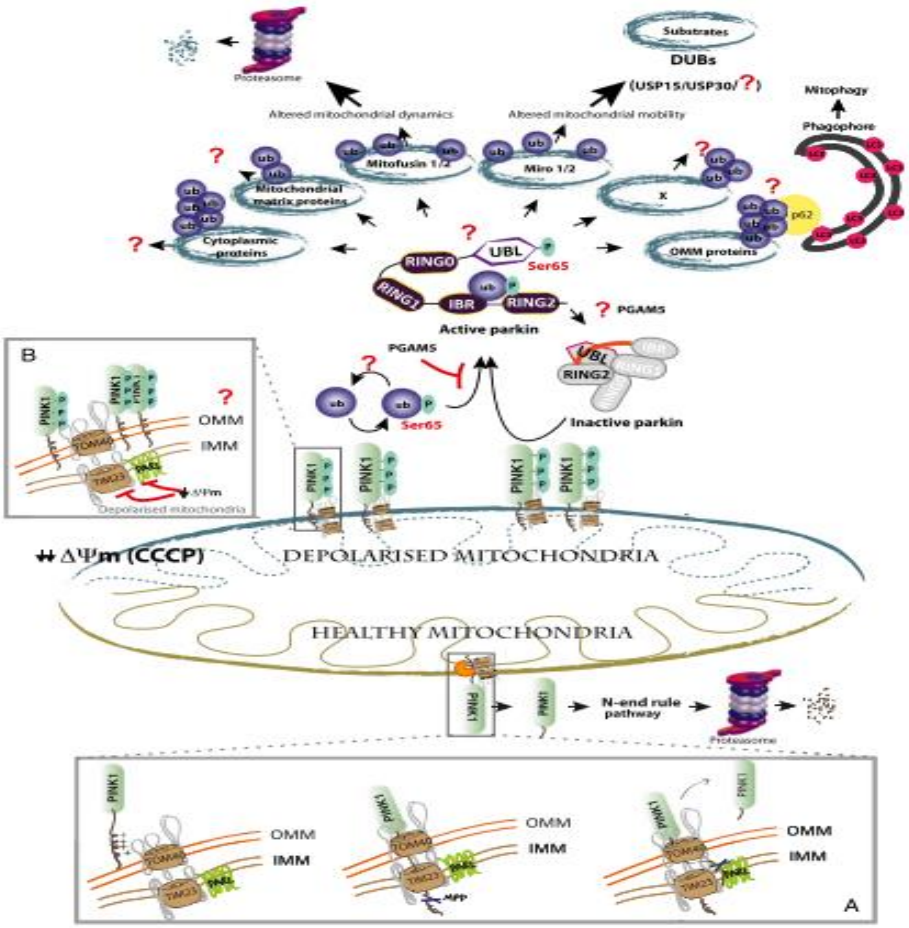

Picture 7: PINK1-Parkin signaling (under healthy conditions / upon mitochondrial depolarization) (A. Kazlauskaite and M.M. K. Muquit, *FEBS Journal* 282, 2015)

In addition to parkin's role in the clearance of dysfunctional and damaged mitochondria, it also mediates the activation of mitochondrial transcriptional coactivator PGC-1a[114]. This is done through the ability of parkin to degrade PARIS, which normally inhibits the activity of PGC-1a. Stabilization and activation of PGC-1a through the parkin-mediated degradation of PARIS leads to activation of the transcription factors nuclear respiratory factor 1 and 2 (NRF1/2), which will switch on mitochondrial probiogenesis factors such as mitochondrial transcription factor A (TEAM). Loss of parkin function, which is the case in PARK2-related PD, results in the accumulation of PARIS and, therefore, to sustained repression of PGC-1a activity[117]. This will eventually lead to the inhibition of mitochondrial biogenesis.

Proteomic, structural, and functional analyses were applied in a recent study using human isogenic iPSC-derived neurons with and without a PARK2

knockout (KO)[118]. This study identified dysregulation of several proteins in the PARK2 KO neurons that are involved in oxidative stress, mitochondrial respiration and morphology, cell cycle control and cell viability. Furthermore, the structural and functional analyses showed accumulation of enlarged and elongated mitochondria, which is consistent with the function of parkin in mitochondrial quality control. These functions of parkin highlight its pivotal role in the production and degradation of mitochondria as well as its essential function in the ubiquitin-proteasome system.

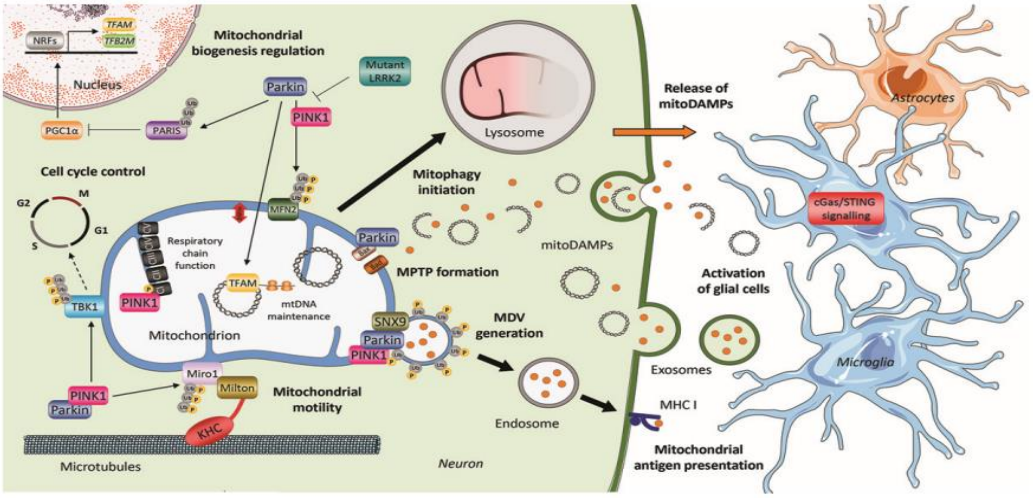

Picture 8: Involvement of PINK1 AND Parkin in mitochondrial processes. (M. Borsche et al. / *Mitochondria and PD*)

1.1.9 Fragility of the *PRKN* gene

The *PRKN* gene is located in the so-called FRA6E region on chromosome 6, one of the most fragile areas of the human genome. Typically, chromosomal fragile sites are hotspots for deletions and amplifications, and fragility of the FRA6E region is likely caused by replication problems linked to transcription of the extremely large *PRKN* gene. Thus, even though the mature *PRKN* mRNA is only about 4 kb, the *PRKN* gene and primary transcript is about 1,4 Mb, which mainly consists of introns. Since, the size of the region is conserved in vertebrates, the non-coding DNA may possess some unknown regulatory function. A recent study has shown that the large introns do not seem to be important for *PRKN* expression, but may through the fragility of the region contribute to an increased risk of de novo germline variants in *PRKN*. Moreover, the fragility of the *PRKN* gene likely increases the risk of

somatic *PRKN* mutations, which based on Parkin's possible role as a tumor suppressor, could have implications for cancer susceptibility[178].

1.1.10 Parkin –associated PD

More than 100 PD-associated mutations in the 12 exons of the *PARK2* gene have been identified including missense mutations, large chromosomal deletions and duplications, truncation mutations, and promoter mutations[119,120]. The general view is that parkin-related PD arises from similar mechanisms. The simplest explanation is that parkin mutations serve to lead to a loss of parkin function. Parkin-linked PD where deletions span several exons is certainly consistent with a loss of parkin function. Nonsense-mediated decay would serve to destabilize any truncated transcripts that might be expressed leading to the absence of protein expression. Indeed, there is little evidence that truncated parkin protein is expressed in patients with exon deletions[121]. Many missense mutations also appear to lead to a loss of parkin function through decreased catalytic activity, aberrant ubiquitination and impairment of proteasomal degradation of parkin substrates. Thus, the general view is that disease-causing mutations in parkin lead to a loss of parkin function, albeit through different mechanisms[122-125].

Parkin may also have a role in sporadic PD. It may be inactivated due to nitrosative stress[126,127], dopaminergic stress[128] and oxidative stress[129,130], which are key pathogenic processes in sporadic PD as well. Carriers of PD-associated *PARK2* mutations have generally a characteristic clinical picture that is more restricted than sporadic PD[131,132]. More distinctive clinical phenotypes associated with *PARK2* mutations include earlier age of onset, frequent dystonia, and hyperreflexia and slower disease progression despite the early onset with absence of dementia or severe autonomic dysfunction even after prolonged disease duration[131]. Additionally, *PARK2*–associated PD patients have an excellent response towards levodopa treatment but are prone to develop levodopa-mediated dyskinesia[133,134]. Pathologically, *PARK2*-associated PD patients show a significant reduction of neurons in the SNpc and only a moderate decrease of neurons in LC.

1.1.11 Clinical characteristics of Parkin-associated PD

Clinical description: Parkin type of early-onset PD is characterized by the cardical signs of PD: bradykinesia, resting tremor and rigidity. The median age of onset is 31 years (range: 3-81 years). The disease is slowly progressive and disease duration of more than 50 years has been reported. Clinical findings vary, though hyperreflexia is common. Lower-limb dystonia may be a presenting sign and cognitive decline appears to be no more frequent than in normal population. Dyskinesia as a result of treatment with dopaminergic drugs frequently occurs[135]. Women and men are affected with equal frequency. Age at onset is highly variable, even among individuals with the same pathogenic variant. Onset is usually before age of 40 years, the median age at onset being 31 years[136].

Clinical findings at onset , often, include tremor, braydkinesia and dystonia. Dystonia is observed in 65% of affected individuals. Almost half of affected individuals present with hyperreflexia. The diagnosis of PD may be delayed due to unusual clinical features, especially in patients with an early manifestation[137]. Parkin associated PD is not associated with specific behavioral, neuropsychological or psychiatric manifestations[138]. Cognitive impairment is uncommon, and dementia is observed very rarely[139]. The disease is slowly progressive: disease duration of greater than 50 years has been reported. In later disease stages, freezing at gait, posture deformities, and motor fluctuations may be common features, whereas dementia does not develop[140]

Neuroimaging: Routine cranial CT and MRI scans are usually normal. PET/SPECT studies have revealed a reduced striatal ^{18}F-DOPA uptake and a reduced presynaptic dopamine transporter density in individuals with Parkin-associated PD[141]. The putamen is predominantly affected, consistent with the findings in PD of other etiologies. In contrast, however, the loss of dopaminergic striatal innervations is rather symmetric and the progression rate is considerably slower. The postsynaptic D2 receptor density as assessed with ^{21}C-raclopride PET has been shown to be upregulated

untreated affected individuals and downregulated in affected individuals who receive dopaminergic medication.

Voxel-based morphometry revealed a decrease of putaminal gray matter volume and a slight increase of gray matter in the right pallidum in individuals with Parkin-associated PD (i.e. those with biallelic *PRKN* pathogenic variants), whereas asymptomatic individuals heterozygous for a *PRKN* pathogenic variant demonstrated an increase of both putaminal and pallidal gray matter volume. Using $T2^*$ relaxometry, an increased substantia nigra iron load was detected in four symptomatic individuals with Parkin associated PD and two asymptomatic individuals heterozygous for a *PRKN* pathogenic variant[142].

Neuropathology: To date, detailed postmortem studies of nine individuals with biallelic *PRKN* pathogenic variants have been published[143]. The most prominent and most common feature was the finding of neuronal loss in pigmented nuclei of brain stem. Unlike Parkinson disease of other etiologies, the neuronal loss was greater in the substantia nigra pars compacta than in the LC. Typical alpha-synuclein-containing LB were identified in only two affected individuals, whereas one affected individual had basophilic LB –like pathology of pedunculopontine nucleus. Tau-containing neurofibrillary tangles were observed in two affected individuals. In summary, the spectrum of post-mortem findings is broad and thus somewhat reminiscent of the situation in LRKK2 Parkinson's disease[144].

Clinical Phenotype	
Motor features	Bradykinesia
	Resting tremor
Non-motor features	Anxiety
	Psychosis
	Panic attack
	Depression
Other clinical features	Normal cognitive function
	Hyperreflexia
	Frequent focal dystonia
	Sleep benefit
	Benign disease course
	Excellent response to low dose Levodopa
	Prone to develop Levodopa-induced dyskinesias

Picture 9: Clinical phenotypes frequently reported in PD cases with *PARK2* mutations (*Cells*, 2021, 10, 283)

1.1.12 Role of heterozygous *PRKN* pathogenic variants in PD

PARK2 gene mapped to chromosome 6q25.2-q27, has a high mutation rate, and is located in an unstable region in the genome. Thus, more than 100 pathogenic mutations have been reported worldwide. Among them are point mutation and exon rearrangements, which contribute equally to the *PARK2* mutation spectrum. The classical view is that carriers of one risk allele are not affected, although this view is debated. Copy number variants (CNVs) constitute a particular challenge in genetic association studies and the impact of CNVs affecting *PARK2* in heterozygous carriers in large samples remains to be studied.[162]

It is debated whether heterozygous CNV carriers are at risk of developing PD, as heterozygous *PRKN* pathogenic variants have been detected in a large number of individuals with PD[145]. Case control studies revealed a frequency of 0% to 7,9% in people with PD and 0% to 3,7% in neurologically healthy controls[146]. In a comprehensive case-control study, the frequency of heterozygous *PRKN* exon rearrangements was the same among affected persons and controls[147]. Notably, however, the frequency of heterozygous *PRKN* pathogenic variants in presumably healthy individuals in public exon databases is only 0,17%.

Not only association studies but also examination of families has yielded conflicting results[163-165]. Heterozygous family members of homozygous carriers have been described with mild PD signs of late onset, whereas another group found no typical clinical signs of the disease[166]. Another study showed that typical *PARK2*-associated symptoms, such as dystonia and dyskinesia, correlate with the number of mutated *PARK2* alleles[167]. Furthermore, in comparison to homozygous carriers, characterized by an onset before the age of 40 years, some groups showed that heterozygous carriers of CNVs, as well as point mutations, are associated with a later onset[168-170]. Still, an earlier age at onset for *PARK2* mutation carriers compared with that of individuals without mutations in *PARK2* is suspected[171].

The notion that heterozygous carriers may be at increased risk of PD is also supported by neuroimaging and electrophysiological findings. Preclinical

changes such as reduced fluorodopa uptake in the striatum of the asymptomatic heterozygous mutation carriers were connected to the development of PD later in life[172-174].

Multimodal neuroimaging and electrophysiologic studies disclosed latent nigostratial impairment, compensatory hypertrophy of the putamen and pallidum, and increased iron deposition in the substantia nigra is asymptomatic individuals heterozygous for a *PRKN* pathogenic variant, supporting the assumption that heterozygous *PRKN* pathogenic variants are a genetic susceptibility factor for PD[174].

PET/SPECT studies have revealed that asymptomatic individuals heterozygous for a PRKN pathogenic variant have a slight and subclinical impairment of dopaminergic neurotransmission. A longitudinal PET study demonstrated a very subtle progression rate, indicating that only a marginal number of asymptomatic individuals heterozygous for a *PRKN* pathogenic variant may develop clinically overt parkinsonism if no other risk factors are present[148].

Using functional MRI, asymptomatic individuals heterozygous for a PRKN pathogenic variant showed an increased activation of motor-related brain regions when they performed repetitive finger movements. The same mechanism of an increased neuronal recruitment has been illustrated for a facial emotion recognition task[149].

However, based on the currently available data (and lack of prospective evaluations), the role of heterozygous *PRKN* pathogenic variants in disease causation cannot be determined conclusively.

A possible explanation is that mutations may act as susceptibility factors or disease modifiers and might contribute to the heritability of familial and sporadic PD[162]. Haploinsufficiency has been considered a more likely explanation than compound heterozygocity through unidentified recessive mutations. Thus, the impact of heterozygous mutations in *PRKN* should be the focus of future investigations. It is important to further elucidate their role

in PD in order to provide an accurate diagnosis and counseling of mutation carriers.

Of note, sporadic tumors (e.g. ovarian cancer) occurring as single tumors in the absence of any other findings of Parkin-associated PD frequently harbor PRKN somatic variants that are not present in the germline. In these circumstances predisposition to these tumors is not heritable. However, the involvement of *PRKN* pathogenic variants in oncogenesis is ambiguous, as the association with cancer could not be replicated in a population-based study[150].

1.1.13 Contribution of PINK1/Parkin MQC dysfunction to idiopathic PD

While it is clear that genetic loss of PINK1/Parkin contributes to the selective loss of SNpc neurons, these genetic cases represent only a small fraction of PD, which remain in most cases an idiopathic disease with no clear Mendelian genetic etiology[151].

Our understanding of MQC dysfunction in idiopathic PD has arisen largely from surveys of pathological changes in postmortem patient brains and mechanistic studies linking a-synuclein aggregation to deficits in the PINK1/ Parkin pathway . The two broad causes of potential responses that PINK1 / Parkin MQC may exhibit in iPD are either protective activation in response to mitochondrial damage, or inactivation leading to an additional pathway of neurodegeneration. While there is evidence that PINK1 levels are stabilized and increased in PD patient brains[152], Parkin is S-nitrosylated and sequestered into LBs, leading to reduced availability of soluble Parkin to perform its native functions[153]. Because Parkin acts downstream of PINK1 activation, its inactivation in iPD likely blocks the effects of PINK1 accumulation. This is supported by the accumulation of proteins normally targeted for degradation by the PINK1/Parkin system. Consistent with findings of Parkin inactivation in PD brains, protein levels of multiple Parkin substrates-AIMP2, FBP1, PARIS, PDCD2, STEP61 – have been found to be elevated in patient midbrain tissues[154]. PGC-1a, whose levels would be expected to drop with inactivation of the PINK1/Parkin pathway, has likewise been found to be downregulated in PD brains[155].

Current literature suggests that Parkin inactivation may derive from chemical inactivation[156]. Or may occur downstream of a-synuclein aggregation[157]. A number of recent studies have suggested that a-synuclein pathology drives the activation of nonreceptor tyrosine kinase c-Abl, which phoshorylates Parkin at Y143 and inactivates it, leading to accumulation of Parkin substrates such as PARIS[158]. Other potential mechanisms could involve direct sequestration of Parkin into a-synuclein aggregates[159] or the activation of other pathways that add inactivating post-translational modifications on Parkin[160]. Thus, a possible explanation for why genetic Parkin inactivation does not exacerbate a-synuclein toxicity is because it phenocopies the Parkin inactivation induced by a-synuclein.

While there is evidence supporting the role of a-synuclein aggregation in inactivating Parkin, whether a-synuclein-independent pathways of MQC inactivation such as oxidative damage may also be at play requires further study. Regardless, these findings implicated PINK1/Parkin inactivation not just as a cause of selective SNpc degeneration in the small percentage of PD cases associated with monogenic *PRKN* or *PINK1* mutations, but also in the sporadic disease driven by a-synuclein aggregation as well.

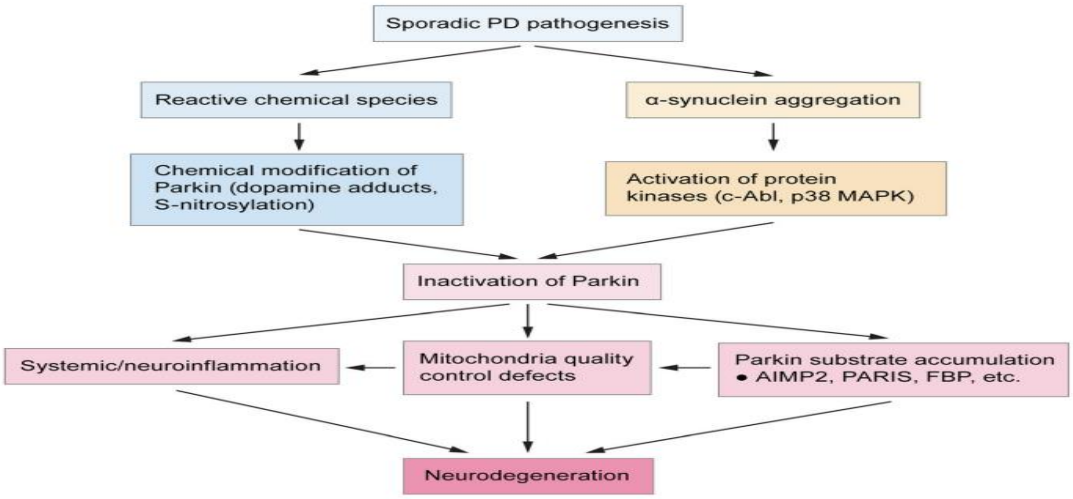

Picture 10: Mechanisms of Parkin inactivation in idiopathic PD (Ge et al, *Molecular Neurodegeneration*, 2020)

1.2 Aim of the study

While the neurodegenerative effects of *PARK2* mutations are well established, to our knowledge, there have been few studies examining whether variants in the *PRKN* gene affect these respective mRNA levels in *PRKN*-carrier PD patients or if such alterations could even occur in sporadic PD patients. To address this issue, we aimed to identify potential alterations in *PRKN* mRNA expression levels in PBMCs isolated from *PRKN*-carrier PD patients compared to iPD patients and healthy controls. In order to further differentiate between heterozygous, biallelic, as well as sporadic PD patients, comparisons between these groups were also undertaken.

PBMCs were chosen as an easily accessible blood cell type that expresses the necessary mRNA and has been shown to be useful in the study of PD-related pathogenic events. PBMCs share some mitochondrial and metabolic characteristics with neurons, making them as attractive surrogate for investigating *PARK2* related dysfunctions[161]. The expression levels of *PRKN* mRNA in PBMCs could serve as a potential biomarker for Parkin-related PD.

Alterations in *PRKN* transcription have already been reported in patients with *PRKN* mutations in our cohort in a previous study[161]. In particular, the work of Papagiannakis et al. (2024) was the first to measure *PRKN* mRNA expression levels in PBMCs and report low *PRKN* mRNA levels in a wide variety of *PRKN* mutation carriers, upon sampling from peripheral sources. More specifically, a major result of this study was that pathogenic variants in the *PRKN* gene result in reduced expression of the respective mRNA in PBMCs. This result was evident not only in biallelic individuals, but also in heterozygous PD patients, suggesting that additional factors may lead to *PRKN* mRNA reduction in these cases. Despite the small number of samples being used, this study was the first to propose an easily accessible screening test for *PRKN* mutations.

This thesis aims at further extending these findings to additional *PRKN* carriers, especially heterozygotes, and independently validate the previous results with a new set of primers. This means investigating alterations in

PRKN mRNA expression at a broader level, as well as refining the method used with the perspective to be further accessible as a potential biomarker for the presence of *PRKN*-related PD. By elucidating also the relationship between *PRKN* expression and PD, this work seeks to enhance our understanding of Parkin'*s* systemic role in disease pathology and explore its potential not only as a diagnostic but also as a therapeutic target as well.

2. SPECIFIC SECTION

2.1 Materials and Methods

2.1.1 Sample selection

The samples are collected from a single center cohort (First Department of Neurology, National and Kapodistrian University of Athens) of 7 samples of patients with *PRKN*-related PD as well as 7 samples of healthy controls and 8 samples of patients with idiopathic PD. The patients'/controls' characteristics are recorded below:

2.1.2 Study design

This study aimed to analyze the mRNA expression levels of the *PRKN* gene in Peripheral Blood Mononuclear Cells (PBMCs) from three distinct groups

- Control group: 7 samples of healthy individuals without a history of PD
- Idiopathic PD group: 8 samples of patients diagnosed with idiopathic PD
- *PRKN* mutation group: 7 samples of patients with PD carrying confirmed mutations in the *PRKN* gene

The samples were collected from a single center cohort (First Department of Neurology, National and Kapodistrian University of Athens) and were analyzed in the Lab of Neurodegenerative Diseases of the Biomedical Research Foundation of the Academy of Athens (BRFAA).

All participants provided informed consent before sample collection. The study protocol was approved by the Institutional Review Board (IRB) of Medical School of National and Kapodistrian University of Athens. The inclusion and exclusion criteria were strictly followed to ensure homogeneity within the groups.

2.1.3 Inclusion Criteria

Control group:

- Healthy individuals with no clinical signs of PD or other neurodegenerative disorders
- Age range: 40-75 years, to match the typical age range of PD patient
- No history of neurological or psychiatric disorder
- No family history of PD (to reduce the probability of genetic predisposition)
- Willing and able to provide informed consent

PRKN mutation group:

- Patients diagnosed with PD carrying confirmed *PRKN* gene mutations (genetic testing required for inclusion)
- Age range 20-75 years (to include both early onset and late onset cases)
- Onset of PD typically before the age of 70 (early –onset PD is common in *PRKN* mutations)
- Confirmed diagnosis based in genetic testing (heterozygous, homozygous or compound heterozygous mutations in *PRKN*)
- Willing and able to provide informed consent

Idiopathic PD group

- Patients diagnosed with idiopathic PD according to the United Kingdom Parkinson's Disease Society Brain Bank Criteria (UKPDSBBC)
- Age range: 40-75 years
- No known genetic mutations related to PD (especially no *PRKN* mutations)
- Onset of PD at an age ≥ 50 years , to increase the probability of sporadic PD (not early onset)
- Disease duration of at least 1 year (to ensure the presence of established disease)
- Willing and able to provide informed consent

2.1.4 Exclusion Criteria (Applicable to all groups)

- Presence of other neurodegenerative or neurological disorder (e.g. Alzheimer's disease, Multiple System Atrophy, Progressive Supranuclear Pulsy)
- History of psychiatric disorders (e.g. schizophrenia, major depression) that could influence gene expression in PBMCs)
- Severe systemic illness (e.g cancer, autoimmune disease) that could affect immune function and gene expression)
- Current use of immunosupressive drugs (e.g. corticosteroids, biologics) or other medications that may alter PBMC function
- Recent infection or inflammation (within the last 2 weeks) , as this could affect mRNA expression in PBMCs
- History of substance use (alcohol or drugs) within the past 5 years
- Pregnancy or breastfeeding (for female participants), as hormonal changes could influence gene expression
- Family history of PD (for the control group), to exclude individuals who may be at genetic risk

2.1.5 Participants characteristics

PD patients and age-matched healthy subjects were enrolled from Eginitio University Hospital, Athens, Greece. Their age and age of onset are shown in **Table 1**, while demographic and clinical characteristics of the study participants are presented in **Table 2**. The control group consisted of 7 individuals (6 females, 1 male) with a mean age of 59.9 (11.6) years. The idiopathic PD group included 8 individuals (5 males, 3 females) with a mean age of 59.9 (7.5) years and a mean disease duration of 1.63 (1.22) years. The *PRKN* mutation group included 7 individuals (4 males, 3 females) with a mean age 0f 46.7 (14.4) years and a mean disease duration of 8.67 (8.03) years. The subjects of this group were divided into two categories: heterozygous (n=4) and biallelic (n=3), comprising both compound heterozygous and homozygous carriers of *PRKN* variants, as shown in **Table 3.** No significant differences in age or sex distribution were observed between

the three groups (p>0,05). The chronological data of the study procedures are shown in **Table 4.**

Patient ID	Type	Age	Age onset
Γ634	iPD	48	45
Γ635	iPD	62	61
Γ636	iPD	46	45
Γ617	iPD	65	55
Γ618	iPD	67	66
Γ622	iPD	66	65
Γ606	iPD	56	54
Γ696	iPD	65	61
Γ505	PRKN	40	33
Γ640	PRKN	54	51
Γ144	PRKN	38	32
Γ550	PRKN	65	39
Γ388	PRKN	22	20
Γ496	PRKN	57	49
ΘΑ765	PRKN	51	43

Table 1: Age/ Age of onset of PD patients

iPD: idiopathic PD patients (blue colour)

PRKN: *PRKN*-related PD patients (red colour)

Characteristics	Controls (n=7)	PD (n=8)	PRKN (n=7)
Mean age (years)	59.9 (11.6)	59.9 (7.5)	46.7 (14.4)
Mean age of onset	-	56.5 (7.71)	38.29 (10.19)
Sex (M/F)	1/6	5/3	4/3
Disease duration (years)	-	1.63 (1.22)	8.67 (8.03)
PRKN mutations (Bial/Het)	-	-	3/4

Table 2: Demographic characteristics of study participants

M: male, F: female, Bial: biallelic, Het: heterozygous

2.1.6 Cell population selection

2.1.6.1. PBMCs

Peripheral Blood Mononuclear Cells (PBMCs) are a heterogenous group of immune cells isolated from blood, including lymphocytes (T cells, B cells, NK cella) and monocytes. They are widely used as a model system in research,

including studies on *PRKN* expression. Studying *PRKN* expression in PBMCs helps explore its role in systemic mitochondrial quality control and its potential link to immune function and neurodegenerative disorders like PD.

PBMCs are easily obtained from blood samples, making them accessible and non-invasive source for studying *PRKN* expression in a physiologically relevant system. PBMCs represent a “normal” cellular content, free for tumorigenic or neural-specific influences. This allows to compare *PRKN* expression in PBMCs with that in specialized cells like neuroblastoma or HEK cells, helping identify cell-type specific patterns of expression.

In PBMCs, *PRKN* may regulate mitochondrial turnover and function during immune activation or stress responses. Studies have linked *PRKN* dysfunction to inflammatory conditions and diseases like Parkinson’s Disease, where systemic immune dysfunction is implicated. PBMCs are also an excellent model for studying the regulation of *PRKN* in response to external stimuli such as: oxidative stress, inflammatory cytokines, mitochondrial toxins or inhibitors.

Dysregulated *PRKN* expression in PBMCs has been implicated in neurodegenerative diseases, like PD[161]. Monitoring *PRKN* expression in PBMCs can provide insights into its systemic effects beyond the central nervous system or cancer.

Limitations of PBMCs

1) Heterogeneity: PBMCs consist of multiple cell types, making it challenging to pinpoint *PRKN* expression to a specific cell population without further sorting
2) Low baseline Expression: *PRKN* may have lower baseline expression in PBMCs compared to neuroblastoma or HEK cells, requiring sensitive selection methods like RT-PCR
3) Limited Culture Lifespan: PBMCs are primary cells and do not proliferate indefinitely, unlike immortalized cell lines

2.1.6.2 Neuroblastoma cells

In purpose of exploring *PRKN* expression in a larger amount of cells, as levels of PBMCs in human blood vary and are influenced by diverse factors, we used also some samples of neuroblastoma cells of a recently produced cell culture in order to evaluate how *PRKN* expression levels are influenced by the cell number. Neuroblastoma cells are easy to culture and provide high RNA yields, which are essential for reliable RT-PCR experiments. Neuroblastoma cell lines, such as SH-SY5Y, are well characterized and widely used, while they also have the advantage of reproducibility. They are derived from neural crest tissues, where *PRKN* plays a critical role in regulating mitochondrial quality and survival[175]. They exhibit diverse levels of *PRKN* expression due to factors like oncogene amplification (e.g. N-myc) and epigenetic modifications, as well as they are particularly sensitive to mitochondrial dysfunction, making them an excellent model for studying the role of *PRKN* in mitophagy and mitochondrial dynamics[176]. Thus, neuroblastoma cells are a relevant and practical model for exploring *PRKN* expression using RT-PCR, given their link to neural tissue and mitochondrial function. These studies can provide insights into the regulation of *PRKN* and its role in distance contexts.

2.1.6.3 HEK cells

In order to further explore the *PRKN* mRNA expression levels in non-neuronal tissues, as well, we used samples of HEK293 cells.

HEK cells, especially HEK293 and derivatives are highly amenable to genetic manipulation. This makes them ideal for overexpressing or knocking down *PRKN*, testing regulatory elements of the *PRKN* promoter and studying mutants of *PRKN* linked to PD.

HEK cells are non-neuronal, providing a baseline to study *PRKN* expression and function outside of its typical neuronal or tumour environment. This allows to identify fundamental mechanisms of *PRKN* regulation, independent of cancer-specific or neural specific factors. HEK cells grow robustly and produce high-quality RNA, which is essential for sensitive and reproducible

RT-PCR studies. They are one of the most well-studied cell lines in biomedical research. Extensive knowledge about their genetics and biochemistry facilitates the interpretation of experimental results. They are often used for mitochondrial studies, where *PRKN* plays a critical role in mitophagy[177]. HEK cells can act as a control or reference in studies comparing *PRKN* expression in specialized cells, like neuroblastoma cells or PBMCs. The contrast helps identify cell-type specific expression patterns or regulatory mechanisms.

Compared to neuroblastoma cells that may have dysregulated *PRKN* due to cancer-specific alterations (e.g. oncogene amplification, epigenetic changes), HEK cells, being non-tumorigenic, provide a complementary system to study normal *PRKN* regulation.

2.1.7 Genetic testing

Screening for *PRKN* variants was undertaken in those PD patients with a high likelihood of a genetic underpinning, i.e suggestive family history, very early age of onset (<40 years old), or suggestive clinical history (early dystonia, predominant lower limb involvement). In total, using Multiplex Ligation-dependent Probe Amplification (MLPA), together with direct Sanger Sequencing of the PRKN gene or Whole Exome Sequencing (WES), PD-related *PRKN* variants were found in a number of patients, seven of whom were selected to be included in this study. Among these patients, 4 are carrying single heterozygous and 3 biallelic variants (**Table 3**). All included variants are considered pathogenic, according to ACMG criteria, except 2 of them, the variant exon6:c540delinsGC:Pv181Rfs*16 and the variant c401T>C which are considered of uncertain significance (**Table 3**). For the heterozygote carriers, long read sequencing was performed in order to identify potential trans genomic alterations in the *PRKN* gene. This led to the identification in one subject of a 540 bp deletion in exon 6 in one allele with additional insertion of GC bp. Because the 540bp deletion is not predicted to cause splicing alterations (splice AI), we have maintained this subject in the heterozygote category. None of the samples studied with long read

sequencing showed insertions in the PRKN gene. For some samples (Γ492, Γ505, Γ640), long read sequencing has not yet been completed, in order to confirm the previously identified *PRKN* mutations or potentially identify other genomic alterations. The samples with the genetic background of c101_102delAG;Exon 7 del (ΘΑ765), Exon 2 del (Γ144) and Exon 6: c540delinsGC:pV181Rfs*16 (Γ388) have already been tested in the previous study of our lab[161], while the samples with c401T>C variant (Γ492), c758G>A variant, exon 2 deletion (Γ505), c101_102delAG variant (Γ550) and c376C>T; exon 4 variant (Γ640) are being tested for the first time, which permits potentially to verify and extend our previous findings.

Patient ID	Mutation	Status	Clinical Significance	Protein
Γ550	**c.101_102delAG**	**Homozygous**	**Pathogenic**	**p.Gln34Argfs*5**
Γ640	c.376C>T (exon 4)	Heterozygous	Pathogenic/likely pathogenic	p.Arg126Trp
Γ144	Exon 2 del	Heterozygous	Pathogenic	-
Γ505	**c.758G>A, Exon 2 del**	**Compound Heterozygous**	**Pathogenic/likely pathogenic**	**p.Cys253Tyr**
Γ388	Exon 6: c540delinsGC:pV181Rfs*16	Heterozygous	Uncertain significance	p.V181Rfs*16
Γ492	c401T>C	Heterozygous	Uncertain significance	p.Leu.134Pro
ΘΑ765	**c101_102delAG;Exon 7 del**	**Compound Heterozygous**	**Pathogenic**	**p.Gln34fs**

Table 3: Type of mutation of *PRKN*-related PD patients and clinical significance (**biallelic mutations** are **in bold**)

2.1.8 *PRKN* Variant Detection

DNA was extracted from peripheral blood. All 12 exons of *PRKN* gene were analysed by Sanger Sequencing following PCR amplification of each exon and exon-introns boundaries. MLPA kit (P051 kit, MRC-Holland, Amsterdam, The Netherlands) was conducted to search for *PRKN* exon deletion or duplications.

WES was carried out in the Greek Genome Center (GGC) of the Biomedical research Foundation of the Academy of Athens (BRFAA). WES Libraries were

prepared with the Twist Library preparation EF 2.0 protocol and the Twist Comprehensive Exome Pane, according to manufacturer;s instructions. Quality of the libraries was verified with Agilent Bioanalyser DNA 1000 and HS chips and quantity with the qubit HS spectrophotometric method. WES libraries were sequenced in the Illumina NovaSeq 6000 sequencer. Bioinformatics analysis was performed using published algorithms including the Burrows-Wheeleraligner tool (BWA), SAM tools, and the Genome Analysis Toolkit (GATK). Sequencing reads were aligned to the GRCh37 (hg19).

2.1.8.1 Long read sequencing: This is a next generation DNA sequencing technology that generates reads significantly longer than those produced by traditional short-read sequencing methods. It provides greater insights into the structure and complexity of genomes, making it specifically valuable for studying repetitive regions, structural variants and epigenetic. All of our samples with identified *PRKN* mutations variants have undergone LRS. However, LRS has not yet been completed for some samples (Г492, Г505, Г640).

Key features of LRS:

1) Read length: LRS can produce reads ranging from several kilobases (kb) to over 100 kb in length
2) High resolution analysis: it excels in resolving repetitive regions, structural variants, and haplotype phasing, which are often missed by short-read technologies
3) Applications: used for de novo genome assembly, trascriptomics , metagenomics, and studyingcompex genomic rearrangements

- **Technologies for Long - Read Sequencing**

1) PacBio Pacific Bioscences) Single-Molecule-Real-Time (SMRT) Sequencing: produces reads averaging 10-15 kb, with some exceeding 100 kb. It uses a single molecule of DNA as a template. It provides high accuracy with “HiFi” reads (high-fidelity reads) and it is useful for detecting epigenetic modifications such as DNA methylation.

2) Oxford Nanopore Technologies (ONT): It can generate ultra-long reads, with some exceeding 2 Mb. It employs nanopores embedded in a membrane; DNA or RNA molecules are sequenced as they pass through the pore, disrupting an electrical current. It provides portable options like MinION which make it versatile for fieldwork.

- **Advantages of Long Read Sequencing:**

1) Improved Genome Assembly: resolves repetitive regions, telomeres and centromeres and enables de novo genome assembly with fewer gaps
2) Detection of Structural Variants: identifies large insertions, deletions, inversions, and translocations that short reads may miss.
3) Haplotype phasing: allows assignement of genetic variants to specific parental chromosomes
4) Analyses of Complex Regions: effective for regions with high GC content or other sequencing challenges
5) Epigenetic Studies: it can detect modifications like DNA methylation directly from the row sequencing data

- **Limitations of LRS:**

1) Higher error rates: compared to short-read sequencing, long read technologies can have higher error rates, though this has improved significantly with newer methods like PacBio HiFi
2) Cost: historically more expensive than short-read sequencing though costs are decreasing
3) Lower throughput: may produce fewer total bases compared to short-read sequencing

- **Applications of LRS:**

1) Human Genomics: characterizing structural variations and resolving compex genomic regions and applications in rare diseases research and cancer genomics

2) Microbial genomics: improved assembly of microbial genomes and analysis of metagenomics samples
3) Transcriptomics: full length RNA sequencing to characterize splice variants and isoforms
4) Plant and Animal Genomics: used for the assembly of large and complex genomes in plants and animals
5) DNA modifications and their roles in gene regulations

LRS was carried out in the NGS Competence Center in Tubingen. Genomic integrity was assessed using puls-field capillary electrophoresis with the Genomic DNA 165 kb Analysis Kit on a FemtoPulse (Agilent) instrument. Quanification of DNA was assessed using the dsDNA High Sensitivity assay on a Qubit 3 fluorometer (ThermoFischer) and purity was assessed by Nanodrop. A total of 2-4 µg of genomic DNA was sheared with Megaruptor 3 (Diagenode) from samples harbouring high-molecular weight. DNA fragments followed by a clean-uo with AMPure XP heads (Beckman Calter). Libraries were prepared with the ID Ligation SQK-LSK114-XL Sequencing kit (Oxford Nanopore Technologies). Each library was diluted to 15 fmol for loading on a single PromethION Bio flow cell. A nuclease flush was performed for re-loading library at 24hour after run start or when required.

2.1.8.2MLPA: Multiplex Ligation-dependent Probe Amplification is a molecular biology technique widely used for detecting copy number variations (CNVs) in DNA. It is a reliable, sensitive and efficient method often employed in genetic diagnostics and research . More specifically, MLPA is a technique designed to quantify DNA or RNA sequences, specifically identifying variations such as deletions, duplications or other abnormalities. It is commonly used for analyzing gene dosage and detecting mutations associated with genetic disorders

- **How MLPA works:**
  1) Sample preparation: DNA is extracted from cells or tissue to serve as the template

2) Probe Hybridization: Two synthetic oligonucleotide probes are designed to hybridize to adjacent regions on the target DNA sequence. Each probe has a unique sequence for target specificity and a universal binding site.
3) Ligation: When both probes bind correctly to the target DNA they are joined together by a DNA ligase enzyme, forming a complete probe.
4) Amplification (PCR):The ligated probes are amplified with Polymerase Chain Reaction (PCR). Each probe generates a product of specific size, which corresponds to a particular target sequence.
5) Analysis: The amplified products are separated by capillary electrophoresis and their relative intensities are measured. The intensity reflects the quantity of the target DNA sequence

- **Applications of MLPA:**
  1) Genetic Diagnostics: Detecting chromosomal abnormalities like deletions and duplications / screening for hereditary cancers (e.g. mutation in BRCA1/BRCA2)
  2) Cancer research: identifying copy number changes in oncogene or tumor suppressor genes
  3) Prenatal and postnatal testing: diagnosing genetic syndromes such as Down syndrome or Di George syndrome
  4) Neurological disorders: detecting mutations associated with diseases like spinal muscular atrophy (SMA)

Advantages of MLPA:

- High specificity and sensitivity
- Ability to analyze up to 50 targets in a single reaction
- Cost effective compared to other methods like array-CGH or Next Generation Sequencing for CNV analysis

Limitations of MLPA:

- It requires prior knowledge of the target sequence to design probes
- It is not ideal for detecting point mutations unless combined with other methods

2.1.8.3 Sanger sequencing: Also known as the dideoxy chain – terminations method, is a DNA sequencing technique developed by Frederick Sanger and colleagues in 1977. It was the first widely used method for sequencing DNA and remains a gold standard for high-accuracy sequencing of short DNA fragments. It relies in the incorporations of chain-terminating nucleotides (dideoxynucleotides, ddNTPS) during DNA synthesis. These ddNTPs lack the 3'-OH group required for forming a phosphodiester bond, leading to termination of DNA extension when incorporated

- **Steps:**
  1) Template Preparation: The DNA to be sequenced (template) is isolated and prepared. A single-stranded DNA template is ideal for the process.
  2) Reaction set-up: The sequencing reaction mixture includes: DNA template, a single primer complementary to the template, DNA polymerase, Deoxynuclotides (dNTPs: A, T, G,C) for elongation , Fluorecently or radioactively labeled dideoxynucleotides (ddNTPs)
  3) DNA synthesis and Chain termination: DNA polymerase extends the primer by adding dNTPs complementary to the template strand. Occasionally, a ddNTP is incorporated instead of a dNTP, terminating the chain
  4) Separation by size: the resulting DNA fragments of varying lengths are separated by size using capillary electrophoresis or gel electrophoresis
  5) Detection: fluorescent labels on the ddNTPs are detected by a laser during electrophoresis. Each ddNTP emits a different color corresponding to its base (A,T,G,or C)

6) Data Interpretation: The sequence of DNA is determined by analyzing the order of fluorescent signals, which corresponds to the terminated fragments

- **Applications of Sanger Sequencing:**

1) Validation of Next –Generation Sequencing Results: used to confirm variants detected by next-generation sequencing (NGS)
2) Targeted Sequencing: sequencing single genes or small genomic regions, such as in genetic testing or studying mutations
3) Small-scale Projects: ideal for sequencing plasmids, PCR products and individual clones
4) Clinical Diagnostics: used to detect specific mutations associated with diseases

- **Advantages of Sanger Sequencing:**

1) High accuracy: provides very accurate base-by-base information, especially for short sequences
2) Reliable: suitable for sequencing individual genes or small regions
3) Established technique: decades of use and optimization make it a trusted method

- **Limitations of Sanger Sequencing:**

1) Low throughput: can only sequence one DNA fragment at a time, making it inefficient for large-scale projects
2) Cost: More expensive and slower compared to high – output NGS technologies
3) Read lengths: Maximum read length is typically about 500-1000 base pairs

2.1.8.4 Whole Exome Sequencing: is a genomic technique that focuses on sequencing the exome, which consists of all the protein-coding regions of the

genome. These regions make up about 1-2% of the human genome but are responsible for the majority of known diseases.

- **Key features of WES:**

1) Target : WES sequences only the exons, which are the coding regions of genes
2) Size: the human exome comprises approximately 20.000 genes, spanning about 30 million base pairs
3) Purpose: it identifies genetic variants (e.g. single nucleotide variants, insertions, deletions) in protein-coding regions to help diagnose diseases, especially rare genetic disorders

- **Steps:**

1) DNA extraction: DNA is extracted from a sample, such as blood or saliva
2) Library preparation: The DNA is fragmented into smaller pieces and adapters are added for sequencing
3) Exome enrichement: Specialized probes (capture probes or baits) are used to hybridize and isolate exonic regions from the entire genome
4) Sequencing: The enriched DNA is sequenced using high-throughput sequencing technologies (e.g. illuming platforms)
5) Data Analysis: Sequencing reads are aligned to a reference genome. Variants are called and annotated to identify mutations, which are then evaluated for their clinical significance

- **Applications of WES:**

1) Rare Disease Diagnosis: Identifies mutations causing Mendelian disorders. Detects pathogenic variants in diseases with unknown etiology
2) Cancer genomics: Analyzes mutations in cancer-related genes to guide personalized therapy
3) Pharmacogenomics: Explores genetic variants affecting drug response
4) Prenatal and Pediatric Testing: Identifies genetic conditions in fetuses or children with unexplained developmental disorders

5) Research: Used to discover novel disease-related genes and understand genotype-phenotype correlations

- **Advantages of WES:**

1) Efficiency: By focusing on coding regions, WES provides a cost-effective alternative to Whole Genome Sequencing (WGS)
2) Clinical Relevance: captures most mutations with direct links to diseases since most known pathogenic variants are in exons
3) Comprehensive Analysis: Covers all protein-coding genes, while targeted panels are limited to a subset of genes

- **Limitations of WES:**

1) Misses Non-Coding Variants: non-coding regions (introns, regulatory elements) are excluded, even though they may influence gene function or disease
2) Incomplete Coverage: Some exons may be poorly captured or sequenced due to technical limitations
3) Interpretations Challenges: Identifies many variants of uncertain significance (VUS), making it challenging to determine their clinical impact
4) Structural Variants: large insertions, deletions and rearrangements are difficult to detect with whole genome sequencing

2.2 Study Procedures : The chronological data with the study procedures are shown in **Table 4 .**

Samples	Type	Age	Sex	PRKN mutation	Blood collection	PBMCs collection	RNA extraction	CDNA synthesis	RT-PCR
Г641	CT	48	F	-	04.04.23	05.04.23	25.09.24	25.09.24	26.09.24
Г683	CT	61	F	-	05.12.23	06.12.23	12.09.24	12.09.24	13.09.24
Г590	CT	66	F	-	24.05.22	25.05.22	02.10.24	02.10.24	03.10.24
Г594	CT	49	F	-	07.06.22	08.06.22	02.10.24	02.10.24	03.10.24
Г595	CT	73	F	-	16.06.22	17.06.22	02.10.24	02.10.24	03.10.24
Г564	CT	74	M	-	15.02.22	16.02.22	02.10.24	02.10.24	03.10.24
Г576	CT	48	F	-	12.04.22	13.04.22	02.10.24	02.10.24	03.10.24
Г634	PD	48	M	-	28.02.23	29.02.23	15.09.24	15.09.24	26.09.24
Г635	PD	62	M	-	07.03.23	08.03.23	25.09.24	25.09.24	26.09.24
Г636	PD	50	F	-	07.03.23	08.03.23	25.09.24	25.09.24	26.09.24
Г617	PD	65	M	-	22.11.22	23.11.23	02.10.24	02.10.24	03.10.24
Г618	PD	67	M	-	22.11.22	23.11.23	02.10.24	02.10.24	03.10.24
Г622	PD	66	F	-	13.12.22	14.12.23	02.10.24	02.10.24	03.10.24
Г606	PD	56	F	-	04.10.22	05.10.22	02.10.24	02.10.24	03.10.24
Г696	PD	65	M	-	26.03.24	27.03.24	02.10.24	02.10.24	03.10.24
Г505	PRKN	40	M	+	28.05.21	29.05.21	25.09.24	25.09.24	26.09.24
Г640	PRKN	54	M	+	04.04.23	05.04.23	25.09.24	25.09.24	26.09.24
Г144	PRKN	38	M	+	07.09.18	08.09.18	02.10.24	02.10.24	03.10.24
Г550	PRKN	65	M	+	09.11.21	10.11.21	02.10.24	02.10.24	03.10.24
Г388	PRKN	22	F	+	19.11.19	20.11.19	02.10.24	02.10.24	03.10.24
Г492	PRKN	57	F	+	13.04.21	14.04.21	02.10.24	02.10.24	03.10.24
ΘА765	PRKN	51	F	+	16.06.16	17.06.16	02.10.24	02.10.24	03.10.24

Table 4: Chronological dates of study procedures

2.2.1 Isolation of Peripheral Blood Mononuclear Cells (PBMCs)

Peripheral blood (8-10 ml) was collected from each subject using EDTA-coated or Li-heparin – coated tubes. The blood samples were processed within 2-24 hours of collection for the isolation of PBMCs. Biocoll Separating Solution (Biochrom AG) density gradient centrifugation was used to isolate PBMCs.

PBMCs isolation Procedure:

1) Dilution: Whole blood was diluted in an equal volume of phosphate – buffered saline (PBS)
2) Layering: Diluted blood was gently layered over 3 ml of Biocoll Separating Solution in a 15 ml conical tube
3) Centrifugation; Tubes were centrifuged at 500g for 30 minutes at 4^{o}C

4) PBMCs layer collection: The PBMC layer, located at the plasma-Ficoll interface was carefully collected
5) Washing: PBMCs were washed with PBS (centrifugion at 500g for 30 minutess) to remove remaining platelets and Ficoll
6) PBMCs resuspention: The PBMCs pellet was resuspended in a small volume of PBS (1ml) to ensure an even cell suspension before the 1st and 2nd washing so as to measure the PBMCs number

PBMCs number measurement

To measure the concentration and viability of PBMCs, an hemocytometer with a viability stain like trypan blue was used

Materials needed: PBMCs suspension, Trypan blue solution (0,4%), hemocytometer , microscope

Procedure:

1) Cell dilution with Trypan Blue: 10µL of the PBMCs suspension was mixed with 10µL of trypan blue (1:1 ration) to stain the cells. Trypan blue stains dead cells, which appear blue, while live cells remain unstained
2) Hematocytometer loading: A small amount (10Ml) of the stained cell mixture was placed onto the hemocytometer, carefully loading it under the cover slip
3) Cell counting; Under a microsope, the unstained (live) cells and the blue-stained (dead) cells were counted in the four corner squares of the hemocytometer grid
4) Concentration and Viability concentration: The total count was multiolied by the dilution factor and the hemocytometer factor (10^4) to get the number of cells per ml. The cell viability was calculated as follows:

Viability (%)= (number of live cells/ total cells (live+ dead)] x 100

Freezing and PBMC storage

For optimal cryopreservation of PBMCs, we used a freezing solution that includes Dimethyl Sulfoxide (DMSO) , Fetal Bovine Serum (FBS) and Rosewell Park Memorial Institute (RPMI), with a procedure as follows:

1) Freezing Solution Preparation: 10% DMSO, 40 % FBS, 50 % RPMI-1640 medium was mixed and the freezing solution was kept on ice to minimize cell stress during preparation
2) Pellet collection: the PBMCs were centrifuged (as above) and the supernatant was carefully removed, leaving a cell pellet
3) PBMCs' resuspension in Freezing Solution: the PBMCs pellet was gently resuspended in the cold DMSO/FBS/RPMI solution at a concentration of approximately 2 millions cells per ml. This medium was gently mixed with a pipette to ensure even distribution of cells.
4) Aliquots and Freezing : The cell suspension was transferred to labeled cryovials, ensuring each vial is properly marked with sample information and date. The vials were placed in a freezing container for gradual cooling. The ideal rate is -1^{o} C per minute until reaching -80^{o}C.
5) Storage: Once frozen, the vials were transferred to a -80^{o}C freezer for medium-term storage. For long term storage (longer than 6 months), the vials are ideally transferred to liquid nitrogen

This combination of DMSO, FBS, RPMI helps maintain cell viability and RNA integrity for future analyses and downstream applications like RNA extraction

DMSO (Dimethyl Sulfoxide): is a polar solvent often used as a crypotent to prevent the formation of ice crystals during cell freezing, which can damage cell membranes and lead to cell death

FBS (Fetal Bovine Serum): is a nutrient-rich supplement derived from the blood of fetal cows, containing growth factors, hormones, proteins, vitamins that support cell growth and maintenance in culture

RPMI (Rosewell Park Memorial Institute) Medium: RPMI-1640 is a commonly used cell culture medium formulated to support the growth of

various cell types, especially human immune cells like lymphocytes. It contains essential nutrients, vitamins, aminoacids and a buffering system to maintain physiological PH . RPMI can be included in freezing solutions as a base medium, typically mixed with FBS and DMSO, to provide a balanced environment that supports cell viability during freezing and subsequent procedures.

PBS (Phosphate Buffered Saline): is a balanced salt solution commonly used in biological research. It typically contains sodium chloride (Nacl), potassium chloride (KCL) and sodium phosphate, creating an isotonic solution with a pH similar to that of the human body (around Ph=7,4). This helps maintaining a stable pH, which is crucial for many biological reactions and cell integrity. Thus, it can also be used for isotonic environment, cell washing and maintenance and sample dilution.

Bicoll Separating Solution: is a density gradient medium used for isolating specific cell types, particularly mononuclear cell (such as lymphocytes and monocytes) from blood and other biological samples. It is commonly employed in immunology, cell biology and clinical research, especially for isolating PBMCs from whole blood. Bicoll typically has a density of around 1.077 g/ml, ideal for separating mononuclear cells from red blood cells and granulocytes. It contains substances like polysaccharides and sodium diatrizoate (a type of contrast agent), which create a density gradient to allow for cell separation by centrifugion.

2.2.2 RNA Extraction and Quantification /Qualification

Total RNA was extracted from the isolated PBMCs, using the TRIzol Reagent (Ambion), according to the manufacturer's protocol as follows:

1) Homogenization: PBMCs were homogenized in 1 ml of TRIzol reagent. Then, the samples were centrifuged at 12.000 g for 10 minutes at 4^{o}C. The resulting pellet contains extracellular membranes, polysacharides, and high molecular weight DNA, while the supernatant contains RNA. The clear homogenate solution was transferred to a fresh tube and proceeded to the next step.

2) Phase separation: The homogenized samples were incubated for 5 minutes at 15-30^{o}C. Chloroform (o,2ml per 1 ml of TRIzol reagent) was added.Sample tubes were capped securely. Tubes were shaked vigorously by hand for 15 seconds and incubated at 15-30^{o}C for 2-3 minutes. The samples were then centrifuged at 12.000 g for 15 minutes at 4^{o}C. Following centrifugation, the mixture separates into a lower red, phenol-chloroform phase, an interphase, and a colorless upper aqueous phase. (RNA remains exclusively in the aqueous phase)
3) RNA precipitation: The aqueous phase was transferred to a fresh tube and organic phase was saved if isolation of DNA or protein is desired. The RNA from the aqueous phase was precipitated by mixing with isopropyl alcohol (0,5 ml of isopropyl alcohol per 1 ml of TRIzol reagent). The samples were incubated at -20^{0}C for 2-24 hours and then centrifuged at 12.000 g for 15 minutes at 4^{o}C (The RNA precipitate, often visible before centrifugation, forms a gel-like pellet on the side and bottom of the tube)
4) RNA wash: The supernatant was removed and the RNA pellet was washed once with 75% ethanol (adding at least 1 ml of 75% ethanol per 1 ml of TRIzol reagent used for the initial homogenization). The samples were mixed by vortexing and centrifuged at 7.500 g for 5 minutes at 4^{o}C.
5) Redisolving the RNA: The RNA pellet was briefly air-dried and dissolved in RNase free water (20Ml) and the samples were incubated for 10 minutes at 55-60^{o}C. Then, the samples were stored at -80^{o}C.

RNA quality and concentration were measured using a NanoDrop spectrophotometer (Thermo Fisher Scientific, USA). Samples with an A260/280 ratio between 1.8 and 2.0 were considered acceptable for downstream applications.

NanoDrop Spectophotometry: In NanoDrop Spectophotometry , the A260/280 and A260/230 ratios are used to assess the purity of nucleic acid samples, typically DNA and RNA. These ratios provide insight into possible contamination by proteins, phenols or other substances that may affect downstream applications.

1) A260/280 Ratio: The A260/280 ration measures absorbance at 260 nm and 280nm. Nucleic acids absorb UV light most strongly at 260 nm, while proteins (specifically the amino acids tryptophan and tyrosine) absorb most strongly at 280nm.This ratio, therefore, gives an indication of protein contamination in a nucleic acid sample.

Expected values:

- Pure RNA samples typically show an A260/280 ration around 2.0
- Pure DNA samples usually have an A260/280 ratio of about 1.8
- Lower ratios (<1.8 fro DNA and <2.0 for RNA) suggest possible protein contamination or the presence of other contaminants that absorb at 280nm

2) A260/230 ratio: measures absorbance at 260nm and 230 nm wavelengths. While nucleic acids absorb at 260nm, many contaminants, such as phenol, carbohydrates, guanidine, and other organic compounds used in extraction, absorb more strongly at 230 nm. The A260/230 ratio is therefore used to detect these types of contaminants.

Expected values:

- Pure bucolic acid samples generally have an A260/230 ratio of 2.0-2.2
- Lower ratios (<2.0) indicate contamination by substances that absorb at 230nm, such as phenols or guanidine compounds, which are common in certain extraction buffers.

The corrected RNA values in NanoDrop machine refers to RNA concentration readings adjusted to account for the contribution of contaminating substances such as DNA, proteins and other impurities that can absorb at wavelengths similar to RNA. The NanoDrop spectrophotometer uses UV absorbance at specific wavelengths to estimate RNA purity and concentrations.

This correction works as following;

1) Absorbance Measurement: The NanoDrop measures absorbance at several wavelengths:
    - 260 nm: Absorbance of nucleic acids (RNA/DNA)
    - 280nm: Absorbance of proteins, mainly aromatic amino acids
    - 230nm: Absorbance of other contaminants like phenol, guanidine, or other organic compounds.

2) Correction for Contaminants: Contaminants such as proteins or chemicals can show the RNA concentration by contributing absorbance at 260nm . To correct for the contributions, the NanoDrop applies an algorithm: (Corrected RNA Concentration= A_{260} – (f x A_{280}) – (g x A_{230})
    - A_{260}:Raw absorbance at 260 nm
    - A_{280}: Contribution from proteins
    - A_{230}: Contribution from organic contaminants
    - F and G: Empirical factors used to adjust for overlapping absorbance contributions

3) Purity Ratios: The NanoDrop reports purity ratios to help evaluate sample quality:
    - 260/280 Ratio: Ideal for RNA is 2.0 . Lower values indicate protein contamination
    - 260/230 Ratio: Ideal for RNA is 2.0-2.2. Lower values suggest contamination form organic compounds of salts.

4) RNA –specific Analysis:
    - For accurate RNA measurements, DNA contaminant must be minimized (e.g. using DNase treatment, as we did), because DNA absorbs similarly to RNA at 260nm
    - The corrected RNA value helps eliminate overestimations caused by these contaminants

By using corrected RNA values we can obtain more reliable RNA concentration and purity measurements, leading to better downstream experimental results.

Also, the RNA quality was estimated using Agarose Gel Electrophoresis in order to assess RNA integrity and detect any degradation, as follows:

1) Agarose gel preparation:
   - 1,5% agarose powder was weighted out and dissolved in 1x TAE buffer by heating
   - The gel was allowed to cool slightly (around 50-60^{o}C) and RNA stain (5μL ethidium bromide) was added as per the manufacturer's instructions
   - The agarose solution was poured into a gel casting tray with a comb to create wells and allowed to solidify (15-20 minutes)

2) RNA sample preparation:
   - 0,5 μg of RNA was used for each sample and mixed with equal volume of RNA loading dye that contains a denaturating agent like formamide to ensure linear migration and prevent secondary structures

3) Gel loading:
   - The gel was placed in the electrophoresis chamber and filled with 1x TAE buffer
   - RNA ladder and RNA samples were carefully loaded into the wells

4) Gel Running:
   - The gel run at a voltage of 80 V for around 10-30 minutes, or until the dye front has migrated an appropriate distance down the gel

5) Gel visualization:
   - UV or blue light transilluminator was used to visualize the RNA bands

For high-quality RNA we should see two distinct bands: 28s rRNA (around 4.5 kb) band, which should be approximately twice as intense as the 18s rRNA (around 1.9 kb) band.

If smearing or faint rRNA bands are observed, particularly below the 18s position, this indicates RNA degradation

2.2.3 Reverse Transcription Procedure

- **DNase Treatment:** This step is used for the amount of RNA to be used for cDNA synthesis (usually 1.5-2.0 μg) and increases the yield. The reaction takes place in 11μl total volume, in an eppendorf with the following reagents:
  - RNA= 1.5-2.0 μg
  - RQ1 10x buffer= 1μl
  - RQ1 DNase= 1U/μg
  - DEPCpH2O= up to 11 μl

- The samples were incubated for 30 minutes at 37ºC
- 1μl DNase Stop Solution was added and the samples were incubated for 10 min at 65^0C (total final volume 12 μl)
- The samples were kept on ice

- **cDNA synthesis:**

- 1μl oligodTs or random primers/sample was added and the samples were incubated for 5 minutes at 70º C. Then the samples were kept on ice
- Master Mix for cDNA synthesis preparation: In an eppendorf tube, the following reagents were added, by adding first the RT buffer and the dNTPs and at the last minute the Rnase OUT and the Reverse Transcriptase enzyme (M-MLV RT)

- RT buffer 5x= 5μl
- dNTPs (10mM)=5μl
- RNase OUT=1μL

- M-MLV RT (200U)= 1μl

- 12 μl of Master Mix/sample was added and incubated for 60 min at 37^{o}C (total volume=25μl/sample). We also used a sample without adding M-MLV RT, in order to check possible contamination or other determinants
- cDNA samples were stored at -20^{o}C

2.2.4 PCR for *GAPDH* gene

In order to verify the quality of cDNA synthesis we used a simple PCR protocol for the *GAPDH* gene, which is a housekeeping gene and is used as a reference gene for normalization in gene expression studies.

Materials needed:

- cDNA samples (and sample without RT) =1μl /sample
- PCR primers specific to GAPDH (forward 10μM)= 1μl/sample
- PCR primers specific to GAPDH (reverse 10Mμ)= 1μl/sample
- dNTPs=1μL/sample
- Taq buffer=2μl/sample
- Taq polymerase=0.2 μl/ sample
- Nuclease-free water= 13.8 μl/ sample
- Thermal cycler

PCR Reaction Mix preparation: a reaction volume (20μl/ sample) was prepared by combining the above components. All components were gently mixed by pipetting up and down or vortexing briefly.

PCR Thermal Cycling Conditions set-up : The prepared reaction tubes were placed in the thermal cycler with the following conditions:

Step	Temperature	Time	Cycles
Initial Denaturation	95°C	2 minutes	1
Denaturation	95 °C	30 seconds	
Annealing	55-60 °C	30 seconds	30-40
Extension	72 °C	30 seconds	
Final extension	72 °C	5-10 minutes	1

PCR Running: The reaction takes approximately 1.5-2 hours

Gel Electrophoresis:

- After PCR, we perform electrophoresis on an agarose gel (1.5% agarose) to confirm the presence and size of the PCR product
- PCR samples were mixed with 4 µl DNA dye
- From each sample mix 20µl/sample was loaded along with a DNA ladder for reference
- Expected band size for *GAPDH:* around 110 bp (varying between 100-250 bp, depending on the primer pair used)

Visualization and Documentation

- A UV transilluminator was used to view and capture the gel image
- The presence of a clear, single band at the expected size indicated successful amplification

2.3.5 Quantitative Real Time PCR (qRT–PCR)

Quantitative Real Time PCR (qRT–PCR) was performed using the SYBR Green Master Mix (Thermo Fisher-Scientific) on a ABI Prism 7000 Sequence Detection System (Applied Biosystems) to measure the expression of the *PRKN* gene and the *GAPDH* gene, used as an internal control

The primers used had the following sequences:

- GAPDH forward primer: 5'- CCT CTG ACT TCA ACA GCG ACA C-3'
- GAPDH reverse primer: 5'- AGC CAA ATT GGT TGT CAT ACC AG-3'

- PRKN forward primer: 5’ - AAA ACC ACC AAG CCC TGT C-3’
- PRKN reverse primer: 5’ TGC GGA CAC TTC ATG TGC- 3’

qRT –PCR Protocol:

- 1:10 dilution of cDNA samples in RNase free water
- 3 μl of 1:10 diluted RT cDNA product/well was added in a qPCR plate (duplicates/sample) along with 3 μl of 1:10 diluted no RT samples and 3μL of RNase-free water (no-template controls-NTCs, to ensure the absence of contaminants)
- Master Mix’s preparation in an eppendorf tube (one per gene of interest) as follows:

- Forward primer= 0.6 μl/sample
- Reverse primer=0.6μl/sample
- SYBR Green=10μl/sample
- RNase –free water= up to 17μl/sample

- 17 μl /sample of each Master Mix was added in the qPCR plate.

qRT –PCR Running:qRT –PCR was running in the following conditions:

- 50^{o}C for 2 min
- 95^{o} C for 10 min
- 50 cycles of : 95^{o}C for 15 seconds and 60^{o}C for 60 seconds

A melting curve analysis was performed at the end of each run to confirm the specificity of the amplification process

Samples with Ct_{GAPDH} >25 were excluded from the following analysis , as no corresponding to the *GAPDH* expected according literature

Cq values

The Cq (Quantification Cycle), also known as Ct (Cycle Threshold), is a critical value in RT-PCR results. It represents the cycle number at which the

fluorescent signal of the target amplification crosses a set threshold, indicating detectable levels of the target nucleic acid.

During RT-PCR, fluorescence increases as the target nucleic acid is amplified. The threshold is set above the baseline fluorescence (background noise). The Cq value corresponds to the cycle number at which the amplification first surpasses this threshold, signaling the presence of the target.

Interpretation of Cq:

- Lower Cq values: Indicates a higher concentration of the target nucleic acid. The fluorescence reaches the threshold quickly because there was more template to amplify
- Higher Cq values: Suggests a lower initial concentration of the target, requiring more cycles to reach the threshold. If no Cq value is observed the target may be absent or below the detection limit.

Absolute and Relative Quantification:

- In **absolute quantification**, Cq values are compared to a standard curve of known concentrations to determine the exact amount of the target nucleic acid
- In **relative quantification**, changes in Cq values are compared between samples (e.g. treated VS untreated) to assess relative expression levels, often normalized to a reference gene.

Factors affecting Cq values:

- Efficiency of amplification: High-quality primers, optimized reagents, and reaction conditions ensure consistent amplification
- Sample quality: RNA integrity, absence of inhibition, and proper reverse transcription impact Cq
- Instrument sensitivity: Variations in machine sensitivity and calibration can influence results.

Application of Cq in RT-PCR:

- Gene expression analysis
- Quantifying viral or bacterial load in clinical diagnostics
- Detecting mutations or specific gene variants

2.3 Melting Curve Analysis (RT-PCR)

In RT-PCR, the melting curve analysis is used to assess the specificity of the amplified product. It provides insight into whether the amplification has produced the desired target amplicon or if non-specific products or primer dimers have been generated, which could interfere with accurate quantification

- **How melting curve analysis works:**

  1) Post-amplification heating: After the PCR amplification cycles are completed, the instrument gradually increases the temperature

  2) Fluorescence Monitoring: As the temperature rises, the double-stranded DNA (dsDNA) products start to denature, becoming single-stranded DNA. The instrument monitors fluorescence changes using a dye (like SYBR-Green) that binds specifically to dsDNA

  3) Melting Temperature (Tm): Each product has a characteristic melting temperature (Tm), the point at which 50% of the dsDNA has melted into single strands. This Tm is observed as a peak on the meting curve, representing the temperature where the largest decrease in fluorescence occurs.

- Interpreting the melting curve:
  1) Single peak: A single peak at the expected Tm indicates that the PCR has produced a specific, single product (i.e. the target amplicon). This is ideal.
  2) Multiple peaks: Multiple peaks suggest that non-specific products or primers-dimers are present in the sample. Non-specific products usually have different Tm values from the target amplicon

3) Low Tm Peaks: Peaks at a lower Tm than the target typically indicate primer-dimers or smaller non-specific products

- Importance of Melting Curve Analysis:
  1) Validation of Specificty: Ensures that only the target DNA was amplified, which is crucial for the accuracy of gene expression or quantification analyses
  2) Quality control: Helps identify reactions where primers may be binding to unintended targets or where reaction conditions need optimization

2.4 Data Normalization and Expression Analysis

The relative expression levels of the *PRKN* gene were calculated using the comparative Ct method ($2^{-\Delta\Delta CT}$). The expression of *GAPDH* was used as the internal control to normalize the data. The formula used for each sample was:

- $\Delta Ct = Ct_{PRKN} - Ct_{GAPDH}$
- $\Delta\Delta Ct = \Delta Ct_{sample} - \Delta Ct_{control\ group}$
- Fold change= $2^{-\Delta\Delta Ct}$

-The **ΔCt method** normalizes the expression of a target gene to a reference (housekeeping) gene to correct for sample variations. A smaller ΔCt means higher relative expression of the target gene.

-The **ΔΔCt method** is used to compare gene expression between two conditions (e.g. PRKN- carriers and iPD)

-**Fold change** ($2^{-\Delta\Delta Ct}$) quantifies upregulation or downregulation

- If fold change >1, the target gene is upregulated
- If fold change <1, the target gene is downregulated
- If fold change =1, there is no significant change in expression

2.5 Statistical Analysis

Statisitcal analysis was performed using GraphPad Prism9.0 (GraphPad Software).

All data underwent a normality test (Shapiro-Wilk) and were found to be non-normally distributed, except of the comparison between biallelic and heterozygous *PRKN*-PD carriers. The significance of the presence of differences between mean *PRKN* levels in the different groups (controls, iPD, PRKN-carriers) was assessed with Kruskal-Wallis Test (a non-parametric test for comparing more than two groups). Pairwise post-hoc comparisons were performed using Dunn's Test to identify significant differences between groups. Comparisons between biallelic and heterozygous *PRKN*-carriers were done using Welch's Test. A p-value <0.05 was considered statistically significant.

An outlier sample with $Ct_{PRKN}=24$ was excluded from the analysis using Grubb's Test (p-value<0.001). This was a sample in the control group whose levels were measured at more than an order of magnitude higher compared to the highest levels observed in any other sample in this group.

We also performed statistical analysis for differences in sex (Fisher's Exact Test) and differences in age (Kruskal-Wallis, $p>0.05$) between groups.

Receiver Operating Characteristic (ROC) Curve analysis was used to assess the diagnositic value of the different models with Youden's Index to estimate the most appropriate cut-off values (with the optimal combination of sensitivity and specificity)

3. Results

Overall 60 samples (27 controls, 20 idiopathic PD patients, 8 PRKN-related PD patients and 3 samples of neuroblastoma cells and 1 sample of HEK cells) were double-analyzed (before and after adjustements in our methods and protocols) after their PBMCs isolation, following the methods of RNA extraction, RNA Quantification/Qualification, cDNA synthesis, PCR for *GAPDH* and RT-PCR. Of total, 37 samples were rejected from downstream analysis, due to either low RNA quality/quantity, low cDNA quantity/quality (from PCR results for *GAPDH* gene) or not applicable RT-PCR results (due to no quantification or no specificity of the melting curve).

In order to overcome the problem of either low RNA quality/quantity , or low cDNA quantity/quality, we also used as samples some neuroblastoma cells of about 2 $x10^6$ cells/sample [NBA30G, NB(1), NB(2)] and some HEK293 cells, where there is a greater number of cells/sample than human PBMCs and thus it could reproduce better RNA and cDNA quantity and quality, in order to verify our findings. While this was true , as we had a good amount and quality of RNA/cDNA , we did not have such a good quality in the melting curves of *PRKN* primer used in RT-PCR. The *PRKN* primer pair used in these procedures was the following:

- Forward: 5'- AGGATTACCCAGGAGGAGACCGC-3' and
- Reverse: 5'- ATCATGGTCACTGGGTAGGTG -3'

In this case, we decided to try another pair of *PRKN* primer which was the following (described above);

- PRKN forward primer: 5' - AAA ACC ACC AAG CCC TGT C-3'
- PRKN reverse primer: 5' TGC GGA CAC TTC ATG TGC- 3'

The aforementioned primer pair produced better meting curves in the subsequent trial of RT-PCR and so the human samples prepared with this type of *PRKN* primer pair were used in the subsequent analysis.

1 sample of the control group, despite undergoing downstream analysis, was excluded in the following statistical analysis as an outlier (Grubb's test, p-value<0,001)

The results of NanoDrop RNA quantification / qualification (**Table 5**), RNA electrophoresis (**Images 1,2,3**) , PCR (*GAPDH*) electrophoresis (**Images 4,5,6,7**) and RT-PCR (**Table 6**) are shown below:

3.1 NANODROP RNA QUANTIFICATION/QUALIFICATION

Samples	RNA (ng/μl)	cRNA (ng/μl)	A260/280	A260/230
Γ641	414.9	-	1.99	1.05
Γ683	210.1	178.5	1.89	1.24
Γ590	323.2	293.1	1.95	1.25
Γ594	310.5	280.4	1.98	1.08
Γ595	302.6	225.7	1.97	1.78
Γ564	250.2	235.7	1.89	1.19
Γ576	266.2	235.8	1.88	1.21
Γ634	299.2	263.2	1.92	1.06
Γ635	227.4	328.7	1.95	1.27
Γ636	183.2	227.4	1.91	1.32
Γ617	183.2	170.5	1.90	1.25
Γ618	208	200	1.93	1.26
Γ622	198.7	189.2	1.88	1.13
Γ606	230.3	221.8	1.90	1.25
Γ696	315.6	-	1.95	1.70
Γ505	183.7	159.6	1.90	0.95
Γ640	779.5	707	1.95	1.08
Γ144	248.3	230.2	1.92	1.22
Γ550	357.8	305.2	1.87	1.16
Γ388	224.3	200.8	1.84	1.21
Γ492	237.8	221.4	1.93	1.23
ΘΑ765	115.8	100.3	1.85	1.13
HB32	233.6	233.6	1.73	2.14
NBA30G	4612.1	4612.1	2.08	2.21
NB (1)	518.4	518.4	1.98	1.6
NB (2)	704.6	704.6	2.01	1.23
HEK293	69.6	69.6	1,77	0.83

Table 5: NanoDrop results of RNA quantification/qualification

3.2. RNA EXTRACTION/ELECTROPHORESIS

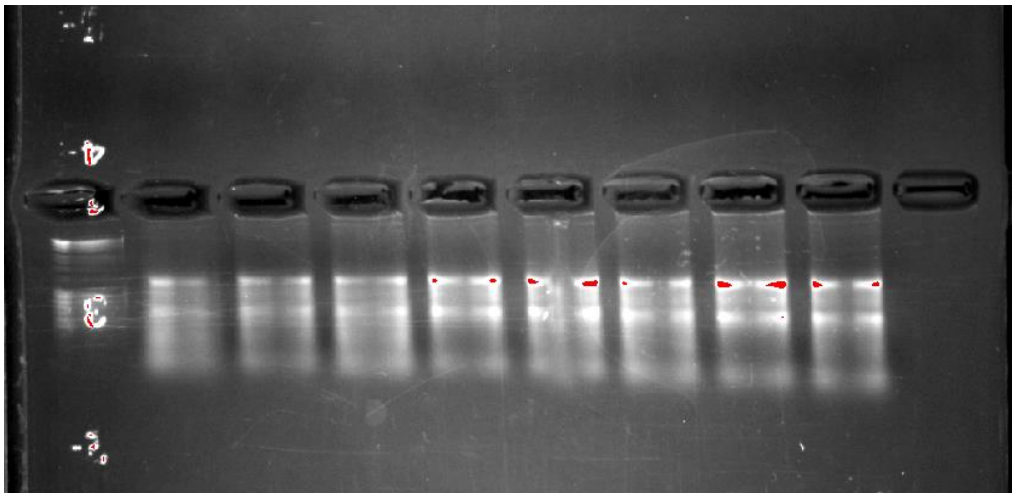

Image1: Sample series: Г641, Г611, Г683, Г634, Г635, Г636, Г505, Г640

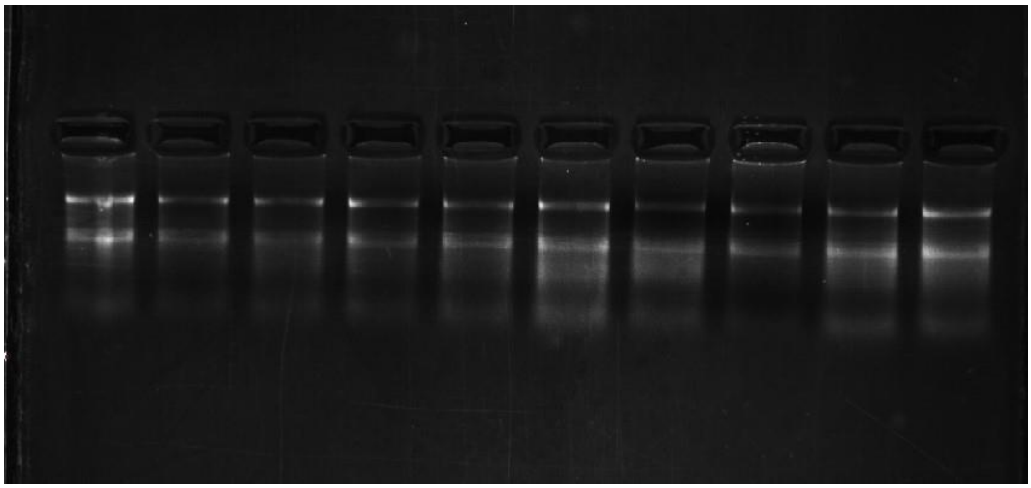

Image 2: Sampleseries: Г590, Г594, Г595, Г564, Г576, Г617, Г618, Г622, Г606, Г696

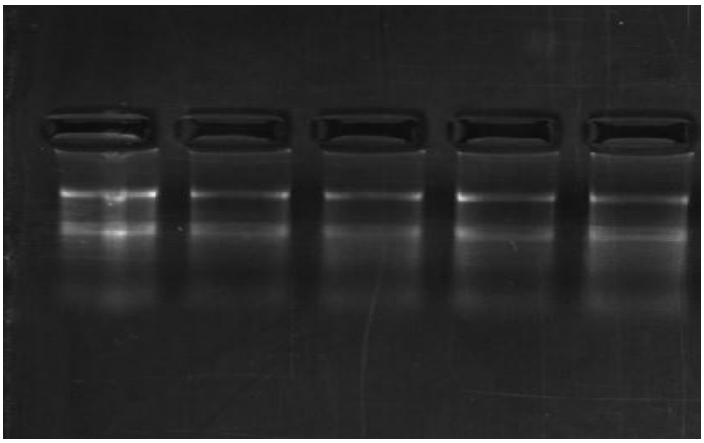

Image 3: Sample series: Г144, Г550, Г388, Г492, ӨА765

3.3 PCR (GAPDH) ELECTROPHORESIS

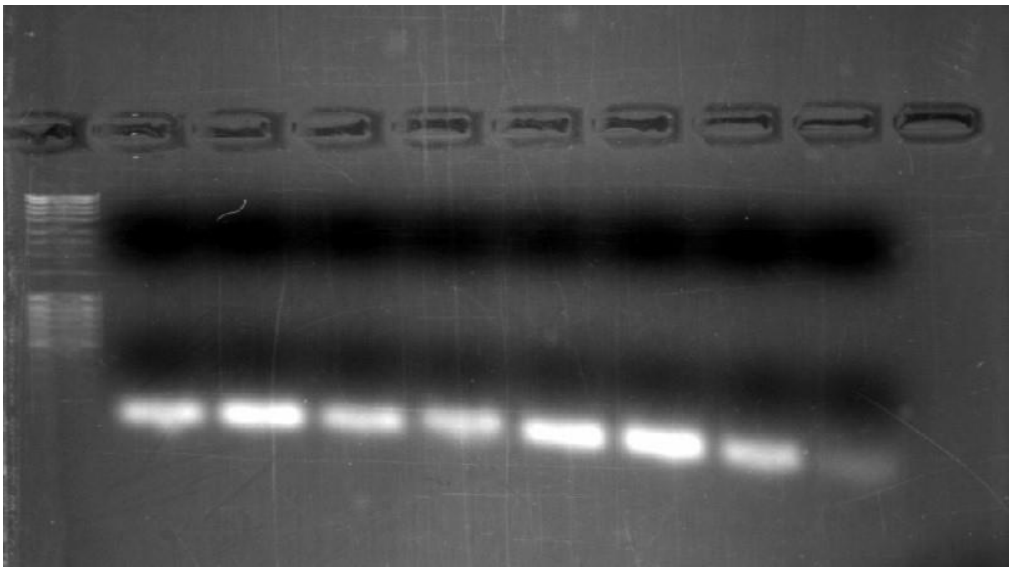

Image 4: Sample series: Г641, Г611, Г683, Г634, Г635, Г636, Г505, Г640

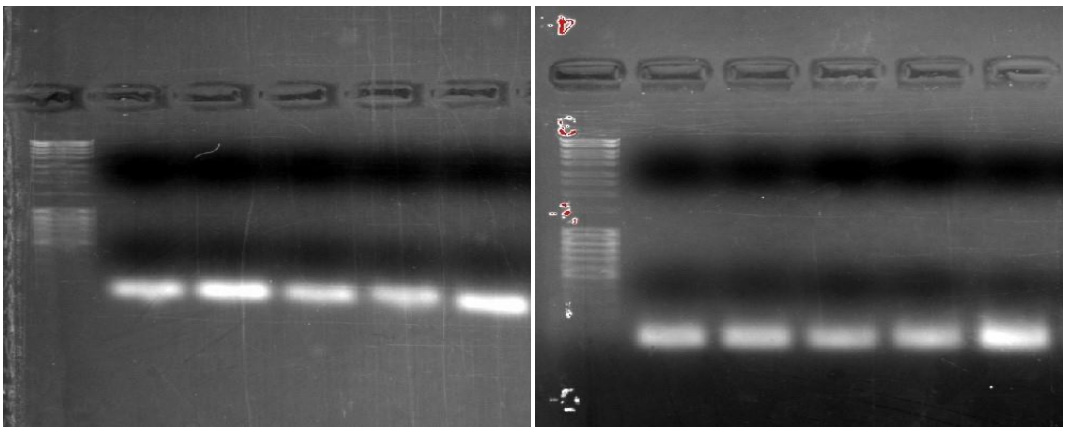

Image 5,6: Sample series: Г590, Г594, Г595, Г564, Г576, Г617, Г618, Г622, Г606, Г696

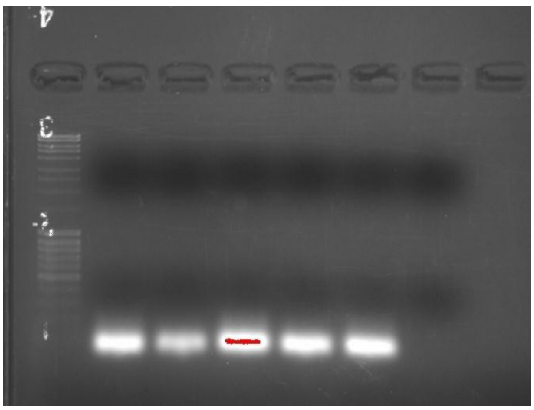

Image 7: Sample series: Г144, Г550, Г388, Г492, ӨА765

3.4 RT-PCR RESULTS

	GAPDH		PRKN		Mean Value of Cq	
SAMPLES	Cq	Cq'	Cq	Cq'	GAPDH	PRKN
Γ641	21.32	21.30	27.82	27.11	21.31	22.47
Γ683	23.12	22.17	29.08	29.01	22.65	30.73
Γ590	24.31	24.09	31.13	32.25	24.20	31.69
Γ594	22.26	22.38	29.17	29.09	22.32	29.13
Γ595	21.15	21.32	28.15	28.23	21.24	28.19
Γ564	20.27	19.95	29.74	29.80	20.11	29.77
Γ576	21.32	21.30	27.82	27.11	21.98	28
Γ634	20.04	20.55	31.04	31.67	20.30	31.36
Γ635	23.81	29.78	30.98	30.47	23.80	30.73
Γ636	18.68	18.85	27.33	27.65	18.77	27.49
Γ617	23.12	22.17	30.92	30.53	22.65	30.73
Γ618	22.81	22.09	31.35	-	22.45	31.35
Γ622	23.35	22.27	30.18	30.09	22.81	30.14
Γ606	20.05	20.52	29.58	29.81	20.29	29.70
Γ696	23.08	21.98	31.95	31.67	22.53	31.81
Γ505	20.59	20.26	36.87	35.45	20.43	36.16
Γ640	22.77	22.17	36.08	37.90	22.47	36.99
Γ144	23.83	23.75	37.09	37.22	23.79	37.16
Γ550	18.63	18.81	33.82	33.95	18.72	33.89
Γ388	20.53	20.21	35.48	35.54	20.37	35.51
Γ492	21.77	22.17	36.04	37.93	21.97	36.99
ΘΑ765	24.58	25.01	38.26	39.02	24.80	38.64
NBA30G	29.99	25.53	28.12	28.27	24.76	33.19
NB (1)	17.84	18.23	26.37	26.44	18.04	26.40
NB (2)	19.38	19.16	30.79	31.42	19.27	31.11
HEK293	23.06	21.68	32.08	33.24	22.37	32.66

Table 6: RT-PCR results , Cq: quantification cycle, NBA30G , NB(1), NB(2):neuroblastoma cells, HEK293: human embryonic kidney cell , GAPDHCq (green colour), PRKNCq (orange colour)

3.5 RT –PCR MELTING CURVES

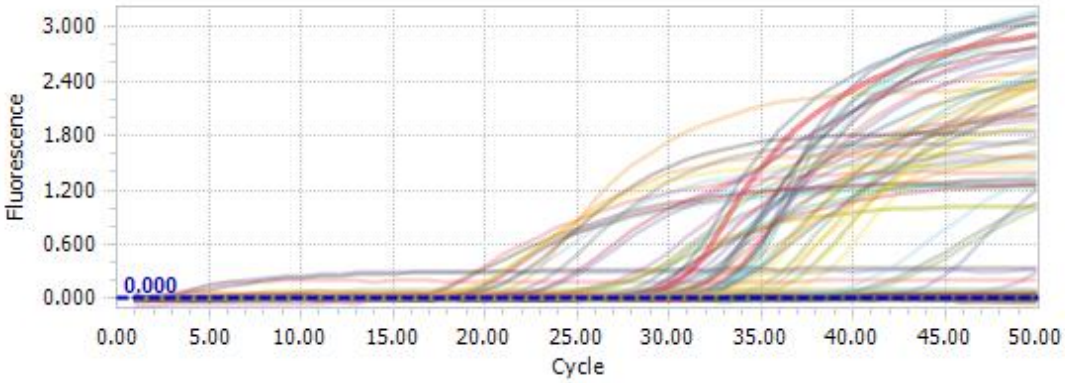

Figure 1: Sample series: Г641, Г611, Г683, Г634, Г635, Г636, Г505, Г640

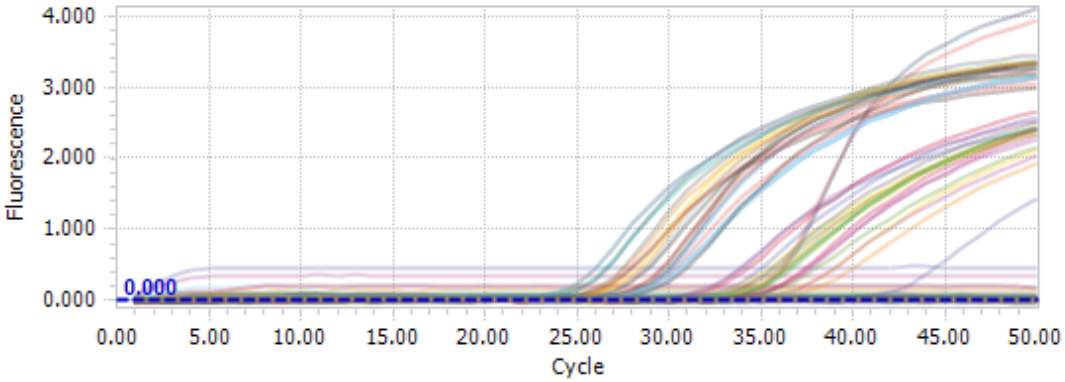

Figure 2: Sample series: Г590, Г594, Г595, Г564, Г576, Г617, Г618, Г622, Г606, Г696, Г144, Г550, Г388, Г492, ΘА765

3.5.1 GAPDH (1)

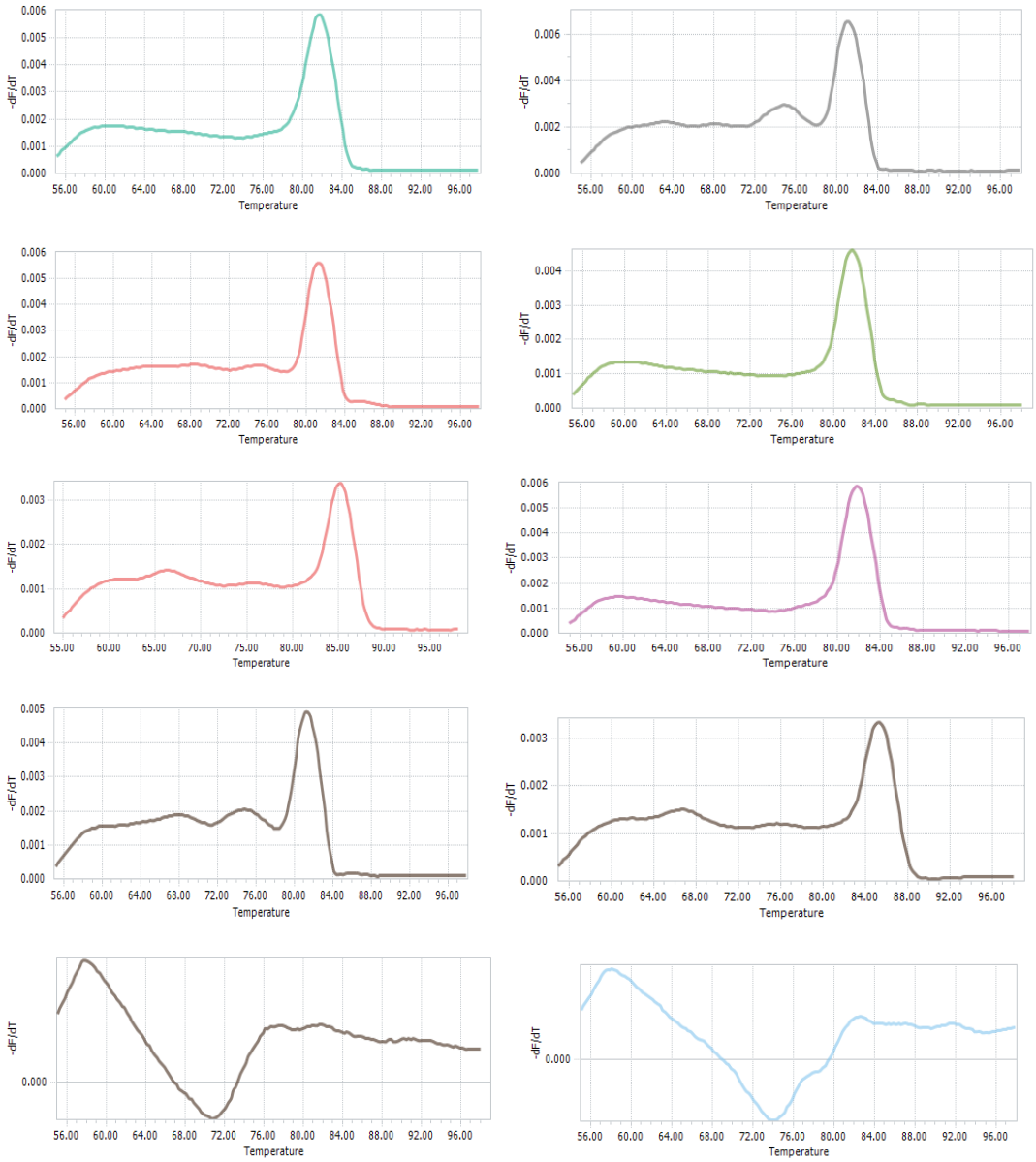

Figures 3-12: Sample series: Г611, Г641, Г683, Г634, Г635, Г636, Г505, Г640, Г640 (no RT), Blank (from left to right order)

3.5.2 PRKN (1)

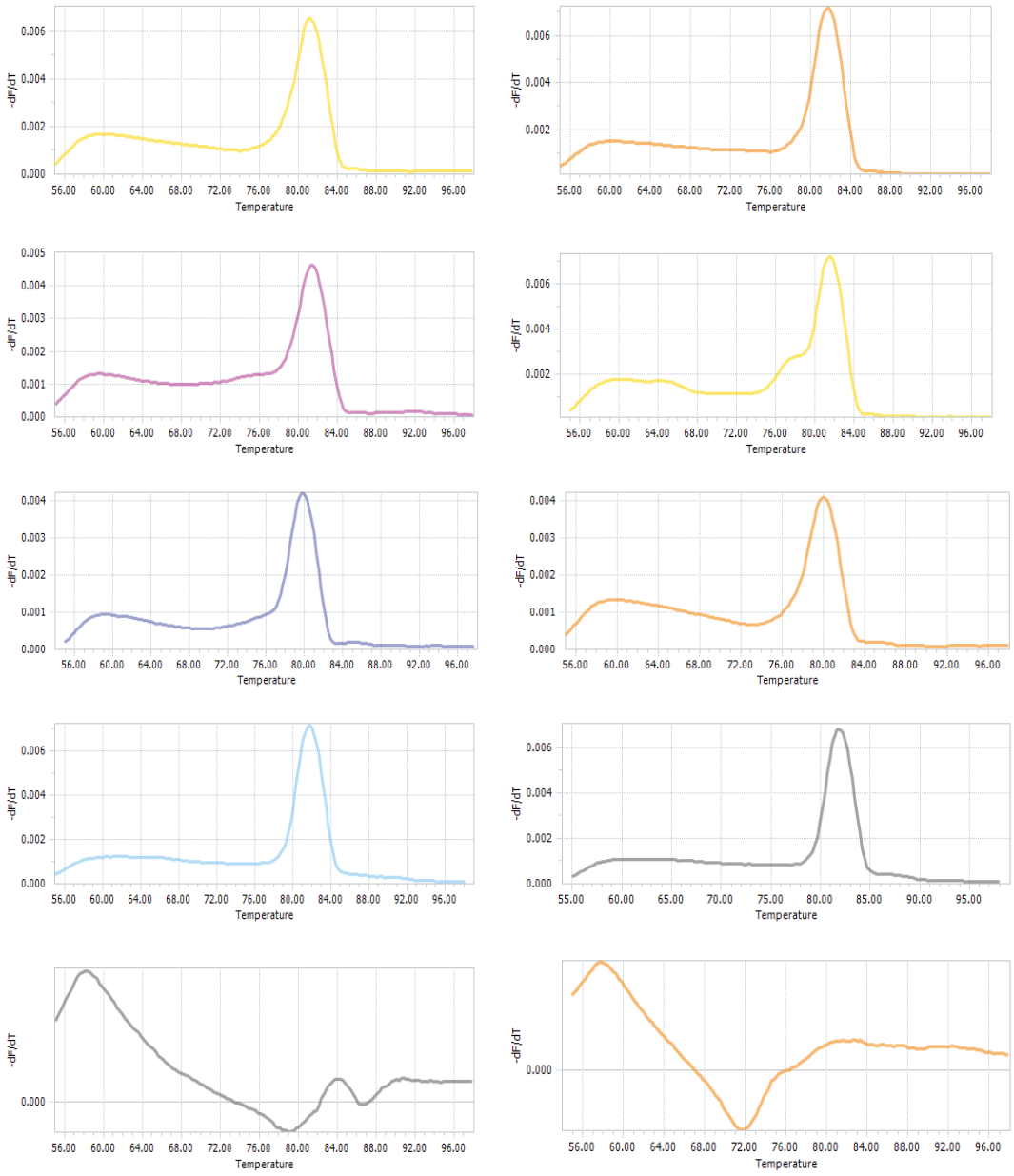

Figures 13-22: Sample series: Г611, Г641, Г683, Г634, Г635, Г636, Г505, Г640, Г640 (no RT), Blank (from left to right order)

3.5.3 GAPDH (2)

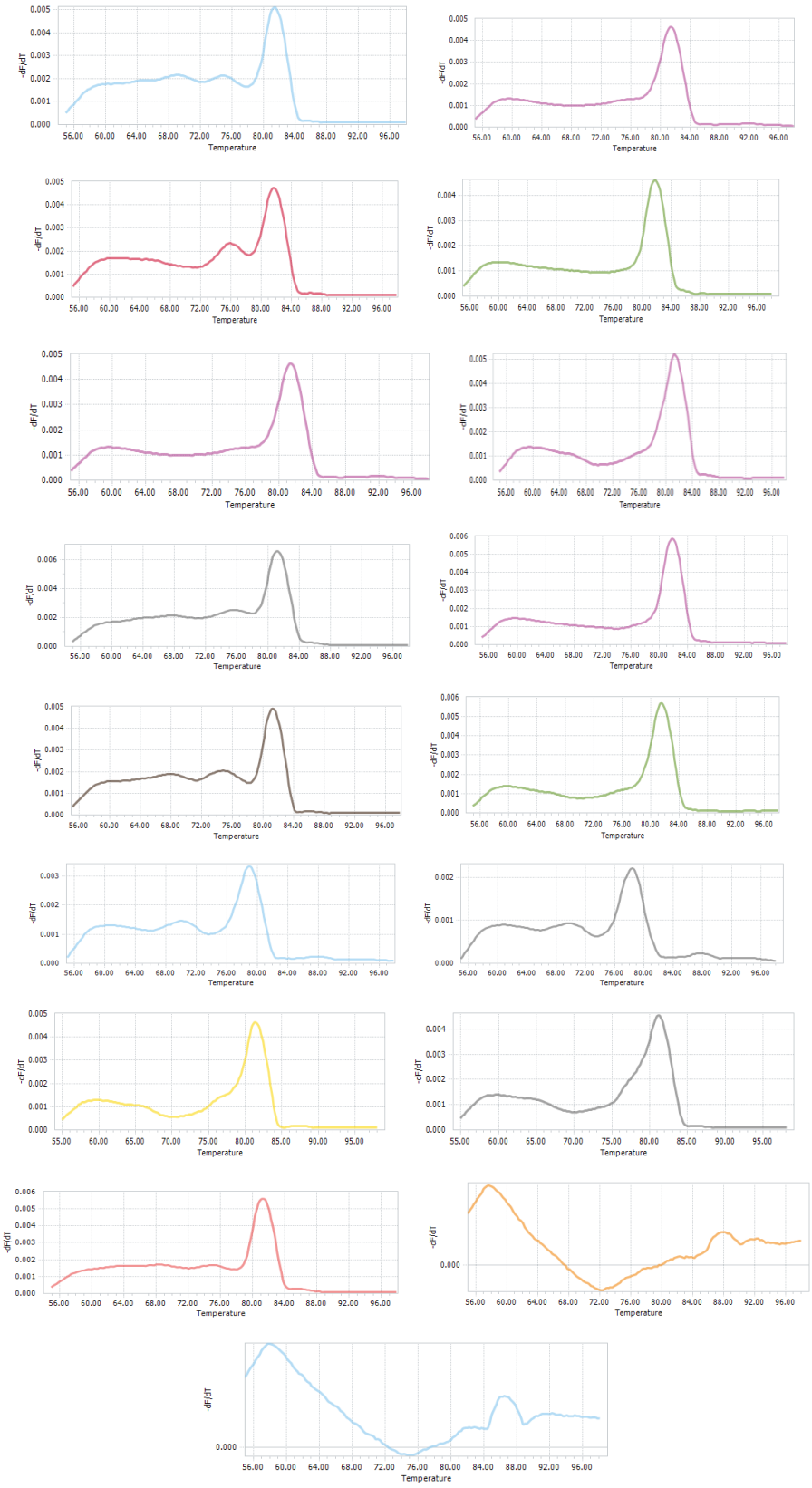

Figures 23-39: Sample series: Г590, Г594, Г595, Г564, Г576, Г617, Г618, Г622, Г606, Г696, Г144, Г550, Г388, Г492, ΘА765, Г595 (no RT), Blank

3.5.4 PRKN (2)

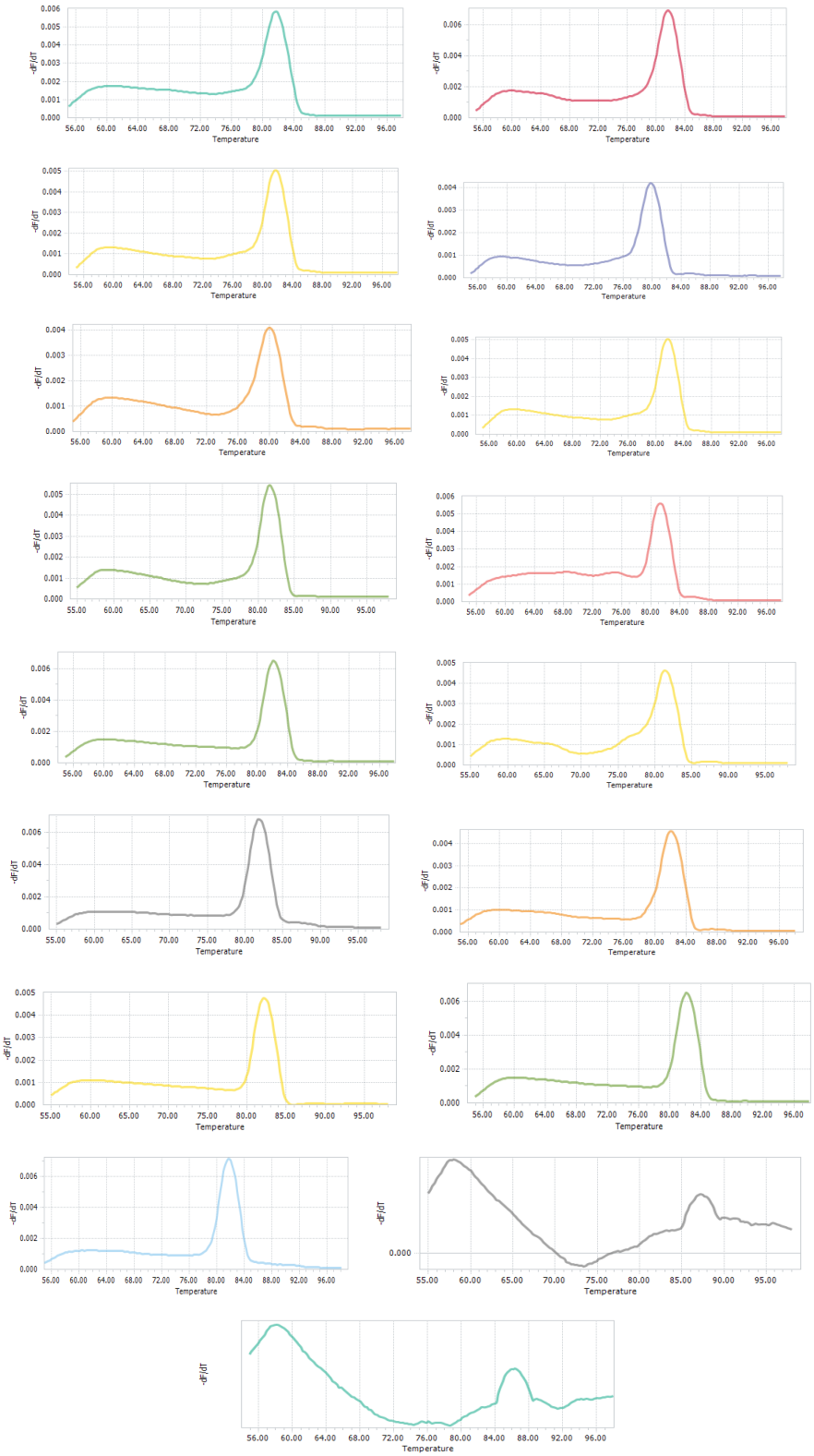

Figures 40-56: Sample series: Г590, Г594, Г595, Г564, Г576, Г617, Г618, Г622, Г606, Г696, Г144, Г550, Г388, Г492, ΘА765, Г595 (no RT), Blank

3.6 DATA NORMALIZATION / EXPRESSION ANALYSIS

SAMPLES	GAPDH	PRKN	ΔCt	Mean ΔCt	ΔΔCt	Fold
Г641	21.31	27.47	6.16	7.31	-1.15	2.21914
Г683	22.65	30.73	8.08		0.77	0.58642
Г590	24.2	31.69	7.49		0.18	0.8827
Г594	22.32	29.13	6.81		-0.5	1.41421
Г595	21.24	28,19	6.95		-0.36	1.28343
Г564	20.11	29.77	9.66		2.35	0.19615
Г576	21.98	28	6.02		-1.29	2.33528

Table 7. Normalisation analysis for the control group

SAMPLES	GAPDH	PRKN	ΔCt	Mean ΔCt	ΔΔCt	Fold
Г634	20.3	31.36	11.06	8.71	3.75	0.07433
Г635	23.8	30.73	6.93		-0.38	1.30134
Г636	18.77	27.49	8.72		1.41	0.37631
Г617	22.65	30.73	8.08		0.77	0.58642
Г618	22.45	31.35	8.90		1.59	0.33217
Г622	22.81	30.14	7.33		0.02	0.98623
Г606	20.29	29.7	9.41		2.1	0.23326
Г696	22.53	31.81	9.28		1.97	0.25525

Table 8. Normalisation analysis for the iPD group

SAMPLES	GAPDH	PRKN	ΔCt	Mean ΔCt	ΔΔCt	Fold
Γ505	20.43	36.16	15.73	13.975	8.42	0.00292
Γ640	22.47	36.99	14.52		7.21	0.00675
Γ144	23.79	37.16	13.37		6.06	0.01499
Γ550	18.72	33.89	15.17		7.86	0.0043
Γ388	20.37	35.51	15.14		7.83	0.00439
Γ492	21.97	36.99	15.02		7.71	0.00478
ΘΑ765	24.8	38.64	13.84		6.53	0.01082

Table 9. Normalisation analysis for the *PRKN*-PD carriers group

For each sample, we performed the **ΔCt method** analysis (*PRKN* gene – *GAPDH* gene), and calculated the mean ΔCt for the control group (**Table 7**).

Afertwards, we perfored the **ΔΔCt method**, in order to compare gene expression between controls, iPD and PRKN-PD carriers, by substrating mean ΔCt of the control group from each ΔCt of samples of control, iPD, *PRKN*-PD carriers group (**Tables 7,8,9**).

And then, we performed the **Fold change** ($2^{-\Delta\Delta Ct}$) method for each sample in order to quantify upregulation or downregulation of *PRKN* expression in each sample (**Tables 7,8,9**).

As it is shown in **Fold column** , in all iPD (except for Γ365) and *PRKN*-PD carriers samples , PRKN expression is downregulated (fold change <1)

3.7 STATISTICAL ANALYSIS

Kruskal-Wallis test

Dunn's multiple comparisons test

GROUPS	MEAN DIFF	FOLD CHANGE	P-VALUE
CT vs PD	4.152	1.25	0.6497 (ns)
CT vs PRKN	13.21	4.3	0.0004 (***)
PD vs PRKN	9.063	3.25	0.0210 (*)

Table 10: Mean differences of expression levels between the 3 groups (CT, PD, PRKN) and their statistical significance (p-value)

- *** (one star):** p-value <0.05 (Significant)
- **** (two stars):** p-value <0.01 (Very Significant)
- ***** (three stars):** p-value <0.001 (Highly Significant)

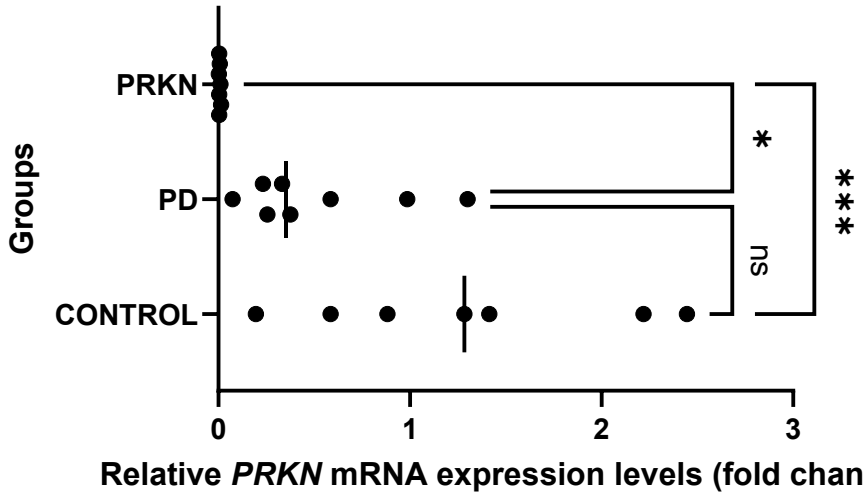

Figure 57: Relative *PRKN* mRNA expression levels among groups (Controls, PD, PRKN), *Kruskal Wallis test/ Dunn's multiple comparisons test*

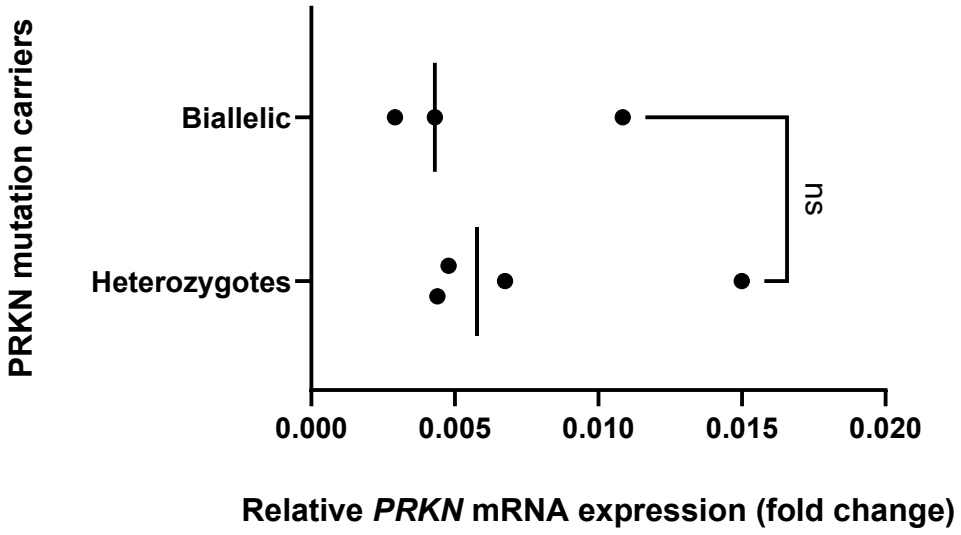

Figure 58: Relative *PRKN* mRNA expression (fold change) among *PRKN* mutation carriers (biallelic, heterozygotes), *Welch's test*

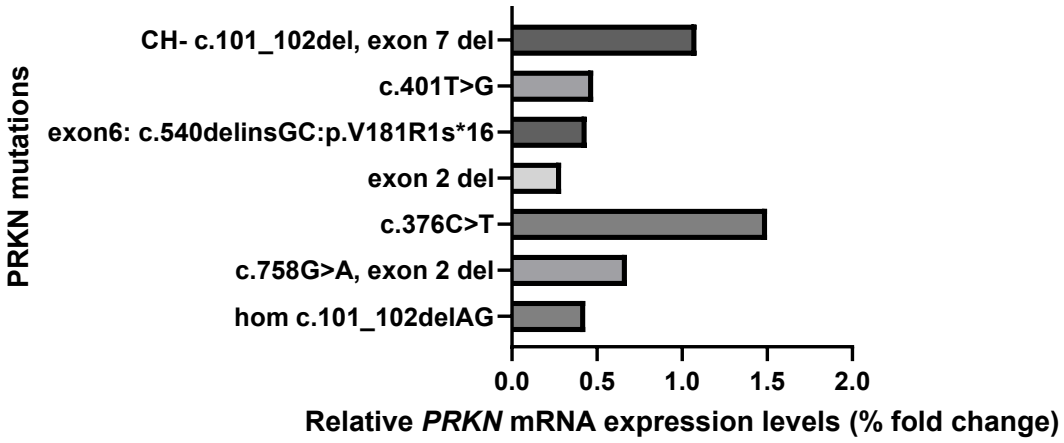

Figure 59: Relative *PRKN* mRNA expression levels (% fold change) among *PRKN* mutations carriers (regarding type of mutation)

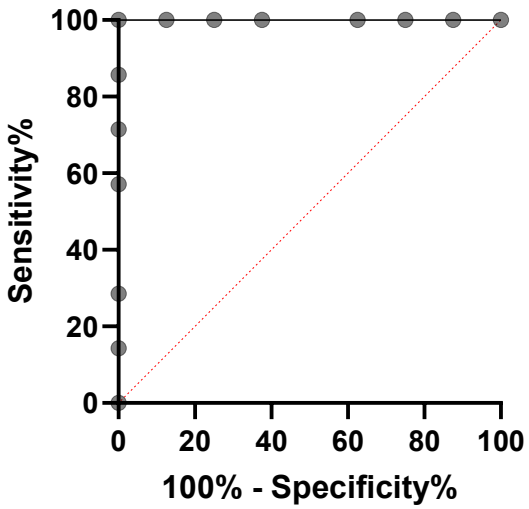

Figure 60: ROC analysis

Cut off values (Youden's Index);

- >32. 85 (100% sensitivity-100% specificity)
- 34.70 (85.71% sensitivity -100% specificity)

Despite the selection effort for lower age controls and iPD patients, *PRKN*-carriers PD patients were younger than these groups, had a lower age of disease onset, and a greater disease duration. However, the statistical analysis for differences in sex (p> 0.05) and age distribution (p>0.05) between groups showed that there was no significant differences in age or sex distribution between these groups (**Table 1, Table 2**). .

A statistically significant difference in PRKN expression was found between these groups (healthy controls, idiopathic PD, PD PRKN-carriers, omnibus p-value <0.0001). Post-hoc analysis revealed practically two different *PRKN*-expression value groups. The first group contained healthy controls and sporadic PD patients, with the other including the *PRKN*-variant carriers. A statistically significant difference was evident between the first and the second group. *PRKN* expression levels were decreased in biallelic and heterozygous *PRKN*-carrier PD patients compared to healthy controls (4,3 times lower) and this relation was statistically significant (p-value=0.0004).

Similarly, mRNA levels were decreased in *PRKN* carrier PD patients compared to sporadic patients (3,25 times lower), and this relationship was statistically significant as well (p-value=0.0210). *PRKN* mRNA levels were, also, slightly decreased in sporadic PD patients compared to healthy controls (1,25 times lower), but this relationship was not statistically significant (p-value=0.6497) (**Figure 57**).

PRKN mRNA levels were uniformly very low in all *PRKN* mutation carriers, even heterozygotes. In fact heterozygote mRNA levels were not statistically different from biallelic carriers (p-value=0.6458) (**Figure 58**).

There was only one subject in our study for each type of variant present and levels were uniformely very low in all mutation carriers, subject to a floor effect. As a result, it is not possible to make any inferences about the individual effects of specific variants on mRNA levels. *PRKN* expression levels corresponding to each of the *PRKN*-carrier PD patients are shown in **Figure 59**.

ROC analysis was performed to assess the usefulness of *PRKN*-expression levels as discriminator of the presence of *PRKN* variants in PD patients. The area under the curve was 1000 (95% confidence intervals 1.000 to 1.000), for the cut-off value of *PRKN* mRNA expression Ct=32.85, yielding a sensitivity of 100 % (64.57-100%) and a specificity of 100% (67.56-100%). In the context of PD, the positive predictive value of low *PRKN* expression levels for the presence of heterozygote or biallelic *PRKN*-variants was 100% (72.3%-100%) (**Figure 60**).

4. Discussion

Our study provides new insights into the differential expression of *PRKN* mRNA in PBMCs across various groups, including healthy controls, idiopathic PD patients and PD patients carrying *PRKN* variants. The findings underscore the critical role of *PRKN* expression in the pathophysiology of PD and its potential as a biomarker for the identification of *PRKN*-variant carriers.

4.1 *PRKN* mRNA expression in PD patients

A major result of our study is that pathogenic variants in the *PRKN* gene result in reduced expression of the respective mRNA in PBMCs. This result was evident not only in biallelic individuals, but also in heterozygous PD patients. Although the role of heterozygous *PRKN* variants in the pathogenesis of PD remains controversial, our results suggest that a profound *PRKN* expression impairment, beyond what would be expected from a single allele disruption , is present in most heterozygote *PRKN*-variant carriers who have already developed early-onset PD. The significant reduction in *PRKN* mRNA expression among *PRKN* variant carriers, compared to both healthy controls and sporadic PD patients, corroborates the prevailing idea that these genetic variations are strongly associated with reduced *PRKN* activity. Such reduced activity is linked to compromised mitochondrial quality control and dopaminergic neuronal death. Interestingly, sporadic PD patients also exhibited slightly lower *PRKN* mRNA levels compared to healthy controls, albeit not statistically significant (p=0,6497). This non-significant trend may suggest a broader involvement of *PRKN* dysregulation in iPD cases or reflect heterogeneity within this subgroup. Alternatively, it might just be the result of the limited number of samples studied; indeed, in the previous study from the lab, no difference was discerned between iPD and controls regarding PBMC *PRKN* mRNA levels, although again levels in controls were slightly higher[161]. It would be important to perform such studies in a larger scale in the future.

4.2 *PRKN* mRNA levels in Biallelic and Heterozygous Carriers

Apart from the c.401T>G variant and the exon 6: c540delinsGC:pV181Rfs*16 variant, which are classified as of uncertain significance, the rest of the variants reported here are classified as pathogenic according to ACMG criteria. All patients had variants that affect at least the Ubl domain, which is considered crucial for the tertiary structural integrity of Parkin molecule. Additionally, some variants are frame-shift, which are expected to lead to loss of function.

It is quite impressive that in all cases with *PRKN* mutations studied, be it heterozygote or biallelic, levels of *PRKN* mRNA are extremely low (**Figure 1**). Our findings suggest that almost all variants studied here lead to a substantial reduction of *PRKN* mRNA levels. This is true not only for large deletions, and the small deletion c.101_102delAG (which created a premature translational stop signal in the *PRKN* gene), but is also the case even for two single nucleotide variants (c376C>T, c.401T>C). A possible mechanism of mRNA degradation in the case of frameshift mutations produced by deletions is the process of non-sense mediated mRNA decay. A search in free online tools, like SpliceAI (https://spliceailook-up.broadinstitute.org/), did not uncover any probable new splice sited in the case of the various SNPs. With the arrival of new bioinformatics and artificial intelligence tools, further exploration of the different probable mRNA conformations is a possible next step.

It has been suggested that heterozygous *PRKN*-mutation carriers, even when asymptomatic, carry a small degree of dopaminergic nigrostriatal dysfunction. It is highly possible that participants in our cohort did not have the necessary compensatory mechanisms, as they have already developed PD. The fact that in most cases in our study these mutations lead to an important reduction of *PRKN* mRNA levels close to those in biallelic carriers suggest that additional related variants may exist in the other allele, possibly in regulatory regions for *PRKN* expression. Long read sequencing of 4 heterozygote carriers in our original study, however, did not reveal any additional causal genomic alterations. Long read sequencing for the 3 new heterozygote

samples has not been completed yet. It remains quite puzzling why heterozygote mutation carriers have such low *PRKN* mRNA levels, quite similar to those with biallelic mutations. An explanation, apart from a yet unidentified second genetic hit, could be that in these cases there are further epigenetic mechanisms that lead to a substantial reduction of *PRKN* mRNA levels and the resultant early disease manifestation.

It should be noted that our group of heterozygote *PRKN* mutations carriers may not be entirely representative of such carriers in the general population. We only screened for these mutations in our population with young onset PD, with the result being that the heterozygote carriers presented in this study have a mean age of onset even lower that of biallelic carriers. It is likely that *PRKN* heterozygote carriers with a later age of onset may not have such profound reduction in *PRKN* mRNA levels, but this will require further study.

4.3 Reproducibility of the results

These results align with the findings of the previous study of our research group, where some of the samples were used again to verify the results, such as in the case of the compound heterozygous c.758G>A, exon 2 del, the heterozygous exon 2 del and the compound heterozygous c.101_102delAG; exon7 del. It is important that these results were verified in the current study using another primer pair, different from the ones in previous work from the lab, providing an independent verification. The primer pair evaluated in the current work gave the best melting curves and thus would appear to be the best choice at this point for assessing accurately *PRKN* mRNA levels in PBMCs.

4.4 Extension of results

These results of low *PRKN* mRNA levels in *PRKN* mutation carriers were not only verified in these samples previously used, but also extended to 4 additional samples with the following genetic background:

- The homozygous c.101_102delAG mutation

- The heterozygous c.376C>T mutation
- The heterozygous c540delinsGC mutation in exon 6
- The heterozygous 401T>G mutation

All these samples had very low *PRKN* mRNA levels, which is especially notable for the heterozygous cases, as these 3 additional mutations had not been previously assessed. Overall, and in conjunction with the previous study from the lab[161], these results indicate that in young onset *PRKN* heterozygous mutation carriers, *PRKN* mRNA levels are almost universally very low, regardless of the particular mutation. These results need to be confirmed in larger studies, with a wider variety of *PRKN* mutations, while it would be advantageous to also include heterozygote carriers with later age of onset.

4.5 Diagnostic Implications

PBMCs are easily accessible blood cells, and as a result they are very useful as a first screening test to assess for the presence of *PRKN* pathogenic variants. The ROC analysis we have performed shows a high sensitivity and specificity for the recognition of a PD patient with a *PRKN* variant. With a ROC area under the curve of 1.00 and sensitivity and specificity both at 100%, *PRKN* mRNA levels appear to be a robust biomarker for detecting the presence of *PRKN* variants. In fact, the positive predictive value of low PRKN levels with this assay is 100% indicating that the current protocol may be extremely useful for screening for *PRKN*-mutated carrier status in the PD population. This finding has significant implications for clinical practice, as it offers a non invasive and reliable method for identifying genetic subtypes of PD, which may inform personalized therapeutic strategies. To our knowledge, this is one of the few studies to report an easily accessible screening test for *PRKN* mutations status. This could simplify the genetic work-up of PD patients, as genetic testing for *PRKN* mutations, relying on WES and MLPA, is relatively complicated, time-consuming and difficult to perform in large numbers of subjects. This approach would be especially useful in underserved areas, with limited access to genetic testing.

4.6 Limitations and Future Directions

While our results are compelling, several limitations warrant consideration. First, the small sample size, especially in the *PRKN*-carrier PD patient group and the limited number of subjects for each variant type, restricts the generalizability of our findings and precludes statistical inferences about individual variant effects. However, *PRKN* variants are rare, and it is difficult to gather more samples from a single center. Clearly, a larger study , in which subjects with additional *PRKN* variants are included, is warranted in order to examine the generalizability of the present studies. Of special interest is the case of the heterozygote mutation carriers with PD, who appear to have such unexpectedly low levels of *PRKN* mRNA. A study is also needed in asymptomatic *PRKN* variant carriers, especially heterozygotes, to examine whether the low *PRKN* levels identified have may also be present in the absence of overt disease manifestation.

Second, the cross-sectional nature of the study does not allow for the assessment of longitudinal changes in *PRKN* mRNA expression and their relationship to disease progression. Future studies with larger cohorts and longitudinal designs are essential to elucidate the temporal dynamics of Parkin expression in PD.

Another limitation is the fact that most patients in the idiopathic PD group were only tested for the presence of the p.A53T SNCA mutation or variants in GBA1, and there were few (only those with age at onset less than 50 years of age) who were tested for *PRKN* mutations. However, given the rarity of PD-related pathogenic variants, and of PRKN in particular, it is unlikely that this issue could have influenced our results.

Another potential limitation is that dopaminergic drug treatment may influence PBMCs *PRKN* mRNA levels, however, this is highly unlikely, given the fact that in the group of iPD, who were also under dopaminergic treatment, *PRKN* mRNA levels were overall no different from controls.

A final consideration is that total blood-extracted mRNA levels could potentially also be used as a source of mRNA to differentiate *PRKN* mutation carriers from controls. If the results are comparable, total blood RNA could be used instead of PBMCs, thus avoiding the extra step of purifying PBMCs. Unfortunately, total blood -extracted mRNA was not available for the subjects of this study.

5. Conclusions

In conclusion, our study highlights the diagnostic potential of *PRKN*-mRNA expression levels in differentiating PRKN-variant carriers from non–carriers in PD, demonstrating reduced *PRKN* mRNA expression in *PRKN*-associated PD patients. The reduction in *PRKN* expression among biallelic and heterozygous carriers underscores its relevance in the genetic architecture of PD. This reduction is especially pronounced in biallelic carriers, but is interestingly also present in all manifesting heterozygotes studied in the present work, suggesting that additional factors may lead to *PRKN* mRNA reduction in these cases.

This study provides, also, strong evidence that assessment of *PRKN* expression by the standard method of RT-PCR in PBMCs represents a valid screening tool for the identification of *PRKN* mutation carriers in a PD cohort. Such a screening tool could be easily widely available. These findings pave the way for the integration of *PRKN* expression profiling into clinical workflows, offering a promising avenue for personalized diagnostics and therapeutics in Parkinson’s Disease.

However, further larger studies are needed, in a diverse multi-center setting, especially in newly diagnosed PD patients with family history suggestive of autosomal recessive inheritance or young age of onset, to verify and extend these findings, and to unravel the exact mechanisms involved in the reduced PRKN expression, that may lead to the discovery of new therapeutic interventions in *PRKN*–carrier PD patients.

6. References

1. Madsen DA, Schmidt S.I, Blaabjerg M, Meyer M, Interaction between Parkin and a-synuclein in PARK2-Mediated Parkinson's Disease, *Cells*, 2021, 10, 283
2. Balestrino R, Schapira, A.H.V Parkinson disease. *Eur J Neurol,* 2020, 27, 27-22
3. Hendarson MX, Trojanowski JQ, Lee VMY, a-synuclein pathology in Parkinson's disease and related a-synucleinopathies, *Neurosci. Lett,* 2019, 709, 134316
4. Poewe W, Seppi K, Tanner CM , Halliday GM, Brudin P, Volkmann J, Schrag AE, Lang AE, Parkinson disease, Nat, *Rev Dis Primers*, 2017, 3, 17013
5. Pickrell AM, Youle RJ, The role of PINK1, parkin and mitochondrial fidelity in Parkinson's disease. *Neuron*, 2015, 85, 257-273
6. Lee A, Gilbert RM, Epidemiology of Parkinson's Disease. *Neurol Clin*, 2016, 34, 955-965
7. Draoui A, El Hiba O, Aimrane A, El Khiat A, Gamrani H. Parkinson's disease: From bench to bedside. *Rev Neurol (Paris),* 2020, 176, 543-559
8. Lunati A, Lesage S, Brice A, The genetic landscape of Parkinson's disease. *Rev Neurol(Paris),* 2018, 174, 628-643
9. Del Rey NL, Quiroga –Varela A, Grbayo E, Carballo-Carbajal I, Fernandez – Santiago R, Monje MHG, Trigo-Damano I, Blanco –Prieto MJ, Blessa J, Advances in Parkinson's disease: 200 years later. *Front. Neuroanat,* 2018
10. Barodia SK, Creed RB, Goldberg MS, Parkin and PINK1 functions in oxidative stress and neurodegeneration. *Brain Res Bull*, 2017, 133, 51-59
11. Preston Ge, Valina L. Dawson, Dawsaon T.M. PINK1 and Parkin mitochondrial quality control: a source of regional vulnerability in Parkinon's Disease, *Molecular Neurodegeneration* (2020)

12. Braak H, Del Tredia K, Rub U, de Vos RA, Jansen Steur EN, Braak E, Staging of brain pathology related to sporadic Parkinson's disease. *Neurobiol Aging*, 2023, 24 (2): 197-211
13. Surmeler DJ, Obeso JA, Halliday GM, Selective neuronal vulnerability in Parkinson's disease. *Nat Revv Neurosci*, 2017, 18 (2): 101-103
14. Li jy, England E, Holton JL, Soulet D, Hagell P, Lees AJ, et al, Lewy bodies in grafted neurons in subjects with Parkinson's Disease suggest host-to-graft disease propagation. *Nat Med*, 2008, 14: 501-03
15. Kordaver JH, Chu Y, Hower RA, Freeman TB, Olanow CW, Lewy body like pathology in long term embryonic nigral transplants in Parkinon's disease. *Nat Med*, 2008, 14(5), 504-506
16. Volpicelli-Daley LA, Luk KC, Pael TP, Tanil SA, Riddle DM, Stieber A et al, Exogenous alpha –synuclein fibrils induce Lewy body pathology leading to synaptic dysfunction ad neuron death. *Neuron*, 2011, 72 (1): 57-71
17. Luk KC, Kehm V,, Caroll J, Zhang B, O'Brien P, Trojanowski JQ et al, Pathological alpha-synuclein transmission initiates Parkinson's – like neurodegenration in nontransgenic mice. *Science,* 2012, 338 (6109): 949-53
18. Mao X, Du MT, Karuppagounder SS, Kam TI, Yin X, Xiong Y et al, Pathological alpha synuclein transmission initiated by binding lymphocyte-activation gene 3. *Science,* 2016, 353
19. Kim S, Kwon SH, Kam TI, Panider N, Karruppagounder SS, Lee S, et al, Transneuronal propagation of pathologic alpha-synuclein from the gut to the brain models Parkinon's disease. *Neuron*, 2019, 103 (4): 627
20. Uemura N, Yagi H, Uemura MT, Hatanaka Y, Yamakado H, Takahashi R, Inoculation of alpha-synuclein preformed fibrils into the mouse gastrointestinal tract induces Lewy body-like aggregates in the brainstem via the vagus nerve. *Mol Neurodegener,* 2018 , 13 (1): 21
21. Brudin P, Melki R, Prying into the prion hypothesis for Parkinson's disease. *J Neurosci*, 2017, 37 (41): 9808-18
22. Surmeier DJ, Obese JA, Halliday GM, Selective neuronal vulnerability in Parkinon disease. *Nat Rev Neurosc*, 2017, 18 (2): 101-13

23. Giguere N, Burke Nanni S, Trudeau LE. On cell loss and selective vulnerability of neuronal populations in Parkinson's disease. *Front Neurol* , 2018, 9: 455
24. Base A, Beal MF, Mitochondrial dysfunction in Parkinson's disease*. J Neurochem,* 2016, 139 (Suppl 1): 216-31
25. Misgeld T, Schuax T, Mitostasis in neurons: maintaining mitochondria in extended cellular architecture. *Neuron*, 2017, 96 (3), 651-66
26. Spinelli JB, Haigis MC, The multifaceted contributions od mitochondria to cellular metabolism. *Nat Cell Biol*, 2018, 20 (7): 745-54
27. Scarffe L, Stevens D, Dawson V, Dawson TM, Parkin and PINK1: much more than mitophagy. *Trends Neurosci,* 2014, 37 (6):315 -24
28. Amadoro G, Corsetti V, Florenzano F, Atlante A, Bobba A, Nicolin V, et al, Morhological and bioenergetuc demands underlying the mitophagy in post-mitotic neurons: the pink-parkin pathway. *Front Aging Neurosci,* 2014, 6:18
29. Kann O, Kovacs R, Mitochondria and neuronal activity. *Am J Phys Cell Phys,* 2007, 292 (2): 41-57
30. Bolam JP, Pissadaki EK, Living on the edge with too many mouths to feed: why dopamine neurons die, *Mov Disorders*, 2012, 27 (12): 1478-83
31. Moss J, Bolan JP, A dopaminergic axon lattice in the striatum and its relationship with cortical and thalamic terminals*, J. Neurosciences*, 2008, 28 (44): 11221-30
32. Matsuda W, Furuta T, Nahamura K, Hioki H, Fujiyama F, Arai R et al, Single nogostriatal dopaminergic neurons form widely spread and highly dense axonal arborization in the neostriatum. *J. Neurosci*, 2009, 29 (2): 444-53
33. Anden N, Hfuxe K, Hamberger B, Hokfelt T, A quantitative study on the nigro-neostriatal dopamine neuron system in the rat, *Acta Physiol Scand,* 1966, 67 (3): 306-12
34. Pacellin C, Giguerre N, Bourque M, Levesque M, Slack R, Trudeau L, Elevated mitochondrial bioenergetics and axonal arborization size are key contributors to the vulnerability of dopamine neurons. *Curr Biol* 2015, 25 (18): 2349-60

35. Langston J, Ballard P, Tetrud J, Irwin I, Chronic parkinsonism in humans due to a product of meperidine-analog synthesis, *Science*, 1983, 219 (4587): 979-80
36. Tanner C, Kamel F, Ross G, Hopppin J, Goldman S, Korel M et al, Rotenone, paraquat and Parkinson's disease, *Environ Health Perspect*, 2011, 119 (6): 866-72
37. Dhillon A, Tarbutton G, Levin J, Plotkin G, Lowry L, , Nalbone J, et al, Pesticide/ environmental exposures and Parkinon's disease in East Texas*, J Agromedicine* 2009, 13 (1): 37-48
38. Dawson T, Dawson V, Molecular pathways of neurodegenration in Parkinson's disease, *Science*, 2003, 302 (5646): 819-22
39. Schapira A, Cooper J,, Dexter D, Jenner P, Clark J, Marden C, Mitochondrial complex I deficiency in Parkinson's disease, *Lancet*, 1989, 1 (8649): 1269
40. Bindoff L, Birch-Machin M, Carlidge N, Parker W, Turrbull D, Mitochondrial function in Parkinson's disease, *Lancet*, 1989, 2 (8653): 49
41. Giannocaro M, La Morgia C, Rizzo G, Carelli V, Mitochondrial DNA and primary mitochondrial dysfunction in Parkinson's disease, Mov Disord 2017, 32 (3): 346-63
42. Grunewald A, Rygiel K, Heppbewhite P, Morris C, Picard M, Turnball Parkinson disease neurons, *Ann Neurol*, 2016, 79 (3): 366 -78
43. Coxhead J, Kwrzawu – Akanbi M, Husseim R, Pyle A, Chinnery P, Hudson G, Somatic mt DNA variations is an important component of Parkinson's disease, *Neurobiology Aging*, 2016, 38, 217 e1-6
44. Dole C, Flones J, Nido G, Miletic I, Oswaorgww N, Krictoft S, et al, Defective mitochondrial DNA homeostasis in the substantia nigra in Parkinon disease, *Nat Commmunications*, 2016, 7 : 1348
45. Navarro A, Boveris A, Bandez M, Sanchee- Pino M, Gomez C, Muntane G, et al, Human brain cortex: mitochondrial oxidative damage and adaptive response in Parkinson's disease and in dementis with Lewy bodies, *Free Rdic Biol Med*, 2009, 46 (12): 1574-80

46. Braschi E, Goyon V, Zumino R, Mohanty A, Xu L, McBride H, Vps35 mediates vesicle ransport between the mitochondria and peroxisomes, *Curr Biol,*2010, 20 (14):1310-5
47. Wang W, Wang X, Fujioka H, Hoppel C, Whone A, Caldwell M, et al, Parkinson's disease-associated mutant Vps35 causes mitochondrial dysfunction by recycling complexes, *Nat Med*, 2016, 22 (1): 54-63
48. Tang F, Liu W, Hu J, Erion J, Ye J, Mei L, et al, Vps35 deficiency or mutation causes dopaminergic neuronal loss by impairing mitochondrial fusion and function, *Cell Resp* , 015, 12 (10): 1631-43
49. Verma M, Callio J, Otero P, Sekler I, Wills Z, Chu C, Mitochondrial calcium dysregulation contributes to dendrite degeneration mediated by PP/ LBD –associated LRKK2 mutants*. J Neurosci*, 2017, 37 (46): 1151-65
50. Howlett E, Jensen N, Belmonte F, Zafar F, Hu X, Kluss J, et al, LRRK2 G20195 –induced mitochondrial DNA damage is LRRK2 kinase depedent and inhibition restores mtDNA integrity in Parkinson's disease. *Hum Mol Genet*, 2017, 26 (22): 4340-51
51. Ramonet D, Podhajska A, Stafa K, Sonnay S, Tranchikova A, Tsika E et al, PARK9 –associated ATP13A2 localises to intracellular –acidic vesicles and regulates cation homeostasis and neuronal integrity, *Hum Mol Genet*, 2012, 21 (8): 1725-43
52. Park S, Davis R, Sue C, Mitochondrial dysfunction in Parkinson's disease: new mechanistic insights and therapeutic perspectives , *Curr Neurol Neurosc Rep*, 2018, 18 (5): 21
53. Kitada T, Asakawa S, Hattori N, Matsumine H, Yamamura Y, Minoshima S, et al, Mutations in the parkin gene cause autosomal recessive juvenile parkinsonism, *Nature*, 1998, 392 (6676): 605-8
54. Valente E, Abou-Sleiman P, Caputo V, Muquit M, Harvey K, Gispert S, et al, Hereditary early-onset Parkinson's disease caused by mutation in PINK1, *Science,* 2004, 304 (5674): 1158-60
55. Clark I, Dodson M, Jiang C, Cao J, Huh J, Seol S, et al, Drosophila PINK1 is required for mitochondrial function and interacts genetically with parkin, *Nature*, 2006, 441 (7097): 1162-6

56. Park J, Lee S, Lee S, Kim Y, Song S, Kim S, et al, Mitochondria dysfunction in Drosphila PINK1 mutants is complemented by parkin, *Nature,* 2006, 441 (7097): 1157-61
57. Yang Y, Gehrke S, Imai Y, Huang Z, Ouyoug Y, Wang J, et al, Mitochondria pathology and muscle and dopaminergic neuron degenration caused by inactivation of Drosophila PINK1 is rescued by Parkin*, Proc Nat Acad Sci USA*, 2006, 103 (28): 10793-8
58. Houlden H, Singleton A, The genetics and neuropathology of Parkinon's disease, *Acta Neuropathol*, 2012, 124 (3):325 -38
59. Dohery K, Silveira Moriyama L, Parkinnen L, Healy D, Farrel M, Menacci N , et al, Parkin disease, *Acta Neuropathol* , 2012, 124 (3): 325-38
60. Koros C, Simitsi A, Stefanis L, Genetics of Parkinon's disease: genotype-phenotype correlations. *Int Rev Neurobiol,* 2017, 132: 197-231
61. Schneider S, Alcalay R, Neuropathology of genetic synucleionopathies with parkinsonism: review of the literature,*Mov Disord,* 2017, 32 (11): 1504-23
62. Harper J, Ordureau A, Heo J, Building and decoding ubiquitin chains for mitophagy, *Nat Rev Mol Cell Biol*, 2018, 19 (2): 93-108
63. Rub C, Wickening A, Voos W, Mitochondrial quality control by the PINK1/ Parkin system. *Cell tissue Res,* 2017, 367 (1): 11-23
64. Pickrell A, Youle R, The roles of PINK1, parkin and mitochondrial fidelity in Parkinon's disease, *Neuron, 2015*, 85 (2): 257-73
65. Voight A, Berlermann L, Winklhofer K, The mitochondrial kinase PINK1 fonctions beyond mitophagy. *J Neurochem*, 2016, 139 (Suppl) 232-9
66. Rsool S, Soya N, Truong L, Croteau N, Lukacs G, Trempe J, PINK1 autophosporylation is required for ubiquitin recognition, *EMPO Rep,*2018, 19e44891
67. The Uni Prot Consortium, Uni Prot: The universal protein knowledgebase, *Nucleic Acids, Res,*2018, 46 2699
68. Kitada T, Akawa S, Hattori N, Matsumine H, Yamamura Y, Minoshima S, Yokochi M, Mizumo Y, Shimizu N, Mutations in the parkin gene

cause autosomal recessive juvenile parkinsonism, *Nature*, 1998, 392, 605-608

69. Hedrich K, Esketson C, Wilmot B, Marder K, Harris J, Garrels J, Meija – Santana H Vieregge P, Jakobs H, Bressamn S, et al Distribution, type and origin of Parkin mutations: Review and case studies *, Mov Disorders* 2004, 19, 1146-1157
70. Giguere K, Pacelli C, Saumure C, Bourque M, Matheoud D, Levesque D, Slack R, Park D, Trudeau L, Comparative analysis of Parkinon's disease- associated genes in mice reveals altered survival and bioenergetics of Parkin deficient dopamine neurons, *J, Biol, Chem,* 2018, 293, 9580-9593
71. Geisler S, Holmstrom K, Treis A, Skijat D, Weber S, Fiesel F, Kahle P, Spinger W, The PINK1/Parkin-mediated mitophagy is compromised by PD-assocated mutations, *Autophagy*, 2010, 6 , 871-878
72. Spratt D, Walden H, Show G, RBRE3 ubiauitin ligases: New structures, new insights, new questions, *Biochem J*, 2014, 458, 421-437
73. Sarraf S, RRaman M, Gurani – Pereira V, Sawa M, Hurlin E, Gygi S, Harper J, Landscape of the PARKIN-depedent ubiauitylome in response to mitochondrial depolarization , *Nature*, 2013, 496, 372-376
74. Hristova V, Beasley S, Rylett R, Show G, Identification of a novel Zn2+ binding domain in the autosomal recessive juvenile Parkinson- related E3 ligase parin, *J Biol Chem* 2009, 284, 14978-14986
75. Truban D, How X, Causfield TR, Fiesel FC, Springer W, PINK1, Parkin and mitochondrial quality control: What can we learn about Parkinon's disease pathobiology? *J Parkinson's Dis,* 2017, 13-29
76. Hampe C, Ardila-Osorio H, Fournier M, Brice A, Corti O, Biochemical analysis of Parkinson's disease-causing variants of Parkin , an E3 ubiauitin-protein ligase with monoubiquitylation capacity. *Hum Mol Genet,*2006, 15 , 2059-2075
77. Matsuda N, Kitami T, Suzuki T, Mizumo Y, Hattori N, Tanaka K, Diverse effects of pathogenic mutations of Parkin that catalyze multiple monouibiauitylation in vitro, *J Biol Chem*, 2006, 281, 3204-3209

78. Dose-Pepe E, Chen L, Madura K, Alpha-synuclein and parkin contribute to the assembly of ubisuitin lysine 63-linked multiubiauitin chains, *J Biol Chem,* 2005, 280, 16619 -16624
79. Chan N, Salazar A, Pham A, Sweredoski M, Kolawa N, Grahan R, Hess S, Chan D, Broad activation of the ubiauitin –proteasome system by Parkin is critical for mitophagy, *Hum Mol Gent*, 2011, 20, 1726-1737
80. Zheng X, Hunter T, Parkin mitochondrial translocation is achieved through a novel catalytic coupled mechanism, *Cell Res*, 2013, 23, 886-897
81. Seirafi M, Kozlov G, Gehring K, Parkin structure and function, *FEBS* J 2015, 282, 2076-2088
82. Lim K, Tan J, Role of the ubiquitin proteasome system in Parkinon's disease, *BMC Biochem,* 2007, 9 (Suppl 91), 513
83. Bard J, Goodall E, Greene E, Johnson E, Dong K, Martin A, Structure and function of the 26s Proteasome, *Annu Rev Biochem*, 2018, 87, 697 -724
84. Geisler S, Holmstrom K, Skujout D, Fiesel F, Rothfuss O, Kahle P, Springer W, PINK1/ Parkin-mediated mitophagy is dependent on VDAC1 and p62/ SQSTM1, *Nat Cell Bio,* 2010, 12, 119-131
85. Narendra D, Tanaka A, Sven D, Youe R, Parkin-induced mitophagy in the pathogenesis of Parkinson disease, *Autophagy,*2009, 5, 706-708
86. Ge P, Dawson V, Dawson T, PINK1 and Parkin mitochondrial quality control: a source of regional vulnerability in Parkinson's disease, *Molecular Neurodegeneration* , 2020, 15:20
87. Matsuda N, Sato S, Shiba K, Okatsy K, Saisho K, Gautier C, Sau Y, Saiki S, Kauajin S, Sato F et al, PINK1 stabilized by mitochondrial depolarization recruits Parkin to damaged mitochondria and activates latent Parkin for mitophagy, *G cell Biology*, 2020, 189, 211-221
88. Harper J, Ordureau A, Heo J, Building and decoding ubiauitin chains for mitophagy, *Nat Rev Mol Cell Biol*, 2018, 19, 93-108
89. Becker D, Richter J, Tocilescu M, Predborski S, Voos W, Pink1 kinase and its membrane potential (Delta ψ)- depedent cleavage product both localize to alter mitochondrial membrane by uniaue targeting mode, *J Biol Chem*, 2012, 287, 22969-22987

90. Yamano K, Youle R, PINK1 is degraded through the N-end rule pathway, *Autophagy,*2013, 9, 1758-1769
91. Greene A, Grenier K, Aguileta M, Muise S, Farazifard R, Haque M, McBride H, Park D, Fon E, Mitochondrial processing peptidase regulates PINK1 processing, import and Parkin recruitement, *EMBO Rep*, 2012, 13, 378-385
92. Narendra D, Sin S, Tanaka A, Suen D, Gautier C, Shen J, Cookson M, Youle R, PINK1 is selectively stabilized on impaired mitochondria to activate Parkin, *PLDS Biol*, 2010, 8, E1000298
93. RubC, Wilkening A, Voos W, Mitochondrial quality control by the Pink1/Parkin system, *Cell Tissue Res*, 2017, 367 (1): 11-23
94. Pickrell A, Youle R, The roles of PINK1, parkin and mitochondrial fidelity in Parkinon's disease, *Neuron,* 2015, 85 (2) 257-73
95. Ordureau A, Sarraf S, Duda D, Heo J, Jedrychowski M, Svidersky V, et al, Quantitative proteomics reveal a feedforward mechanism for mitochondrial PARKIN translocation and ubiauitin chain synthesis, *Mol Cell,*2014, 56 (3): 360-75
96. Shiba- Fukushima K, Araro T, Matsumoto G, Inoshita T, Yoshida S, Ischihama Y et al, Phosporylation of mitochondrial polyubiaqitin by PINK1 promotes Parkin mitochondrial tethering, *PLOS Genet*, 2014, 10 (12): e1004861
97. Walinda E, Morimoto D, Jugase K, Shirakawa M, Dual function of phosphoubiquitin in E3 activation of Parkin , *J Biol Chem*, 2016, 291 (32): 16879-91
98. Tang MY, Vrana M, Krahn Al, Pundil S, Trempe J, Fon E, Strucutre-guided mutagenesis reveals a hierarchical mechanism of Parkin activation *Nat Commun*, 2017, 8: 14697
99. Kayano F, Okatsu K, Kosako H, Tamura Y, GoE, Kimura M, et al, Ubiquitin is phosporylated by PINK1 to activate parkin*, Nature,*2014, 510 (7503): 162-6
100. Okatsu K, Kayano F, Kimura M, Kosako H, Soveki Y, Tanaka K, et al, Phosorylated ubiauitin chain is the genuine Parkin receptor, *J Cell Biol*, 2015, 209 (1): 11-28

101. Pao K, Stanley M, Han C, Lai Y, Murphy P, Balk et al, Probes of ubiquitin E3 ligases enable systematic dissection of parkin activation , *Nat Chem Biol,* 2016, 12 (5): 324-31

102. Aguire JD, Dunkerey K, Mercier P, Show G, Structure of phosphorylated UBL domain and insights into PINK1-orchestrated parkin activation, *Proc Nat Acad Sci USA*, 2017, 114 (2): 298-903

103. Sarraf S, Raman M, Gurani –Pereira V, Saua M, Hutlin E, Gygi S, et al, Landscape of the PARKIN –depedent ubiquitylome in response to mitochondrial depolarization, *Nature* 2013, 496 (7445): 372-6

104. Rose C, Isasa M, Ordureau A, Prado M, Beausoleil S, Jedrychawski M, et al, Highly multiplexed quantitative mass spectrometry analysis of ubiauitylomes, *Cell Syst*, 2016, 3 (4): 395-403 e4

105. Ko H, von Coelin R, Sriram S, Kim S, Chung K, Pletnikova O, et al, Accumulation of the authentic parkin substrate aminoacyl-tRNA synthetase cofactor, p38/jiv-1, leads to chatecholaminergic cell death, *J Neurosci,*2005, 25 (35): 7968-78

106. Ko H, Lee Y, Shin J, Karuppagowder S, Gadad B, Koleske A, et al, Phosphorylation by the c-Abl protein tyrosine kinase inhibits parkin's ubiquitination and protective function, *Proc Nt Acad Sci USA*, 2010, 107 (38): 16691-6

107. Imam S, Zhou Q, Yamamoto A, Valente A, Ali S, Bains M, et al, Novel regulation of parkin function through c- Abl- mediated tyrosine phosphorylation: implication for Parkinon's disease *, J Neurosci* 2011, 31 (1): 157 – 63

108. Pereira S, Grossmann D, Delcambre S, Herman A, Grunewald A, Novel insights into Parkin-mediated mitochondrial dysfunction and neuroinflammation in Parkinon's disease, *Current Opinion in Neurobiology,* 2023, 80: 102720

109. Lee Y, Karuppagounder S, Shin J, Lee Y, Ko H, Swing D, et al, Parthanatos mediated AIMP2-activated age-depedent dopaminergic neuronal loss , *Nat Neurosc* 2013, 16 (10): 13922-400

110. Wang Y, An R, Umanah G, Park H, Nambiar K, Eacker S et al, A nuclease that mediates cell death induced by DNA damage and poly (ADP-ribose) polymerase -1, *Science*, 2016, 354 and 6872

111. Shin J, Ko H, Kang H, Lee Y, Pletinkova D, et al PARIS (ZNF746) repression of PGC-1 alpha contributes to neurodegenration in Parkinson's disease, *Cell*, 2011, 144 (5): 689-702

112. Stevens D, Lee Y, Kong H, Lee B, Lee Y, Bower A et al, Parkin loss leads to PARIS-depedent declines in mitochondrial mass and respiration , *Proc Nat Acad Sci USA,* 2015, 112 (37): 11696-701

113. Cunningham C, Baughman J, Phu L, Tea J, Yu C, Coons M et al, USP30 an parkin homeostatically regulate atyoical ubiaquitin chain on mitochondria, *Nat Cell Biol*, 2015, 17 (2): 160-9

114. Park J, Laplantine E, Curic S, Genin P, Role of optineurin in the mitochondrial dysfunction: Potential implications in neurodegenerative disease and cancer, *Front Immunol*, 2018, 9, 1243

115. Hang L, Thundyil J, Lim K, Mitochondrial dysfunction and Parkinson's disease; New mechanisitic insights and therapeutic perspective, *Curr Neurol Neurosc Rep*, 2018, 18, 21

116. Shin J, Ko H, Kang H, Lee Y, Pletinkova O, Tnoconso J, Sawson V, Dawson T, Paris (ZNF7146) repression of PGC-1a contributes to neurodegeneration in Parkinson;s disease, *Cell*, 2021, 144, 689-702

117. Stevens D, Lee Y, Kang H, Lee B, Lee Y, Bower A, Jiany H, Kang S, Andrabi S, Dawsin U, et al, Parkin loss leads to PARIS – depedent declines in mitochondrial mass and respiration, *Proc Nat Acad Sci USA*, 2015, 112, 11696-11701

118. Bogetofte H, Jensen P, Ryding M, Schmidt S, Okarmis J, Rutter L, Worm C, Hohnholt M, Azevedo C, Roybon L et al, PARK2 mutation causes metabolic disturbances and impaired survival of human iPSC – derived neurons, *Front Cell Neurosci* , 2019, 13, 297

119. Hedrich K, Eschelon C, Wilmot B, Marder K, Harris J, Garrels J, Meja – Santano H, Vieregge P, Jacobs H, Bressnam S, et al, Distribution, type, and origin of Parkin mutations: Review and case studies, *Mov Disorders*, 2004, 19, 1146-1157

120. Lesage S, Magali P, Lahman E, Lacomblez L, Teive H, Janin S, Cassin P, Dur A, Brice A, French Parkinson's Disease Genetics Study, G Deletion of the parkin and PCRG gene promoter in early –onset parkinsonism, *Hum Mutat*, 2007, 28, 27-32

121. West C, Dawson V, Dawson T, The Role of Parkin in Parkinson's Disease. In: Dawson T, *editor Parkinson's Disease: Genetics and Pathogenesis: Informa Healthcare* USA, Inc 2007, p. 199-218

122. Hamoe C, Ardila – Osorio H, Fournier M, Brice A, Corti O, Biochemical analysis of Parkinson's disease-causing variants of Parkin, an E3 ubiauitin –protein ligase with monoubiquitylation capacity , *Hum Mol Genet,* 2006: 15 (130: 2059 -2075

123. Matsuda N, Kitami T, Suzuki T, Mizumo Y, Hattori N, Tanaka K, Diverse effects of pathogenic mutations of Parkin that catalyze multiple monoubiquitylation in vitro, *J Biol Chem*, 2006, 281 (6): 3204-3209

124. Wang C, Tan J, Ho M et al, Alterations in the solubility and intracellular localization of parkin by several familial Parkinson's disease –linked point mutations. *J Neurochem*, 2005, 93 (2): 422 -431

125. Winklhofer K, Hem I, Kay –Jackson P, Heller U, Tatzett J, Inactivation of Parkin by exidative stress and c-terminal truncations: a protective role of molecular chaperones *J Biol Chem*, 2003, 278 (47): 47199-47208

126. Chung K, Thomas B, Li X, et al, S-nitrosylation of parkin regulates ubiquitination and compromises parkin's protective function. *Science* , 2004, 304 (5675) : 1328-1331

127. Yao D, Gu S, Nakamura T et al, Nitrosative stresslinked to sporaduc Parkinson 's disease : S-nitrosylation of parkin regulates its E3 ubiauitin activity *Proc Nat Acad Sci USA,*2004, 101 (29): 10810-10814

128. La Voie M, Ostaszwewski B, Wihofen A, Schossmacher M, Selkoe D, Dopamine covalently modifies and functionally inactivate parkin , *Nat Med*, 2005, 11 (11): 1214-1221

129. Wang C, Kott S, Thomas B, et al, Stress –induced alteration in parkin solubility promote parkin aggregation and compromise parkin's protective function. *Hum Mol Genet,* 2005, 14 (24): 3885-3897

130. Wong E, Tan J, Wang C , et al, Relative sensitivity of parkins and other cycteine-containing enzymes to stress-induced solubility alterations , *J Biol Chem* 2007, 282 (16): 12310-12318

131. Corti O, Lesage S, Brice A, What genetics tells us about the causes and mechanisms of Parkinon's disease, *Physiol Rev* 2011, 91, 1161-1218

132. Lucking C, Dur A, Bonifati V, Vaughan J, De Michelle G, Gasser T, Harhang B, Meco G, Denefle P, Wood N, et al , Association between early-onset Parkinson's disease and mutation in the parkin gene*, N. Engl J Med,* 2000, 342, 1560-1567

133. Schutte C, Gasser T, Genetic basis of Parkinson's disease: Inheritance, penetrance and expression, *App Clin Genet,* 2011, 4, 67-80

134. Mori H, Kondo T, Yokochi M, Matsumine H, Nakagawa –Hattori Y, Miyake T, Suda K, Mizuko Y, Pathologic and biochemical studies of juvenile parkinsonism linked to chromosome 6q, *Neurology*, 1998, 51, 890-892

135. Bruggeman N, Klein C, Parkin type of early onset Parkinson Disease 2001, Apr 17, Adam M, Feldman J, Mirzava G, et al, editors

136. Chien H, Roche C, Cost M, Breedveld G, Ostia B, Barbara E, Bonifati V, Early-onset Parkinson's disease caused by a novel parkin mutation in a genetic isolate from northeastern Brazil, *Neurogenerics*, 2006, 7, 13-9

137. Borshche M, Balck A, Kasten M, Lohmann K, Klein C, Bruggeman N, The sooner , the later-Delayed diagnosis in Parkinson's disease due to Parkin mutations. *Parkinsonism Relat. Disord*. 2019, 65: 284-5

138. Caccappolo E, Alcalay R, Mejia –Santana H, Tang M, Rakitin B, Rosado L, Louis ED, Cornella C, Colcher A, Jennings D, Nance M, Bressman S, Scott W, Tanner C, Mickel S, Andrews H, Water C, Fahn S, Cote L, Frucht S, Ford B, Rezak M, Novak K, Friedman J, Pfeiffer R,

Marsh L, Hiner B, Siderowf AD, Ross BM, Verbitsky M, Kisseler S, Ottman R, Clark L, Mander K, Neuropsychological profile of Parkin mutation carriers with and without Parkinson's disease: the CORE –PD study , *J Int Neuropsychol Soc,* 2011, 17 : 91-100

139. Benbunan B, Korczyn A, Giladi N, Parkin mutation associated parkinsonism and cognitive decline, comparison to early onset Parkinson's disease. *J Neural Transm,*2004, 111: 47-57

140. Doherty K, Silveria Moriyama L , Parkkinen L, Healy D, Farrell M, Menacci N, Ahmed Z, Brett F, Hardy J, Quinn N, Counihan T, Lynch T, Fox Z, Revesz Lees A, Holton J, Parkin disease: a clinicopathologic entrly ? *JAMA Neurol* , 2013, 70: 571-9

141. Van der Vegt J, van Nuemen B, Bloem B, Klein C, Siiebner H, Imaging the impact of genes on Parkinson's disease. *Neuroscience*, 2009, 104: 191-204

142. Pyatigorskaya N, Sharman M, Corrol J, Valabregue R, Yahia – Cherif L, Poupon F, Cormier- Dequaire F, Siebner H, Klebe S, Vidaihet M, Brice A, Lehericy S, High nigral iron deposition in LRRK2 and Parkin mutation carriers using R2* relaxometry, *Mov Disord* 2015, 30: 1077-84

143. Poulopoulos M, Levy O, Alcalay R, The neuropathology of genetic Parkinson's disease, *Mov Disorders*, 2012, 27, 831-42

144. Kasten M, Hartmann C, Hampf J, Schaake S, Westenberger A, Vollstredt E, Balck A, Domingo A, Vulinovic F, Dulovic M, Zorn I, Madoev H, Zehnle H, Lembeck C, Schawe L, Reginold J, Huang J, Koning I, Bertram L, Marras C, Lohmann K, Lill C, Klein C, Genotype-phenotype relations for the Parkinson's disease genes Parkin, PINK1, DJ1: MDS Gene systematic review, *Mov Disord*, 2018, 33: 730-41

145. Klein C, Lohmann-Hedrich K, Rogaera E, Schossmacher M, Lang A, Deciphering the role of heterozygous mutations in genes associated with parkinsonism, *Lancet Neurol*, 2007, 6: 652-62

146. Grunewald A, Klein C, Parkin-associated Parkinson's disease In: Pfeiffer R, Wszolek Z, Ebadi M, eds Parkinson's Disease , 2 ed Chap 14 Boca Raton, FL: CRC Press: 2012

147. Kay D, Stevens C, Hamza T, Montimurro J, Zabetian C, Factor S, Sami A, Griffith A, Roberts S, Molho E, Higgins D, Gancher S, Moses L, Zareparsi S, Poorkay P, Bird T, Nutt J, Schellenberg GD, Payami H, A comprehensive analysis of deletions, multiplications and copy number variations in PARK2 , *Neurology,* 2010, 75: 1189-94

148. Pavese N, Khan N, Scherfler C, Cohen L, Brooks, Wood N, Bhatia K, Quinn N, Lees A, Piccini P, Nigostratial dysfunction in homozygous and heterozygous parkin gene carriers: an 18F-dopa PET progression study, *Mov Disord*, 2009, 24: 2260-6

149. Anders S, Sack B, Pohl A, Munte T, Pramstaller P, Klein C, Binkofski F, Compensatory premotor activity during affective face processing in subclinical carriers of a single mutant Parkin allele. *Brain*, 2012, 135: 1128-40

150. Alcalay R, Clark L, Marder K, Bradley W, Lack of association between cancer history and PARKIN genotype: a family based study in PARKIN /Parkinson;s families. *Genes Chromosomes Cancer*, 2012: 51 : 1109-13

151. Houlden H, Singleton A, The genetics and neuropathology of Parkinson's disease,*Acta Neuropathol*, 2012, 124 (3): 325-328

152. Muqit M, Abou Sleiman P, Saurin A, Harvey K, Gandhi S, Deas E et al, Altered cleavage and localization of PINK1 to aggresomes in the presence of proteasomal stress*, J Neurochem*, 2006, 98 (1): 156 - 159

153. Schlossmacher M, Frosch M, Gai W, Medina M, Sharma N, Fomo L, et al, Parkin localizes to the Lewy bodies of Parkinson disease and dementia with Lewy bodies, *Am J Pathol*, 2002, 160 (5): 1655-67

154. Kurup P, Xu J, Videira R, Oroneryli , Baltazar G, Lombroso P et al, STEP61 is a substrate of the E3 ligase Parkin and is upregulated in Parkinson's disease. *Proc Nat Acad Sci USA*, 2015, 112 (4): 1202-7

155. Eschbach J, von Eimem B, Muller K, Bayer H, Scheffold A, Morrison B, et al, Mutual exacerbation of peroxisome proliferator-activated receptor gamma coactivator 1alpha deregulation and alpha-synuclein oligomerization . *Ann Neurol* 2015, 77 (1): 15-32

156. Wang C, Ko H, Thomas B, Tsang F, Chew K, Tay S, et al, Stress-induced alterations in parkin solubility promote parkin aggregation and compromise parkin's protective function , *Hum Mol Genet*, 2005, 14 (24); 3885-97

157. Brahmachari S, Karuppagounder SS, Ge P, Lee S, Dawson V, Dawson T, et al, C-abl and Parkinon's disease: mechanisms and therapeutic potential, *J Park Dis* 2017, 7 (4) : 589-601

158. Mahl-Mellier A, Fauret B, Gysbers A, Dikiy I, Oueslati A, Georgeon S et al, C-abl phosphorylates alpha-synuclein and regulated its degradation implication for alpha-synuclein clearance and contribution to the pathogenesis of Parkinson's disease , *Hum Mol Genet*, 2014, 23 (11): 2858-79

159. Kawahara K, Hashimoto M, Bar –On P, Ho G, Crews L, Mizuro H, et al Alpha-synuclein aggregates interfere with Parkin solubility and distribution: role in the pathogenesis of Parkinson's disease , *J Biol Chem,* 2008, 283 (11): 6979-87

160. Chen J, Ren Y, Gui C, Zhao M, Wu X, Mao K et al Phosphorylation of Parkin at serine 131 by the p38 MAPK promotes mitochondrial dysfunction and neuronal death in mutant A53T alpha-synuclein model Parkinson's disease , *Cell death Dis*, 2018, 9 (6): 700

161. Papagiannakis N, Liu H, Koros C, Simitsi AM, Stamelou M, Maniati M, Buena-Atienza E, Kartanou C, Karadima G, Makrythanasis P, Vatsellas G, Valente EM, Gasser T, Stefanis L. Parkin mRNA Expression Levels in Peripheral Blood Mononuclear Cells in Parkin-Related Parkinson's Disease. *Mov Disord*. 2024 Apr;39(4):715-722.

162. Huttenlocher J, Stefansson H, Stienberg S, Helgadottir H, Sveinbjornsdottir S, Riess O, Bower P, Stefansson K, Heterozygote carriers for CNVs in PARK2 are at increased risk of Parkinson's disease, *Human Molecular Genetics,* 2015, Vol.24, No19, 5637-5643

163. Hedrick K, Eskelson C, Wilmot B, Morder K, Harris J, Garrels J, Meija-Santana H, Vieregge P, Jacobs H, Bressman J.B. et al, Distribution, type, and origin of Parkin mutations: reviews and case studies, *Mov. Disord*., 2004, 19, 1146-1157

164. Klein C, Pramstaller P.P, Kis B, Page C.C, Kann M, Leung J, Woodward H, Cartellan C.C, Scherrer M, Vieregge P et al, Parkin deletions in a family with adult-onset, tremor –dominant parkinsonism:expanding the phenotype, *Ann Neurol*, 2000, 48, 65-71

165. Farrer M, Chan P, Chen R, Tan L, Lincoln S, Hernandee D, Forno L, Gwinn-Hardy K, Petrucelli L, Hussey J et al, Lewy bodies and parkinsonism in families with parkin mutations, *Ann Neurol*, 2001, 50, 295-300.

166. Wang L, Nuytemans K, Bademci G, Jauregui C, Martin E, Scatt W.K., Vnce J.M, Zucher S, High-resolution survey in familial Parkinson disease genes reveals multiple independent copy number variation events in PARK2, *Hum Mutat*., 2013, 34, 1071-1074

167. Grunewald A, Kasten M, Ziegler A, Klein C, Next-generaton phenotyping using the parkin example: time to catch uo with genetics, *JAMA Neurol*, 2013, 70, 1186-1191

168. Hedrich K, Mouder K, Hartis J, Kann M, Lunch T, Meija-Santana H, Pramstaller P.P, Schwinger E, Bressman S.B., Fahn S et al , Evaluation of 50 probants with early onset Parkinon's disease for Parkin mutations, *Neurology*, 2002, 58, 1239-1246

169. Sun M, Latourelle J.C., Wooten G.F., Lew M.F., Klein C., Shill H.A., Golbe L.I., Mark M.H., Racette B.A., Perlmutter J.S, et al, Influence of heterozygosity for parkin mutation on onset age in familial Parkinson's disease: the GenePD study, 2006, *Arch Neurol*, 63, 826-832

170. Foroud T, Uriacke S.K., Liu L, Pankratz N, Rudolph A, Halter C, Shults C, Marder K, Conneally P.M., Nichols W.C, Heterozygocity for a mutation in the parkin gene leads to later onset Parkinson's disease, *Neurology*, 2003, 60, 796-801

171. Marder K.S, Tang M.X, Meija-Santana H, Rosado L, Louis E.D, Cornella C.L., Colcher A, Siderauf A.D, Jennings D, Nance M.A et al, Predictors od parkin mutations in early-onset Parkinon's disease: the consortium on risk for early onset Parkinson's disease study, *Arch. Neurol*., 2010, 67, 731-738

172. Hiller A, Hagenah J.M., Djarmati A, Hedrich K, Reetz K, Schneider-Gold C, Kress W, Munchan A, Klein C, Phenotypic spectrum of PINK-1 – associated parkinsonism in 15 mutation carriers from 1 family, *Mov Disord*, 2007, 22, 145-147

173. Hiker R, Klein C, Ghaemi M, Kis B, Strotmann T, Ozelius L.S, Lenz O, Viergge P, Hernolz K, Heiss W.D, et al, Positron emission tomographic analysis of the nigostriatal dopaminergic system in familial parkinsonism associated with mutations in the parkin gene. *Ann Neurol,* 2001, 49, 367-376

174. Khan N.L, Scenfer C, Graham E, Bhatia K.P., Quin N., Lees A.J., Brooks D.J., carriers of a single parkin mutation, *Neurology,* 2005, 64, 134-136

175. Feles S, Overath C, Reichardt S, Diegeler S, Schmitz C, Kronenberg J, Baumstark-Khan C, Hemmersbach R, Hellweg CE, Liemersdorf C. Streamlining Culture Conditions for the Neuroblastoma Cell Line SH-SY5Y: A Prerequisite for Functional Studies. *Methods Protoc*. 2022 Jul 12;5(4):58

176. Zhang HT, Mi L, Wang T, Yuan L, Li XH, Dong LS, Zhao P, Fu JL, Yao BY, Zhou ZC. PINK1/Parkin-mediated mitophagy play a protective role in manganese induced apoptosis in SH-SY5Y cells. Toxicol In Vitro. 2016 Aug;34:212-219

177. Narendra D, Tanaka A, Suen DF, Youle RJ. Parkin is recruited selectively to impaired mitochondria and promotes their autophagy. J Cell Biol. 2008 Dec 1;183(5):795-803

178. Clausen L, Okarmus J, Voutsinos V, Meyer M, Lindorff-Larsen K, Hartmann-Petersen R. PRKN-linked familial Parkinson's disease: cellular and molecular mechanisms of disease-linked variants. Cell Mol Life Sci. 2024 May 20;81(1):223

7. Appendix

Pictures

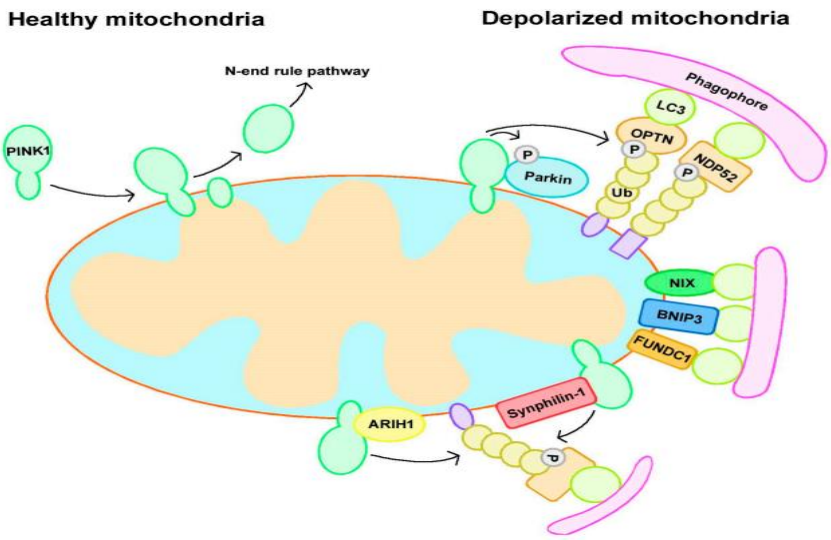

Picture 1: Mitophagy pathways. Mitophagy can be divided into Parkin-dependent or independent pathways. (*Cells* 2019)

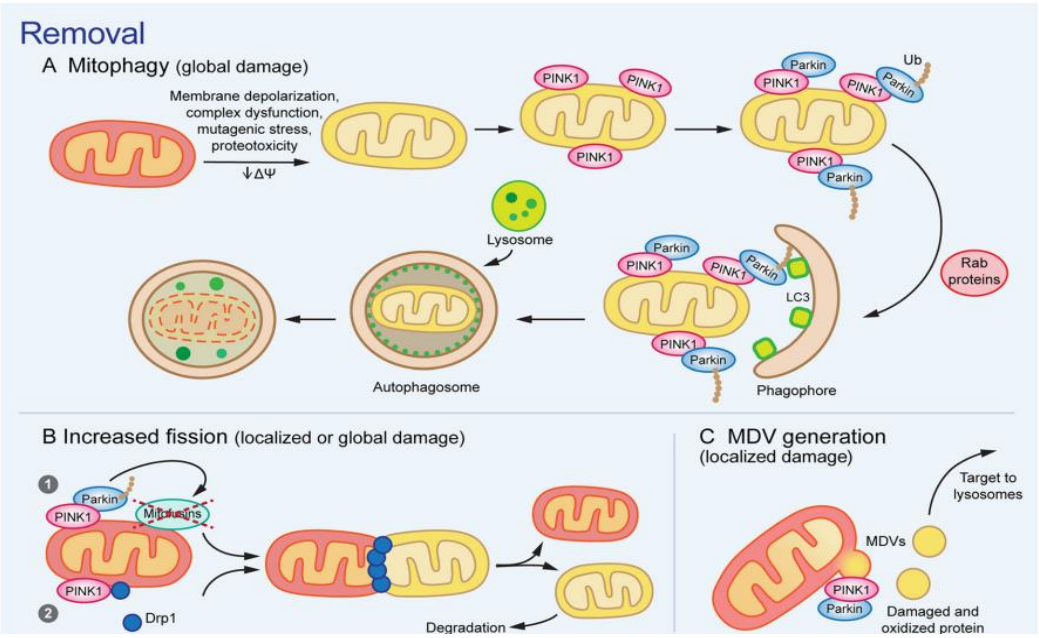

Picture 2[Ge et al. *Molecular Neurodegeneration* (2020)]

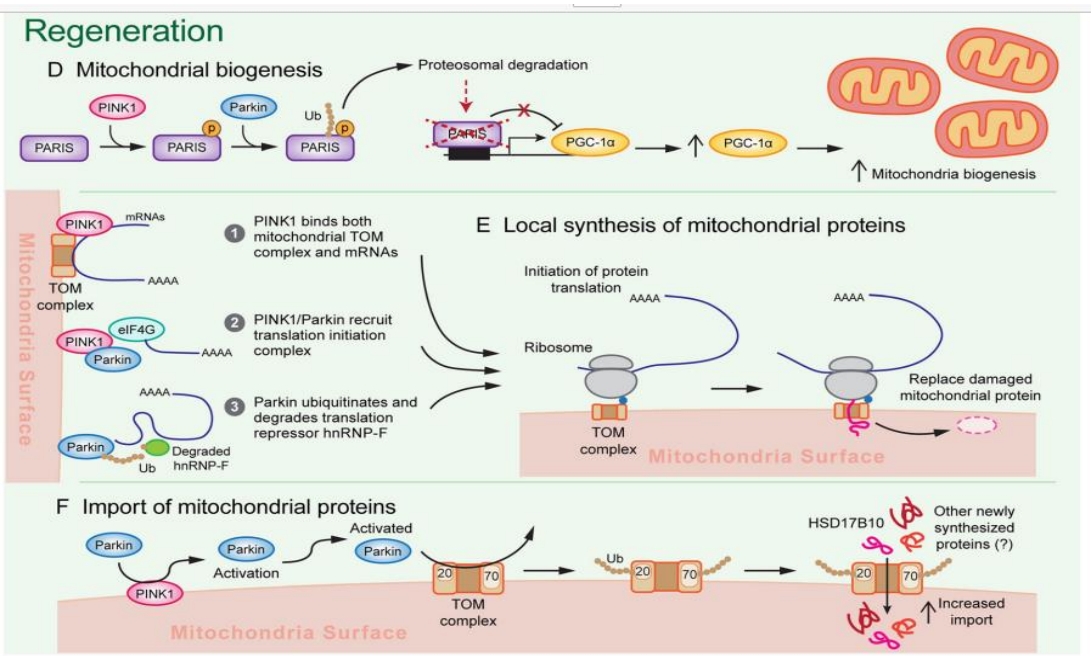

Picture 3 (and Picture 2 above): Model for the multifunctional role of PINK1/Parkin in mitochondrial quality control . Activation of PINK1/ Parkin triggers multiple mechanisms of **a-c** mitochondrial removal and **d,e** mitochondrial regeneration. Different mechanisms of mitochondrial removal are engaged depending in the severity of damage. [Ge et al. *Molecular Neurodegeneration* (2020)]

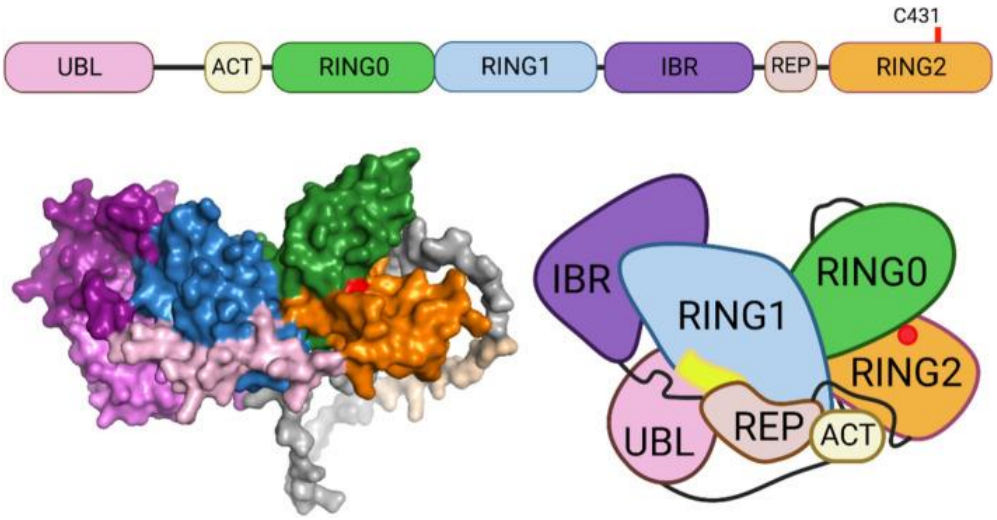

Picture 4: Parkin domain organization and auto-inhibited conformation (Clausen et al, 2024)

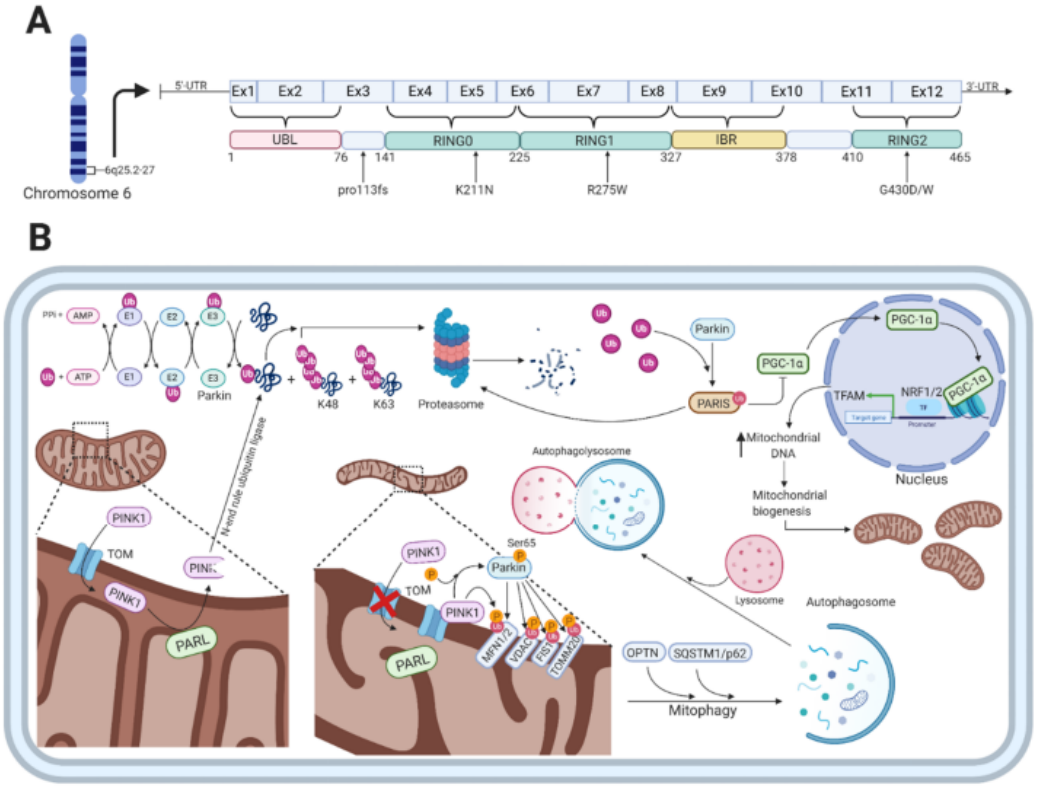

Picture 5: The function of parkin and PARK2-related mutation. **(A)** Shows a schematic representation of parkin on transcripti level, color-coded functional domains, and PARK-2 related mutations**. (B)** Shows the various cellular functions of parkin, which is involved in the ubiquitin-proteasome system as an E3 –ubiquitin ligase, regulation of mitophagy, and mitochondrial biogenesis. (*Cells*, 2021)

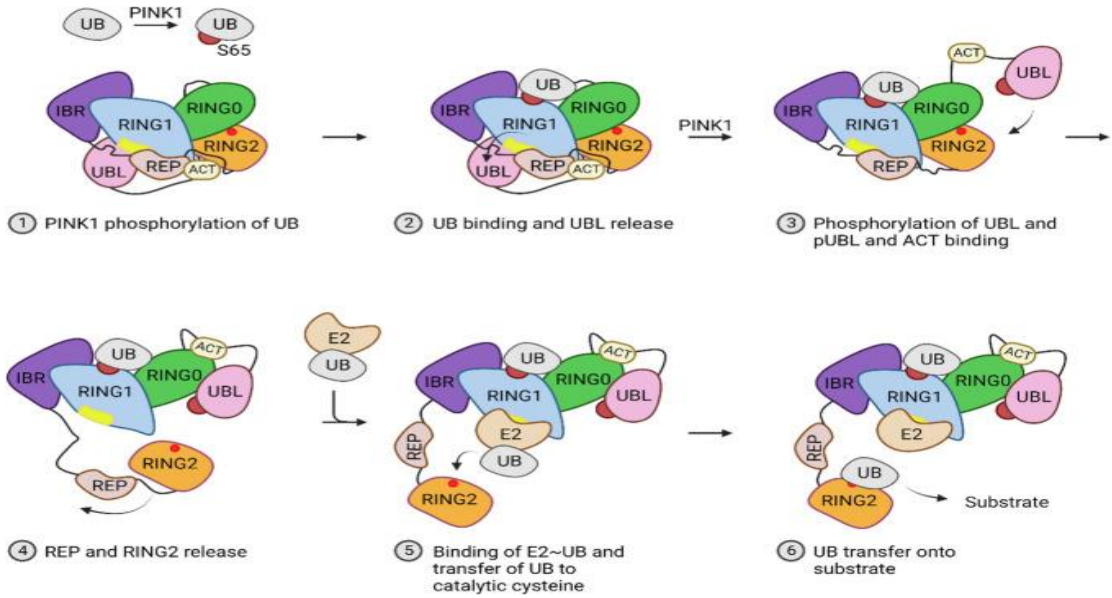

Picture 6: Parkin activation (Clausen et al, 2024)

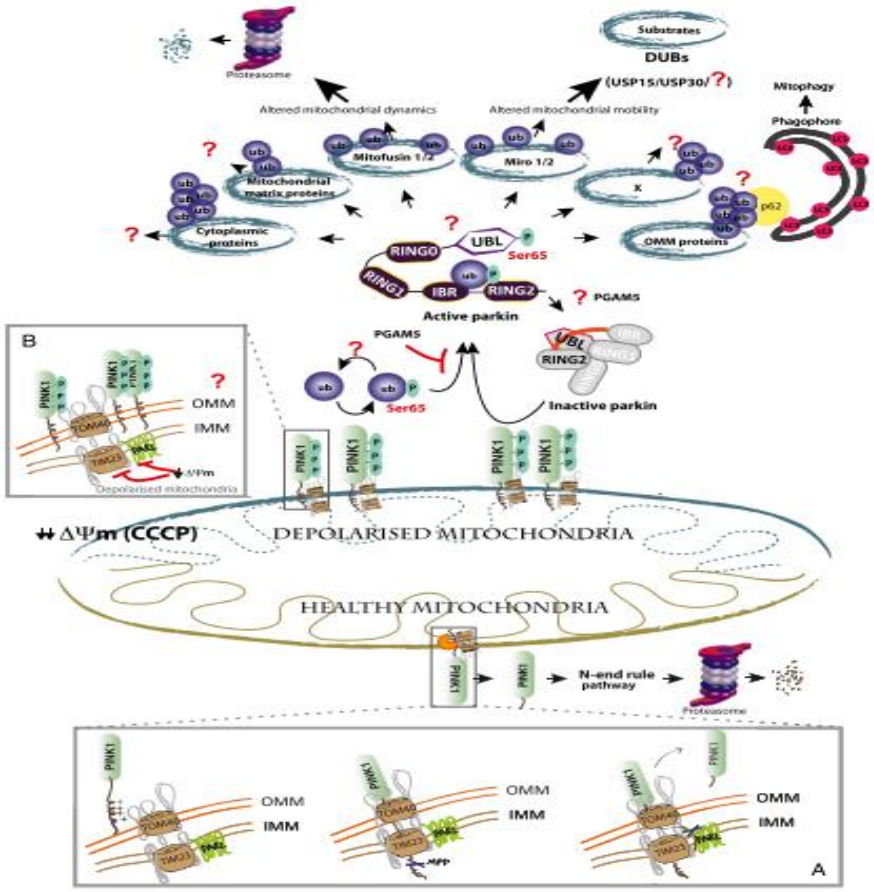

Picture 7: PINK1-Parkin signaling (under healthy conditions / upon mitochondrial depolarization) (A. Kazlauskaite and M.M. K. Muquit, *FEBS Journal* 282, 2015)

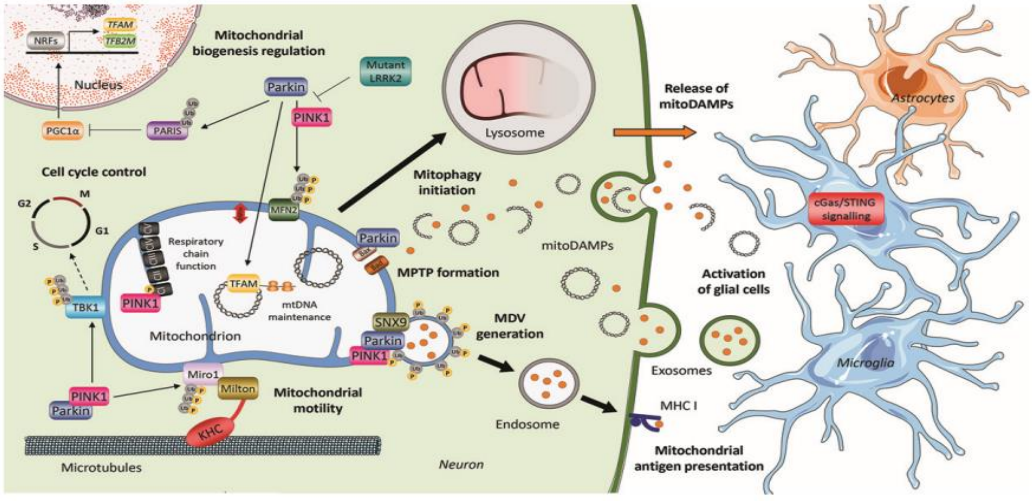

Picture 8: Involvement of PINK1 AND Parkin in mitochondrial processes. (M. Borsche et al. / *Mitochondria and PD*)

Clinical Phenotype	
Motor features	Bradykinesia
	Resting tremor
Non-motor features	Anxiety
	Psychosis
	Panic attack
	Depression
Other clinical features	Normal cognitive function
	Hyperreflexia
	Frequent focal dystonia
	Sleep benefit
	Benign disease course
	Excellent response to low dose Levodopa
	Prone to develop Levodopa-induced dyskinesias

Picture 9: Clinical phenotypes frequently reported in PD cases with *PARK2* mutations (*Cells*, 2021, 10, 283)

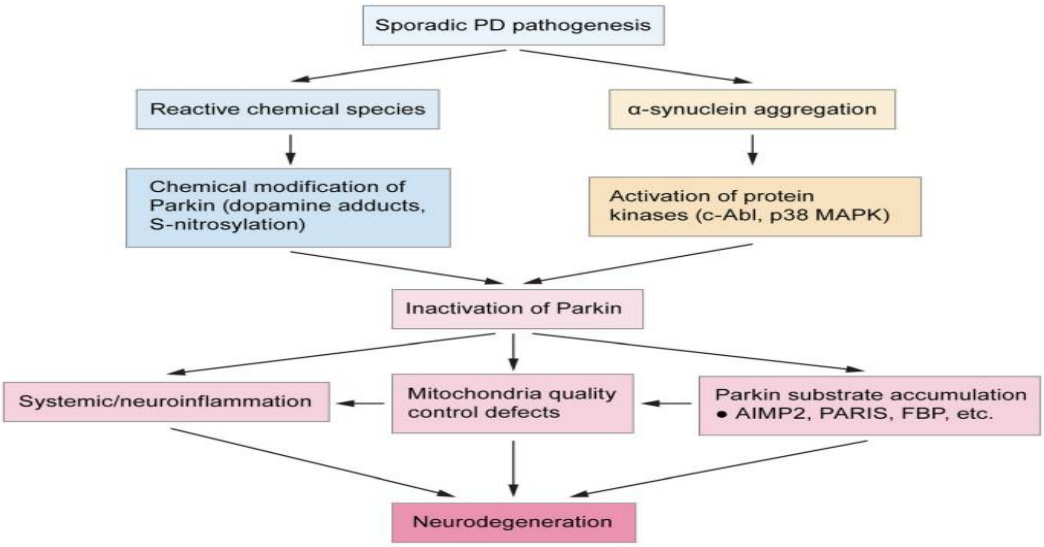

Picture 10: Mechanisms of Parkin inactivation in idiopathic PD (Ge et al, *Molecular Neurodegeneration*, 2020)

Tables

Patient ID	Type	Age	Age onset
Γ634	iPD	48	45
Γ635	iPD	62	61
Γ636	iPD	46	45
Γ617	iPD	65	55
Γ618	iPD	67	66
Γ622	iPD	66	65
Γ606	iPD	56	54
Γ696	iPD	65	61
Γ505	PRKN	40	33
Γ640	PRKN	54	51
Γ144	PRKN	38	32
Γ550	PRKN	65	59
Γ388	PRKN	22	20
Γ496	PRKN	57	49
ΘA765	PRKN	51	43

Table 1: Age/ Age of onset of PD patients

iPD: idiopathic PD patients (blue colour)

PRKN: *PRKN*-related PD patients (red colour)

Characteristics	Controls (n=7)	PD (n=8)	PRKN (n=7)
Mean age (years)	59.9 (11.6)	59.9 (7.5)	46.7 (14.4)
Mean age of onset	-	56.5 (7.71)	38.29 (10.19)
Sex (M/F)	1/6	5/3	4/3
Disease duration (years)	-	1.63 (1.22)	8.67 (8.03)
PRKN mutations (Bial/Het)	-	-	¾

Table 2: Demographic characteristics of study participants

M: male, F: female, Bial: biallelic, Het: heterozygous

Patient ID	Mutation	Status	Clinical Significance	Protein
Г550	c.101_102delAG	Homozygous	Pathogenic	p.Gln34Argfs*5
Г640	c.376C>T (exon 4)	Heterozygous	Pathogenic/likely pathogenic	p.Arg126Trp
Г144	Exon 2 del	Heterozygous	Pathogenic	-
Г505	c.758G>A, exon 7 del	Compound heterozygous	Pathogenic/likely pathogenic	p.Cys253Tyr
Г388	Exon 6: c540delinsGC:pV181Rfs*16	Heterozygous	Uncertain significance	p.V181Rfs*16
Г492	c401T>C	Heterozygous	Uncertain significance	p.Leu.134Pro
ӨА765	c101_102delAG;Exon 7 del	Compound Heterozygous	Pathogenic	p.Gln34fs

Table 3: Type of mutation of *PRKN*-related PD patients and clinical significance

Samples	Type	Age	Sex	PRKN mutation	Blood collection	PBMCs collection	RNA extraction	CDNA synthesis	RT-PCR
Г641	CT	48	F	-	04.04.23	05.04.23	25.09.24	25.09.24	26.09.24
Г683	CT	61	F	-	05.12.23	06.12.23	12.09.24	12.09.24	13.09.24
Г590	CT	66	F	-	24.05.22	25.05.22	02.10.24	02.10.24	03.10.24
Г594	CT	49	F	-	07.06.22	08.06.22	02.10.24	02.10.24	03.10.24
Г595	CT	73	F	-	16.06.22	17.06.22	02.10.24	02.10.24	03.10.24
Г564	CT	74	M	-	15.02.22	16.02.22	02.10.24	02.10.24	03.10.24
Г576	CT	48	F	-	12.04.22	13.04.22	02.10.24	02.10.24	03.10.24
Г634	PD	48	M	-	28.02.23	29.02.23	15.09.24	15.09.24	26.09.24
Г635	PD	62	M	-	07.03.23	08.03.23	25.09.24	25.09.24	26.09.24
Г636	PD	50	F	-	07.03.23	08.03.23	25.09.24	25.09.24	26.09.24
Г617	PD	65	M	-	22.11.22	23.11.23	02.10.24	02.10.24	03.10.24
Г618	PD	67	M	-	22.11.22	23.11.23	02.10.24	02.10.24	03.10.24
Г622	PD	66	F	-	13.12.22	14.12.23	02.10.24	02.10.24	03.10.24
Г606	PD	56	F	-	04.10.22	05.10.22	02.10.24	02.10.24	03.10.24
Г696	PD	65	M	-	26.03.24	27.03.24	02.10.24	02.10.24	03.10.24
Г505	PRKN	40	M	+	28.05.21	29.05.21	25.09.24	25.09.24	26.09.24
Г640	PRKN	54	M	+	04.04.23	05.04.23	25.09.24	25.09.24	26.09.24
Г144	PRKN	38	M	+	07.09.18	08.09.18	02.10.24	02.10.24	03.10.24
Г550	PRKN	65	M	+	09.11.21	10.11.21	02.10.24	02.10.24	03.10.24
Г388	PRKN	22	F	+	19.11.19	20.11.19	02.10.24	02.10.24	03.10.24
Г492	PRKN	57	F	+	13.04.21	14.04.21	02.10.24	02.10.24	03.10.24
ӨА765	PRKN	51	F	+	16.06.16	17.06.16	02.10.24	02.10.24	03.10.24

Table 4: Chronological dates of study procedures

Samples	RNA (ng/µl)	CRNA (ng/µl)	A260/280	A260/230
Г641	414.9	-	1.99	1.05
Г683	210.1	178.5	1.89	1.24
Г590	323.2	293.1	1.95	1.25
Г594	310.5	280.4	1.98	1.08
Г595	302.6	225.7	1.97	1.78
Г564	250.2	235.7	1.89	1.19
Г576	266.2	235.8	1.88	1.21
Г634	299.2	263.2	1.92	1.06
Г635	227.4	328.7	1.95	1.27
Г636	183.2	227.4	1.91	1.32
Г617	183.2	170.5	1.90	1.25
Г618	208	200	1.93	1.26
Г622	198.7	189.2	1.88	1.13
Г606	230.3	221.8	1.90	1.25
Г696	315.6	-	1.95	1.70
Г505	183.7	159.6	1.90	0.95
Г640	779.5	707	1.95	1.08
Г144	248.3	230.2	1.92	1.22
Г550	357.8	305.2	1.87	1.16
Г388	224.3	200.8	1.84	1.21
Г492	237.8	221.4	1.93	1.23
ΘА765	115.8	100.3	1.85	1.13
НВ32	233.6	233.6	1.73	2.14
NBA30G	4612.1	4612.1	2.08	2.21
NB (1)	518.4	518.4	1.98	1.6
NB (2)	704.6	704.6	2.01	1.23
НЕК293	69.6	69.6	1,77	0.83

Table 5: NanoDrop results of RNA quantification/qualification

	GAPDH		PRKN		Mean Value of Cq	
SAMPLES	Cq	Cq'	Cq	Cq'	GAPDH	PRKN
Γ641	21.32	21.30	27.82	27.11	21.31	22.47
Γ683	23.12	22.17	29.08	29.01	22.65	30.73
Γ590	24.31	24.09	31.13	32.25	24.20	31.69
Γ594	22.26	22.38	29.17	29.09	22.32	29.13
Γ595	21.15	21.32	28.15	28.23	21.24	28.19
Γ564	20.27	19.95	29.74	29.80	20.11	29.77
Γ576	21.32	21.30	27.82	27.11	21.98	28
Γ634	20.04	20.55	31.04	31.67	20.30	31.36
Γ635	23.81	29.78	30.98	30.47	23.80	30.73
Γ636	18.68	18.85	27.33	27.65	18.77	27.49
Γ617	23.12	22.17	30.92	30.53	22.65	30.73
Γ618	22.81	22.09	31.35	-	22.45	31.35
Γ622	23.35	22.27	30.18	30.09	22.81	30.14
Γ606	20.05	20.52	29.58	29.81	20.29	29.70
Γ696	23.08	21.98	31.95	31.67	22.53	31.81
Γ505	20.59	20.26	36.87	35.45	20.43	36.16
Γ640	22.77	22.17	36.08	37.90	22.47	36.99
Γ144	23.83	23.75	37.09	37.22	23.79	37.16
Γ550	18.63	18.81	33.82	33.95	18.72	33.89
Γ388	20.53	20.21	35.48	35.54	20.37	35.51
Γ492	21.77	22.17	36.04	37.93	21.97	36.99
ΘΑ765	24.58	25.01	38.26	39.02	24.80	38.64
NBA30G	29.99	25.53	28.12	28.27	24.76	33.19
NB (1)	17.84	18.23	26.37	26.44	18.04	26.40
NB (2)	19.38	19.16	30.79	31.42	19.27	31.11
HEK293	23.06	21.68	32.08	33.24	22.37	32.66

Table 6: RT-PCR results , Cq: quantification cycle, NBA30G , NB(1), NB(2):neuroblastomacells, HEK293: human embryonic kidney cell , GAPDHCq (green colour), PRKNCq (orange colour)

SAMPLES	GAPDH	PRKN	ΔCt	Mean ΔCt	ΔΔCt	Fold
Γ641	21.31	27.47	6.16	7.31	-1.15	2.21914
Γ683	22.65	30.73	8.08		0.77	0.58642
Γ590	24.2	31.69	7.49		0.18	0.8827
Γ594	22.32	29.13	6.81		-0.5	1.41421
Γ595	21.24	28,19	6.95		-0.36	1.28343
Γ564	20.11	29.77	9.66		2.35	0.19615
Γ576	21.98	28	6.02		-1.29	2.33528

Table 7. Normalisation analysis for the control group

SAMPLES	GAPDH	PRKN	ΔCt	Mean ΔCt	ΔΔCt	Fold
Γ634	20.3	31.36	11.06	8.71	3.75	0.07433
Γ635	23.8	30.73	6.93		-0.38	1.30134
Γ636	18.77	27.49	8.72		1.41	0.37631
Γ617	22.65	30.73	8.08		0.77	0.58642
Γ618	22.45	31.35	8.90		1.59	0.33217
Γ622	22.81	30.14	7.33		0.02	0.98623
Γ606	20.29	29.7	9.41		2.1	0.23326
Γ696	22.53	31.81	9.28		1.97	0.25525

Table 8. Normalisation analysis for the iPD group

SAMPLES	GAPDH	PRKN	ΔCt	Mean ΔCt	ΔΔCt	Fold
Γ505	20.43	36.16	15.73	13.975	8.42	0.00292
Γ640	22.47	36.99	14.52		7.21	0.00675
Γ144	23.79	37.16	13.37		6.06	0.01499
Γ550	18.72	33.89	15.17		7.86	0.0043
Γ388	20.37	35.51	15.14		7.83	0.00439
Γ492	21.97	36.99	15.02		7.71	0.00478
ΘΑ765	24.8	38.64	13.84		6.53	0.01082

Table 9. Normalisation analysis for the *PRKN*-PD carriers group

GROUPS	MEAN DIFF	FOLD CHANGE	P-VALUE
CT vs PD	4.152	1.25	0.6497 (ns)
CT vs PRKN	13.21	4.3	0.0004 (***)
PD vs PRKN	9.063	3.25	0.0210 (*)

Table 10: Mean differences of expression levels between the 3 groups (CT, PD, PRKN) and their statistical significance (p-value)

Images

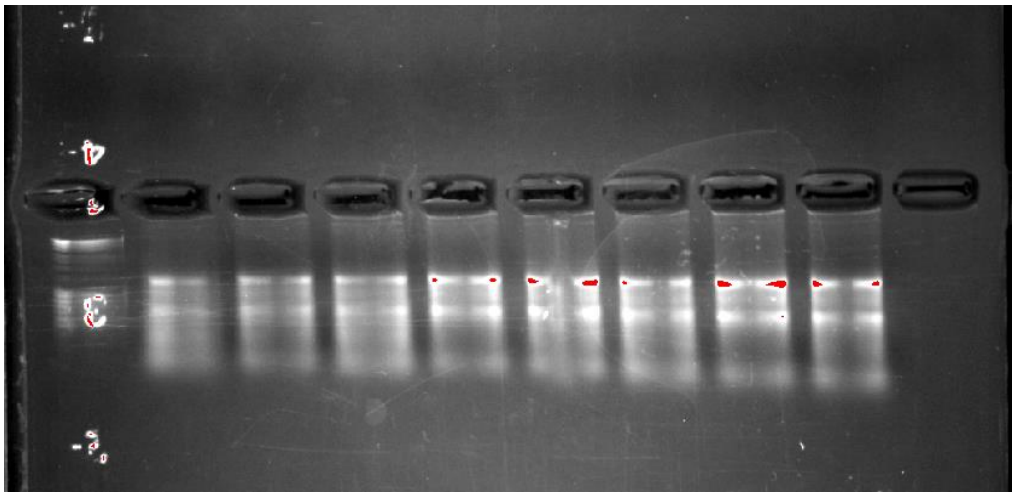

Image1: Sample series: Г641, Г611, Г683, Г634, Г635, Г636, Г505, Г640

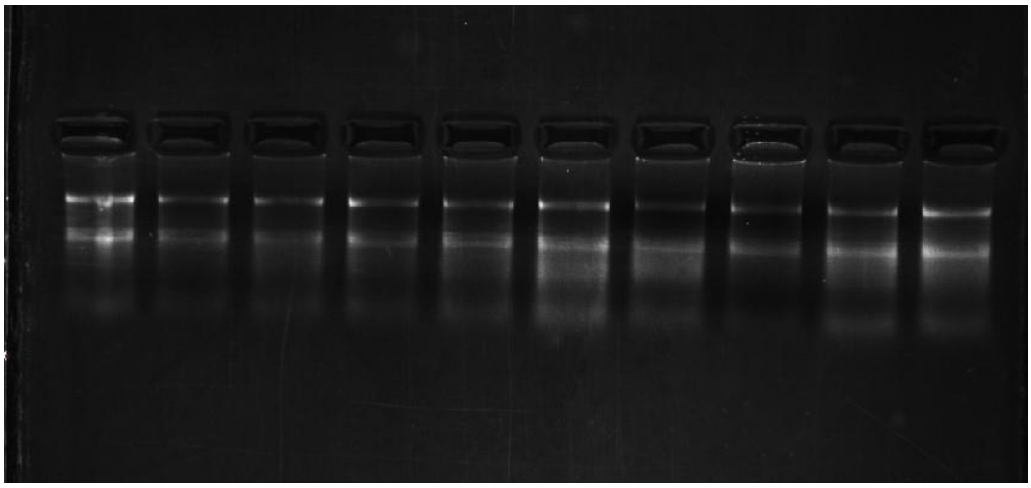

Image 2: Sample series: Г590, Г594, Г595, Г564, Г576, Г617, Г618, Г622, Г606, Г696

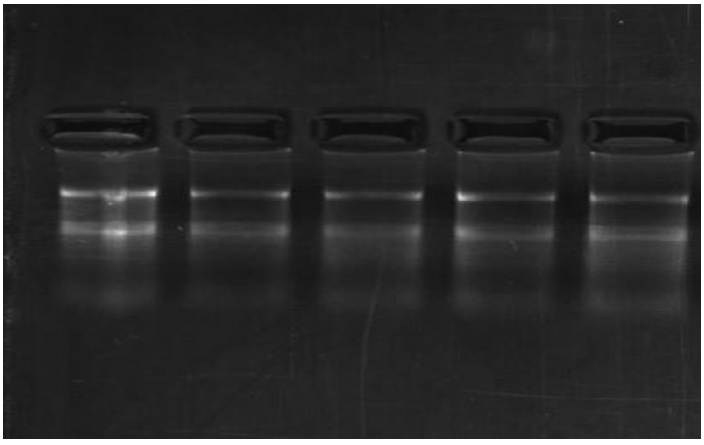

Image 3: Sample series: Г144, Г550, Г388, Г492, ӨА765

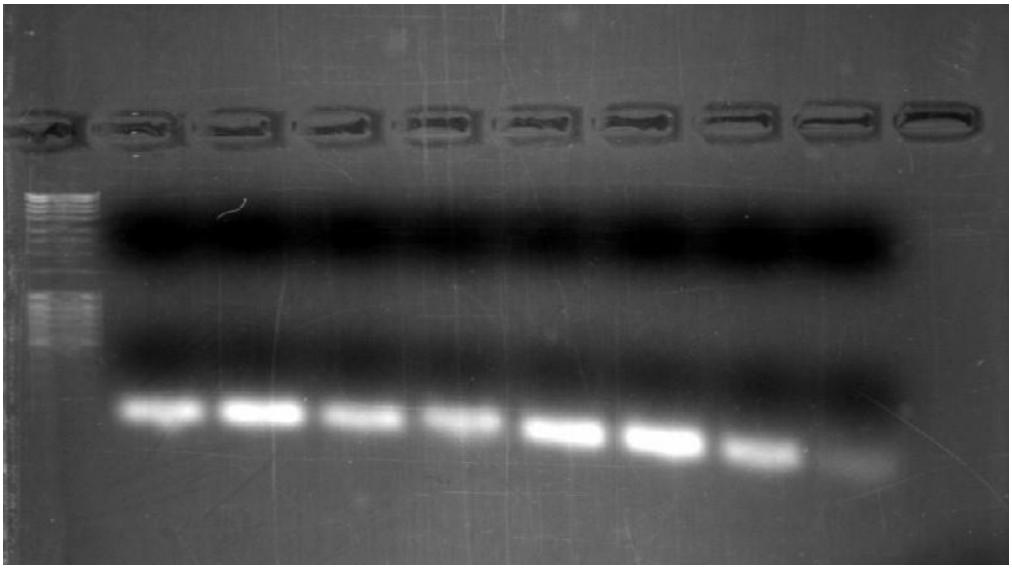

Image 4: Sample series: Г641, Г611, Г683, Г634, Г635, Г636, Г505, Г640

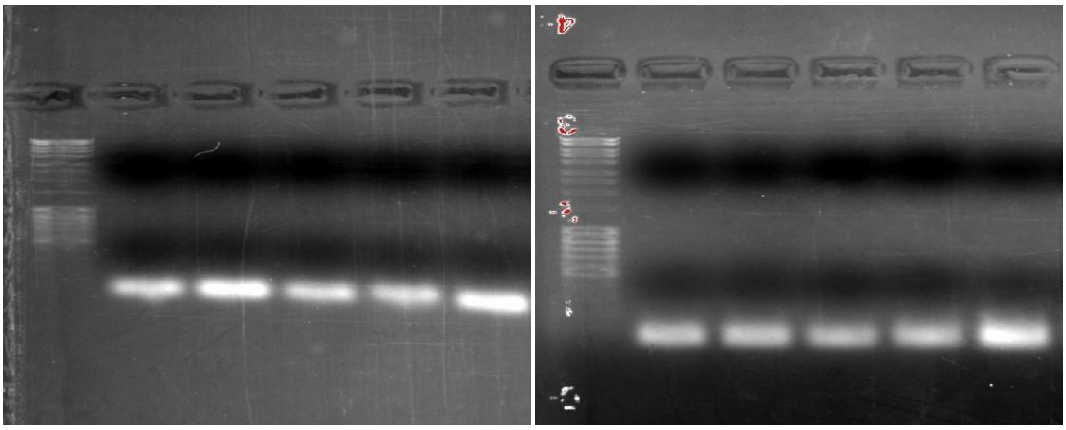

Image 5,6: Sample series: Г590, Г594, Г595, Г564, Г576, Г617, Г618, Г622, Г606, Г696

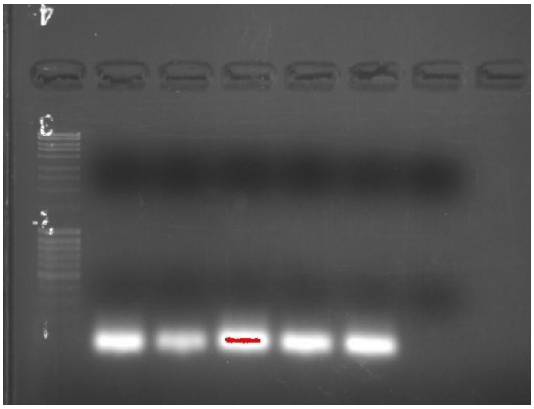

Image 7: Sample series: Г144, Г550, Г388, Г492, ӨА765

Figures

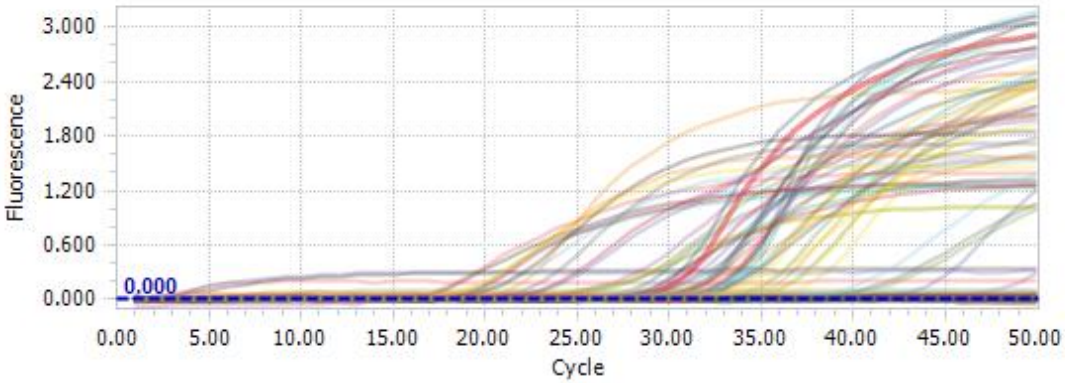

Figure 1: Sample series: Г641, Г611, Г683, Г634, Г635, Г636, Г505, Г640

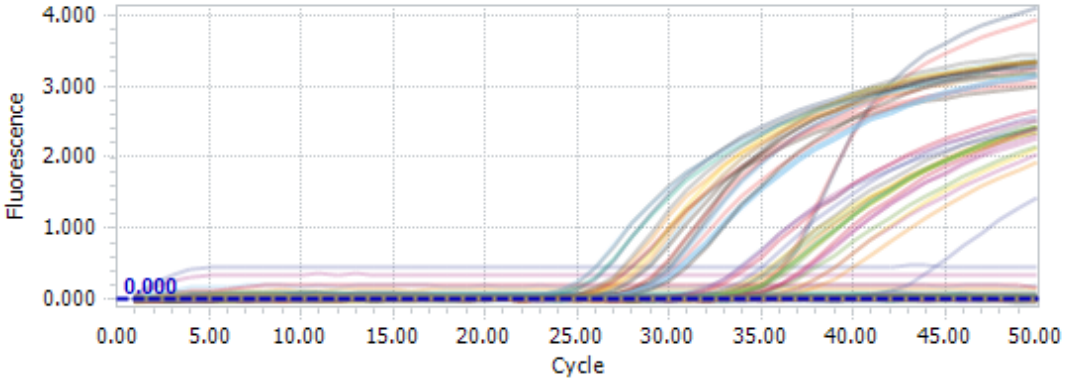

Figure 2: Sample series: Г590, Г594, Г595, Г564, Г576, Г617, Г618, Г622, Г606, Г696, Г144, Г550, Г388, Г492, ӨА765

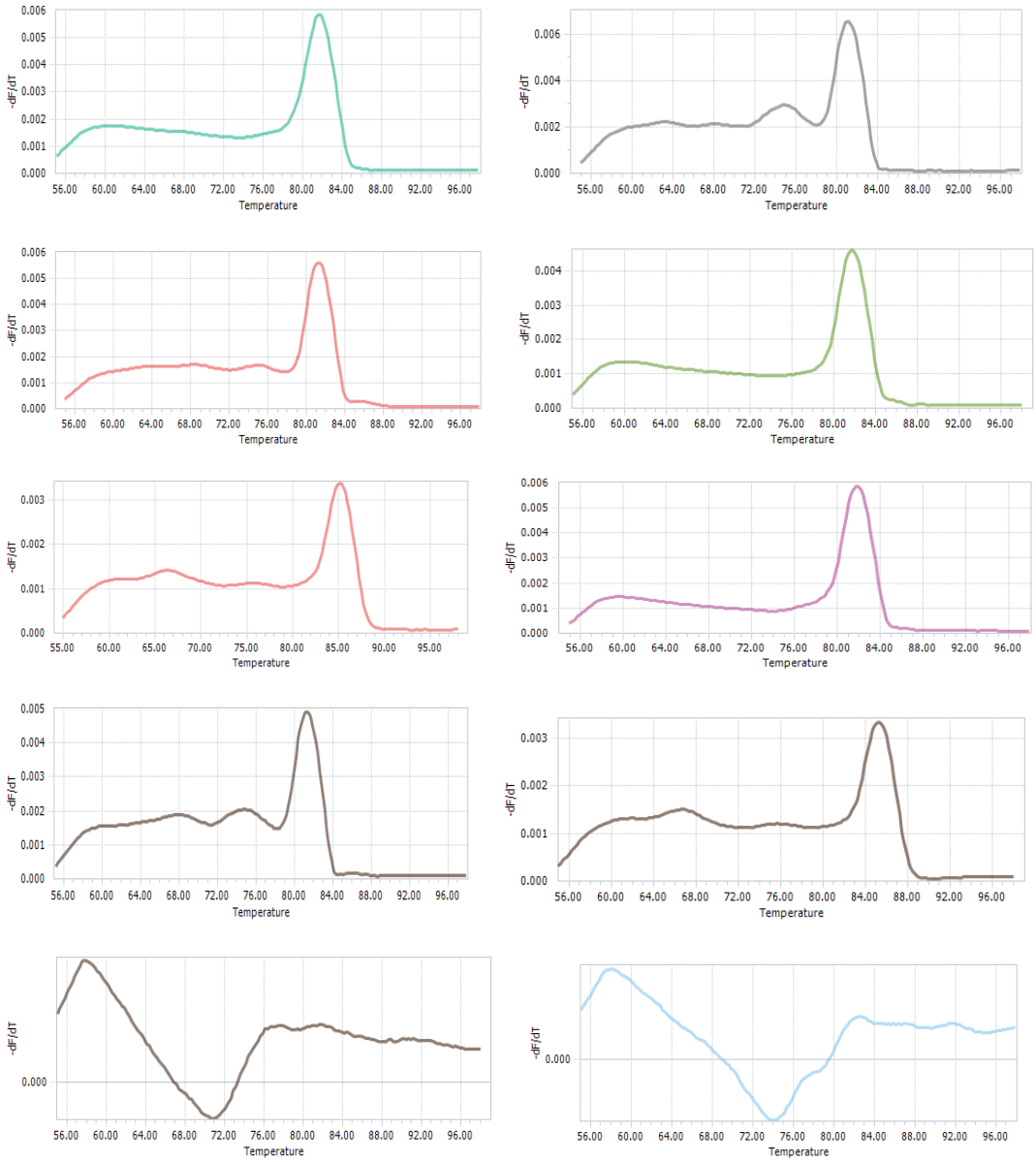

Figures 3-12: Sample series GAPDH (1): Г611, Г641, Г683, Г634, Г635, Г636, Г505, Г640, Г640 (no RT), Blank (from left to right order)

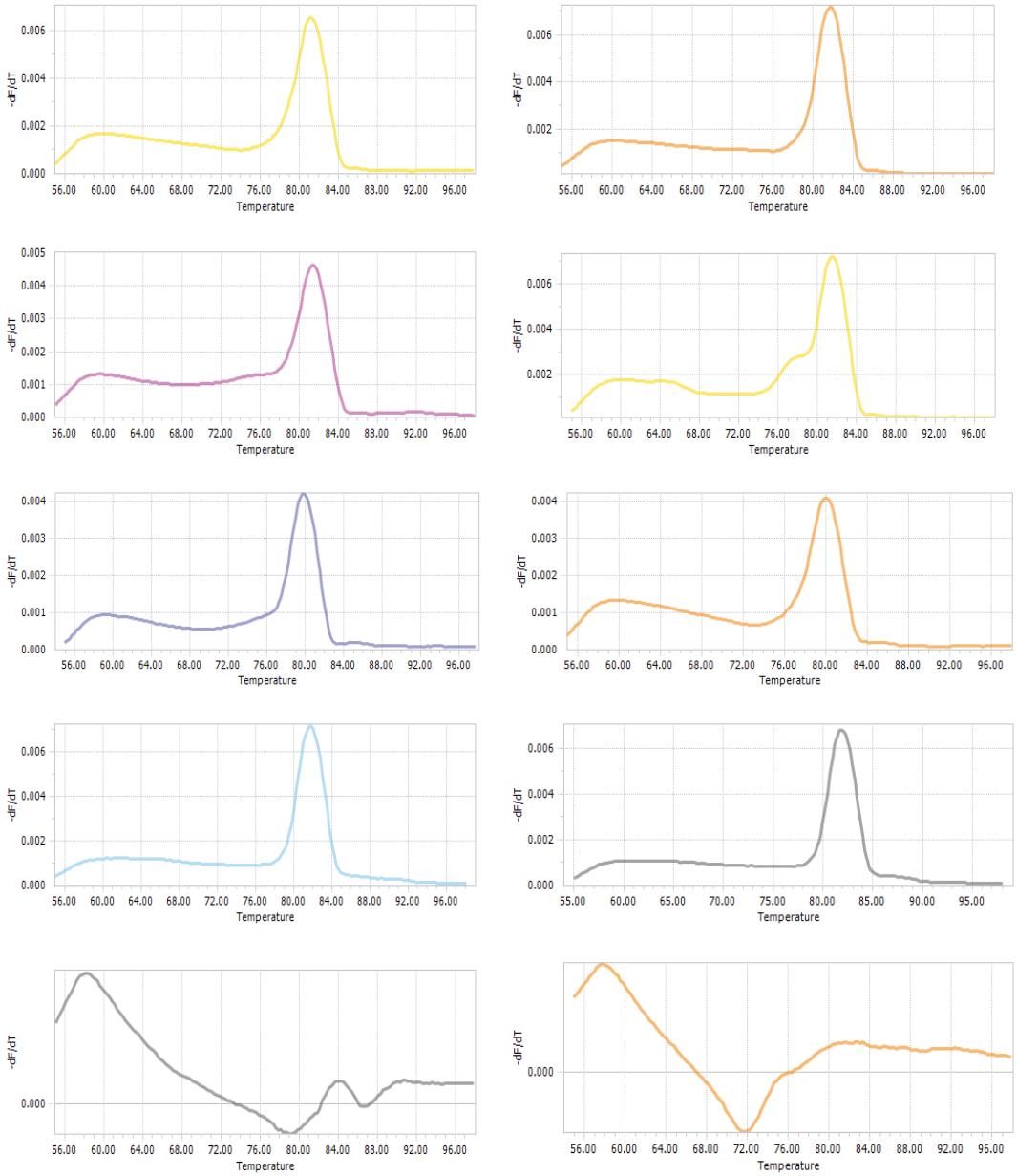

Figures 13-22: Sample series PRKN (1): Г611, Г641, Г683, Г634, Г635, Г636, Г505, Г640, Г640 (no RT), Blank (from left to right order)

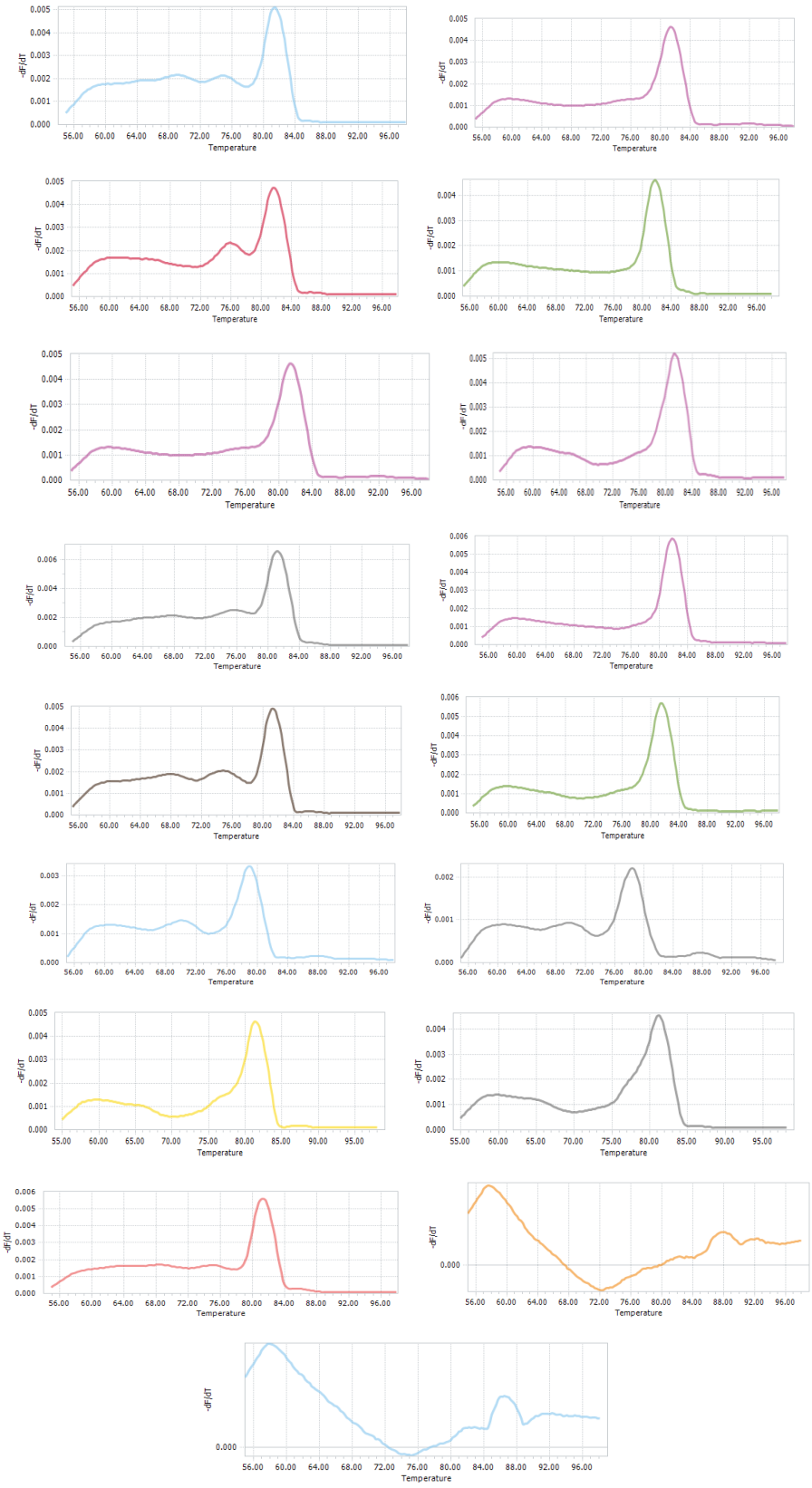

Figures 23-39: Sample series GAPDH (2):Г590, Г594, Г595, Г564, Г576, Г617, Г618, Г622, Г606, Г696, Г144, Г550, Г388, Г492, ΘА765, Г595 (no RT), Blank

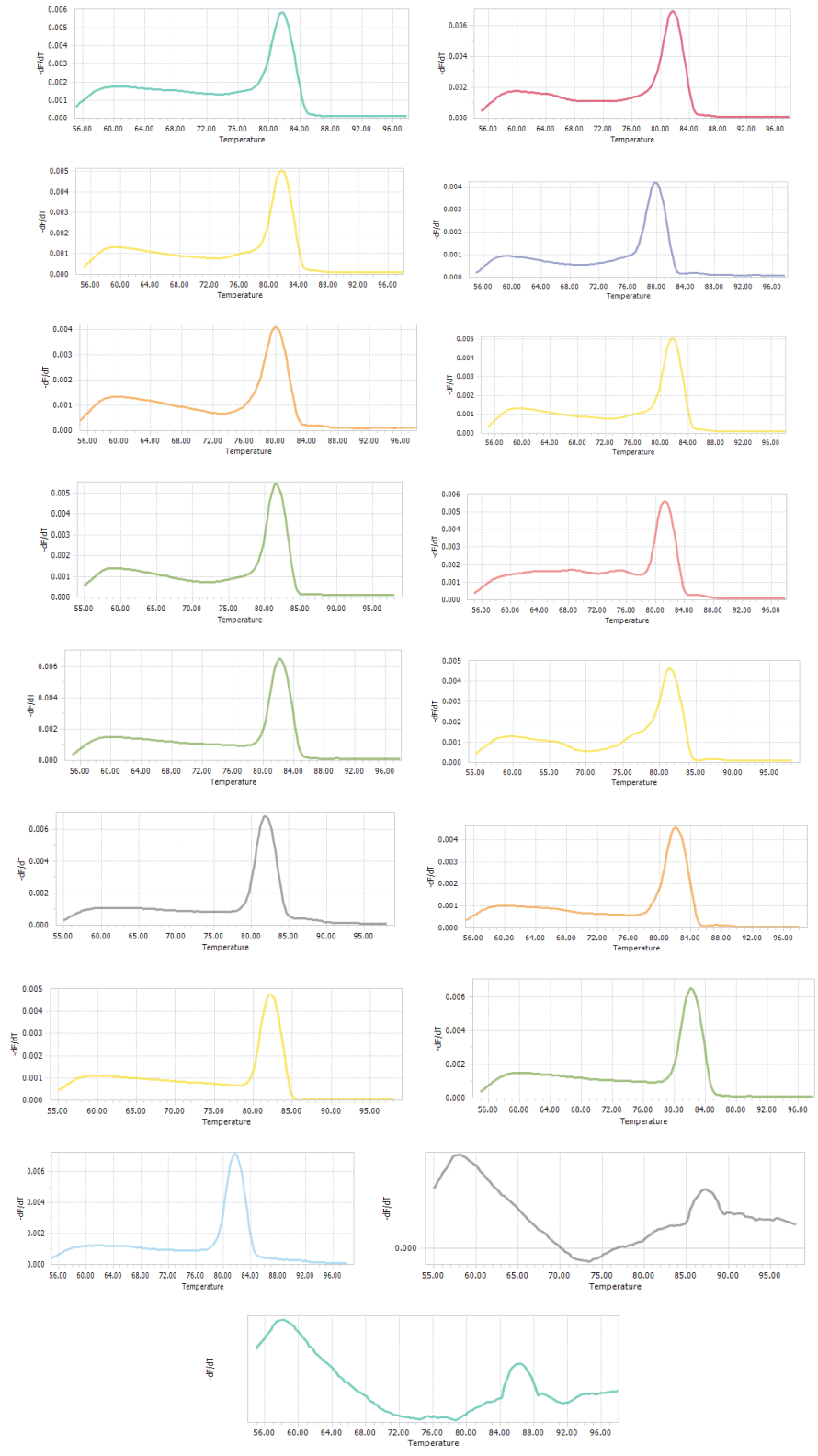

Figures 40-56: Sample series PRKN (2):Г590, Г594, Г595, Г564, Г576, Г617, Г618, Г622, Г606, Г696, Г144, Г550, Г388, Г492, ΘА765, Г595 (no RT), Blank

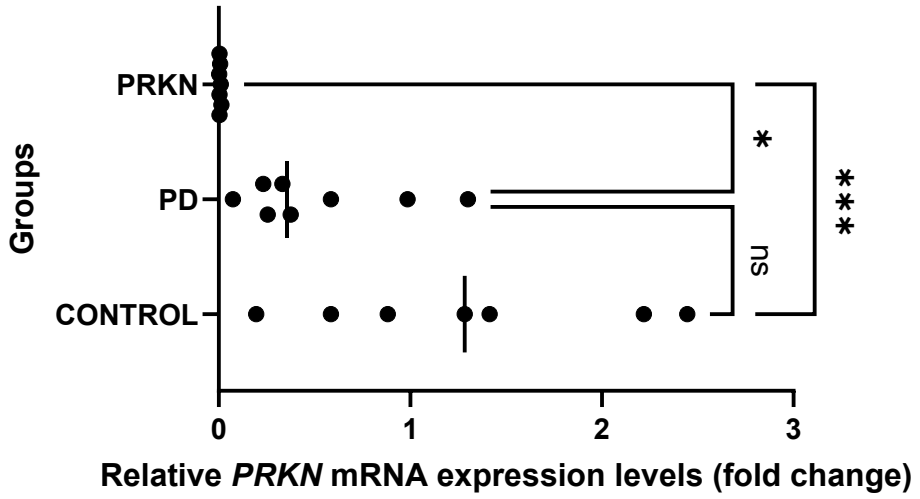

Figure 57: R*elative PRKN* mRNA expression (fold change) among groups (Controls, PD, PRKN)

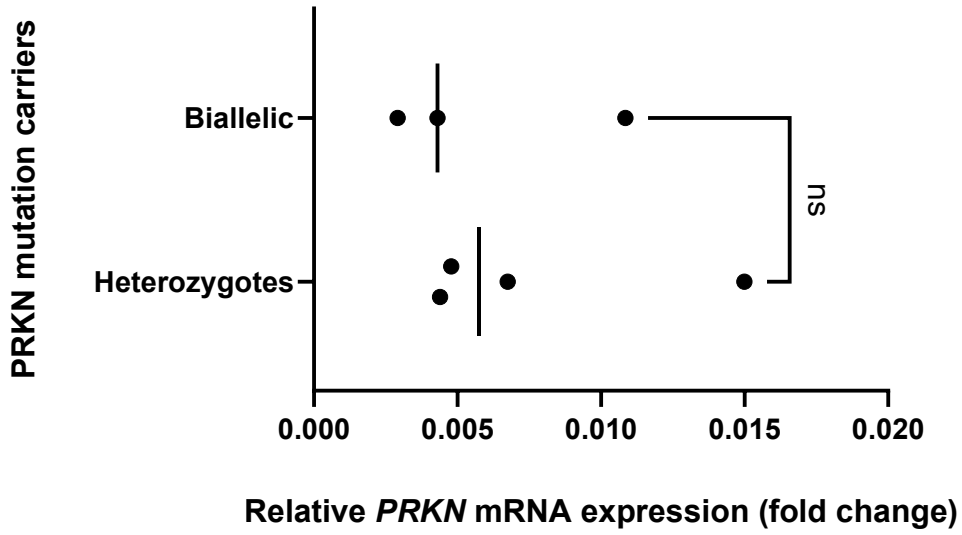

Figure 58: Relative *PRKN* mRNA expression levels (% fold change) among *PRKN* mutation carriers (bialellic, heterozygotes)

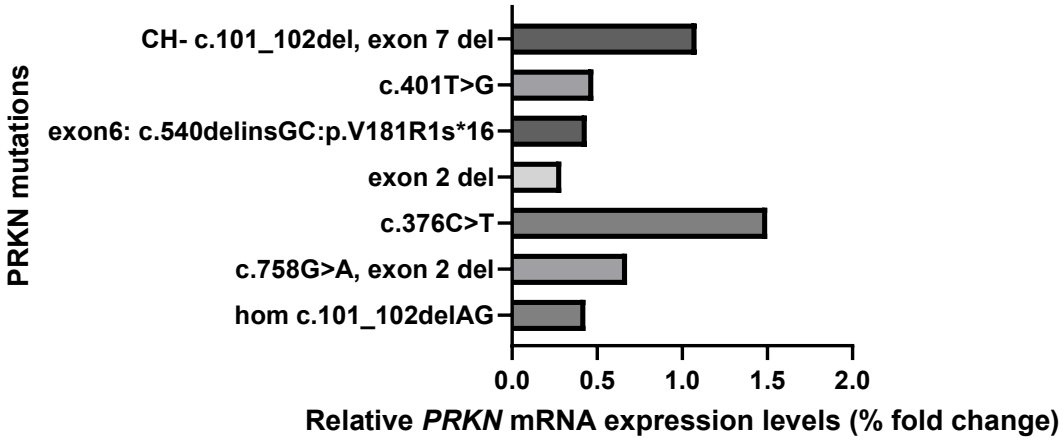

Figure 59: Relative *PRKN* mRNA expression levels (% fold change) among *PRKN* mutations carriers (regarding type of mutation)

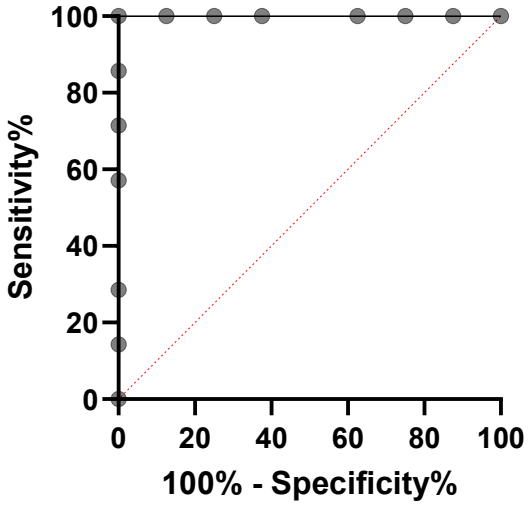

Figure 60: ROC analysis